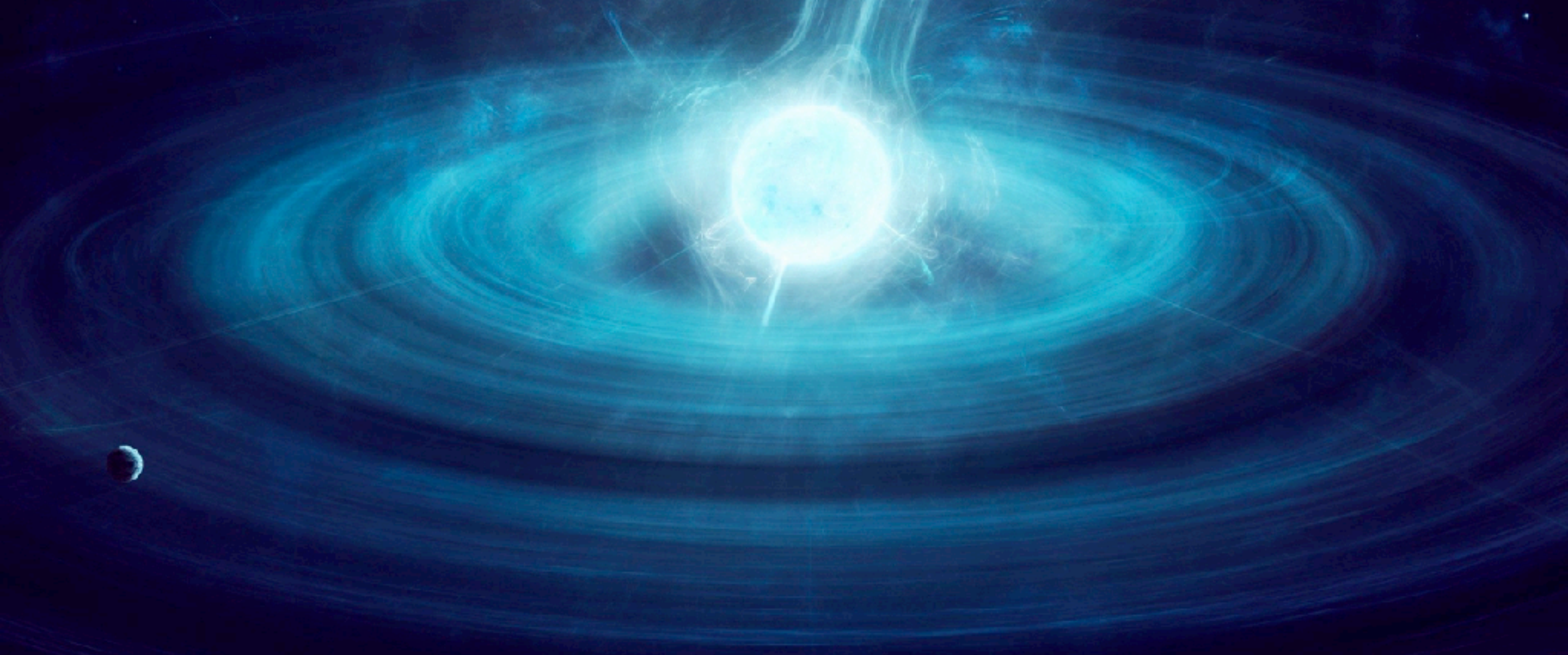

TIM LINDEN

THE RISE OF THE LEPTONS

PULSAR EMISSION DOMINATES THE TEV GAMMA-RAY SKY

Stockholm OKC Colloquium

June 20, 2017

THE OHIO STATE UNIVERSITY

CENTER FOR COSMOLOGY AND ASTROPARTICLE PHYSICS

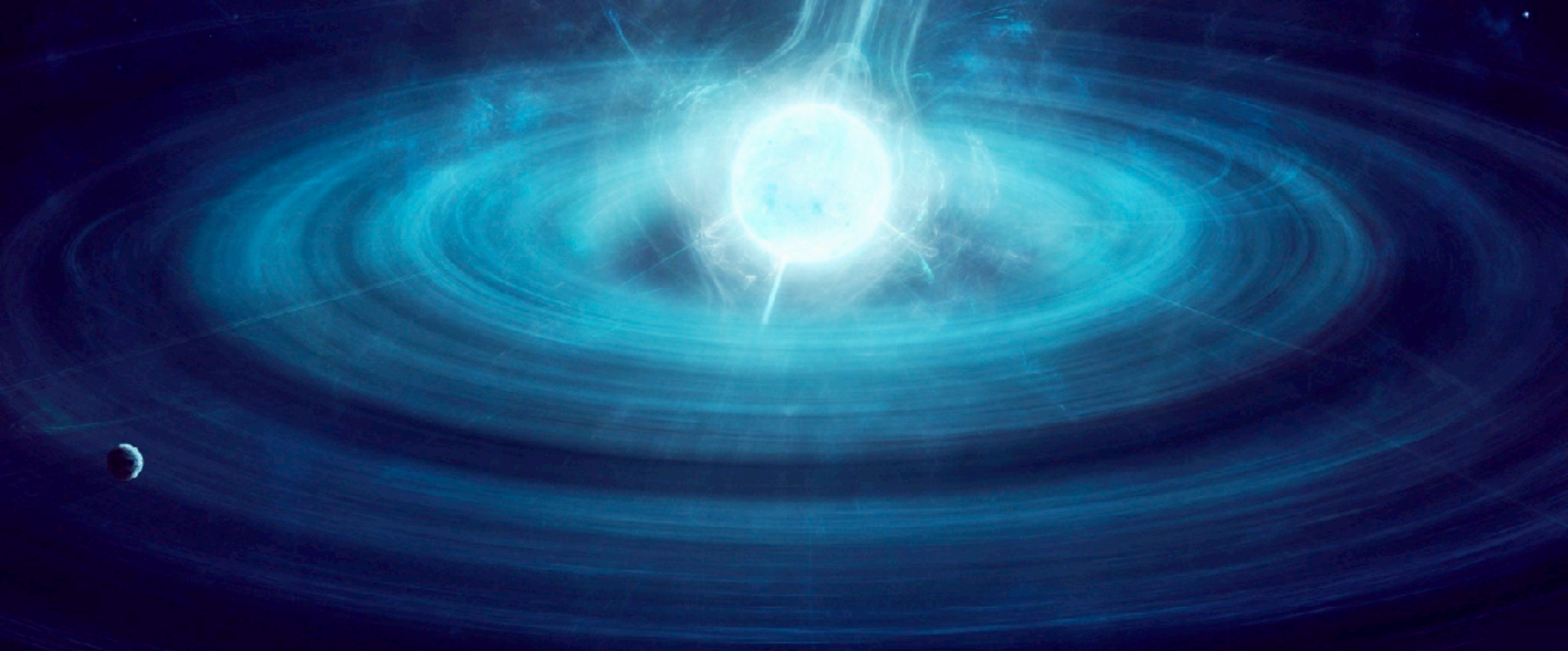

TIM LINDEN

THE RISE OF THE LEPTONS

PULSAR EMISSION DOMINATES THE TEV GAMMA-RAY SKY

WITH: KATIE AUCHETTL, BEN BUCKMAN, JOSEPH BRAMANTE, ILIAS CHOLIS, KE FANG, DAN HOOPER, SHIRLEY LI

Start with a source of relativistic cosmic-rays

- Supernova Explosions
- Supernova Remnants
- Pulsars
- Shocks/Mergers

COSMIC-RAY ACCELERATION AND PROPAGATION

Start with a source of relativistic cosmic-rays

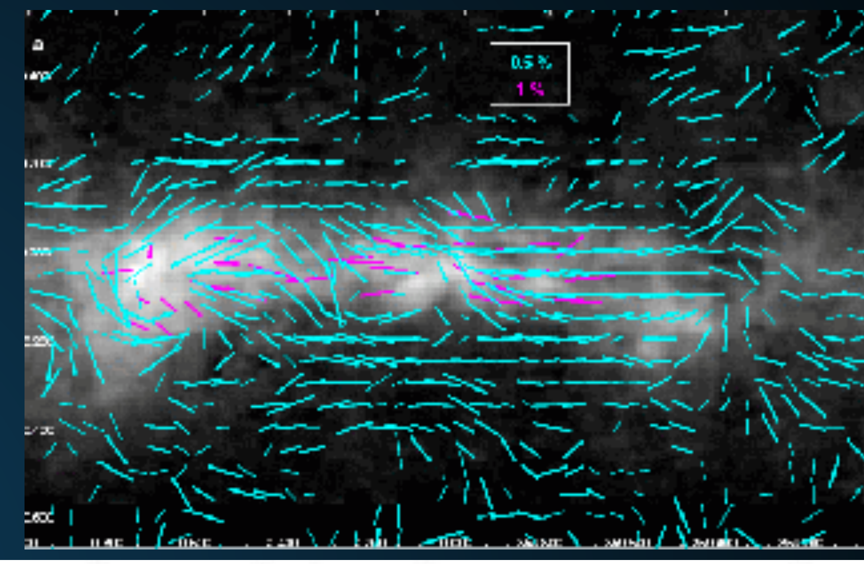

cosmic rays propagate

$$\frac{\partial \psi}{\partial t} = q(\vec{r}, p) + \vec{\nabla}\cdot(D_{xx}\vec{\nabla}\psi - \vec{V}\psi) + \frac{\partial}{\partial p} p^2 D_{pp} \frac{\partial}{\partial p}\frac{1}{p^2}\psi - \frac{\partial}{\partial p}\left[\dot{p}\psi - \frac{p}{3}(\vec{\nabla}\cdot\vec{V})\psi\right] - \frac{1}{\tau_f}\psi - \frac{1}{\tau_r}\psi$$

Solved Numerically:
e.g. Galprop

- If they propagate to Earth, can be detected:
  - AMS-02/PAMELA
  - CREAM/HEAT/CAPRICE

COSMIC-RAY ACCELERATION AND PROPAGATION

Start with a source of relativistic cosmic-rays

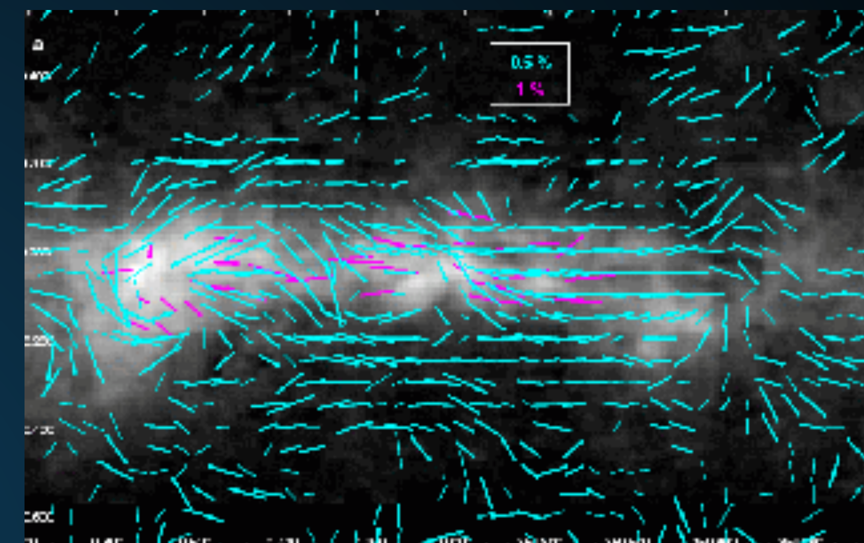

cosmic rays propagate

$$\frac{\partial \psi}{\partial t} = q(\vec{r}, p) + \vec{\nabla} \cdot (D_{xx} \vec{\nabla} \psi - \vec{V} \psi) + \frac{\partial}{\partial p} p^2 D_{pp} \frac{\partial}{\partial p} \frac{1}{p^2} \psi - \frac{\partial}{\partial p} \left[\dot{p} \psi - \frac{p}{3} (\vec{\nabla} \cdot \vec{V}) \psi \right] - \frac{1}{\tau_f} \psi - \frac{1}{\tau_r} \psi$$

Solved Numerically:
e.g. Galprop

Gas/ISRF

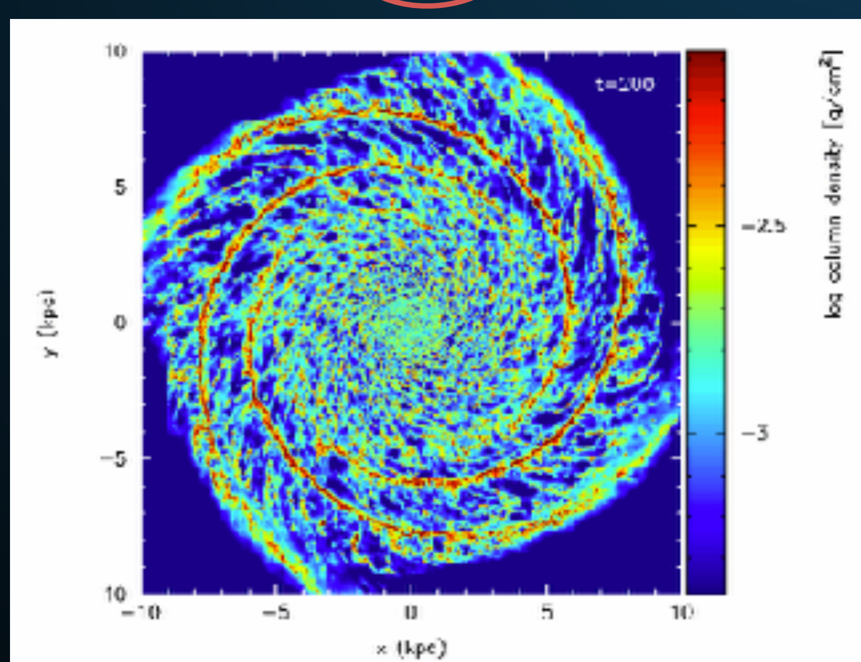

- **Alternatively can collide with Galactic gas or the interstellar radiation field.**

COSMIC-RAY ACCELERATION AND PROPAGATION

Start with a source of relativistic cosmic-rays

cosmic rays propagate

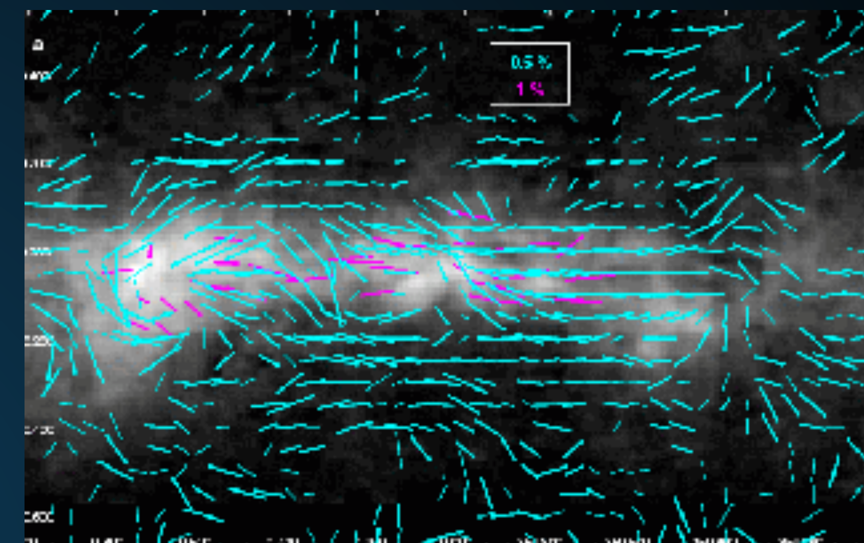

$$\frac{\partial \psi}{\partial t} = q(\vec{r}, p) + \vec{\nabla}\cdot(D_{xx}\vec{\nabla}\psi - \vec{V}\psi) + \frac{\partial}{\partial p} p^2 D_{pp} \frac{\partial}{\partial p}\frac{1}{p^2}\psi - \frac{\partial}{\partial p}\left[\dot{p}\psi - \frac{p}{3}(\vec{\nabla}\cdot\vec{V})\psi\right] - \frac{1}{\tau_f}\psi - \frac{1}{\tau_r}\psi$$

Solved Numerically:
e.g. Galprop

Gas/ISRF

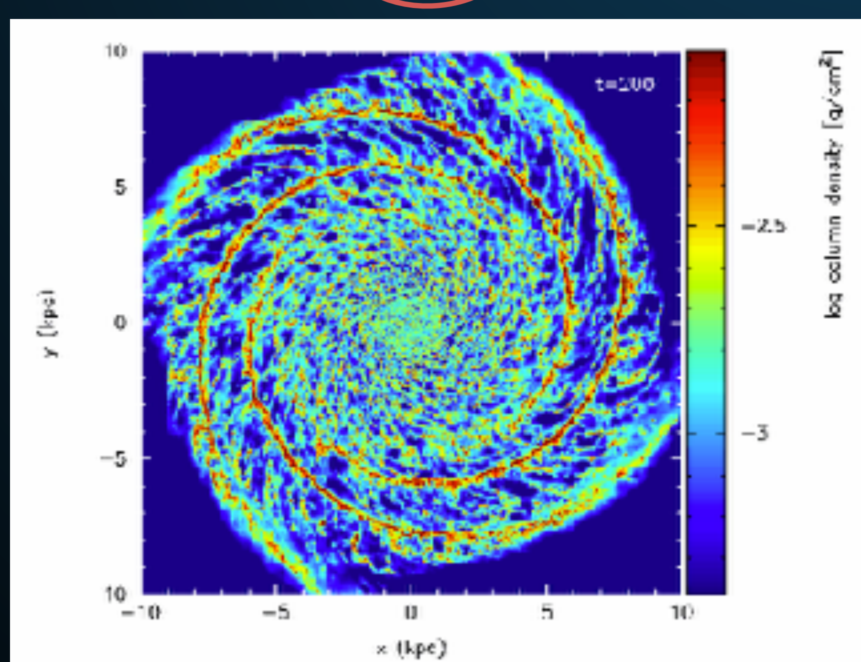

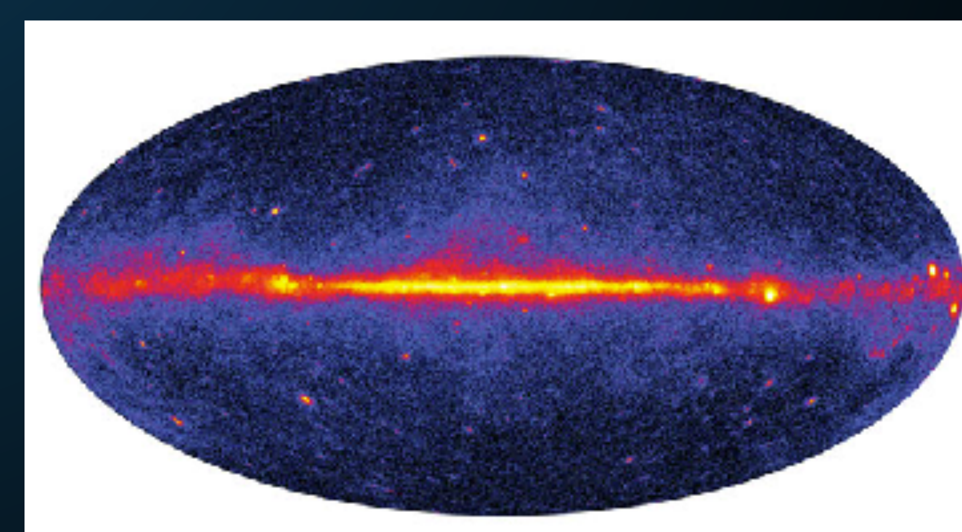

TWO DIFFERENT SOURCES OF INFORMATION

- This provides us two ways to learn about cosmic rays:
  - Investigating the cosmic-rays that directly hit satellites on Earth
    - Can directly detect cosmic-ray species
    - Only a local measurement
    - Solar Modulation
  - Investigating the gamma-ray signal from cosmic-ray interactions
    - Can understand propagation near sources
    - Don't directly know the cosmic-ray species, or even if the gamma-ray is galactic
    - Line of sight

A UNIVERSE DOMINATED BY PROTONS

slide via Don Ellison

- Supernova remnants provide the only source energetic enough to explain the full energy spectrum of cosmic-ray protons up to PeV energies.

- First order Fermi acceleration naturally predicts protons dominate supernova energetics.

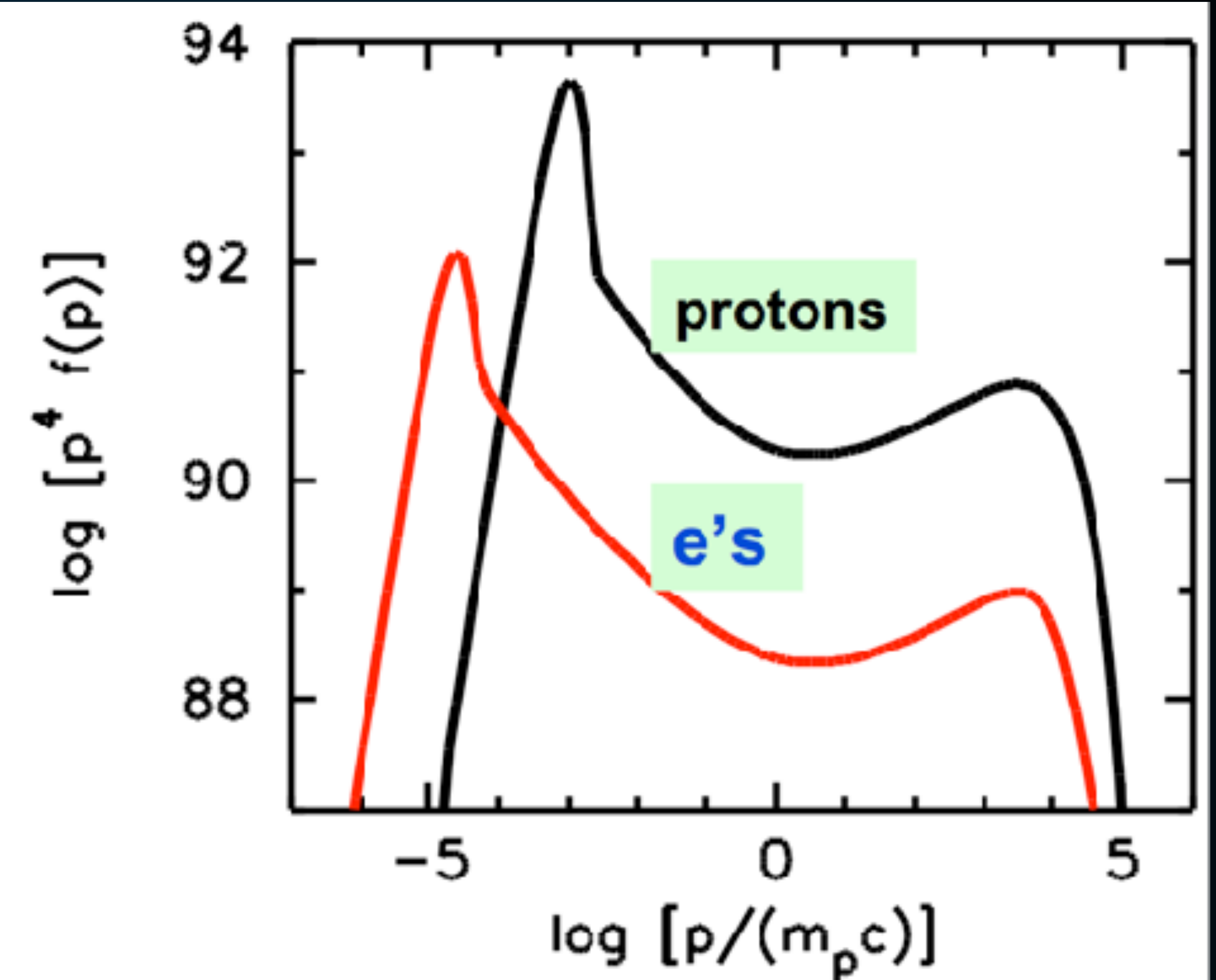

Spectra calculated with semi-analytic model of Blasi, Gabici & Vannoni 2005

- Observationally confirmed by X-Ray observations of SNR synchrotron and gamma-ray measurements of hadronic interactions.

LOCAL COSMIC-RAY OBSERVATIONS

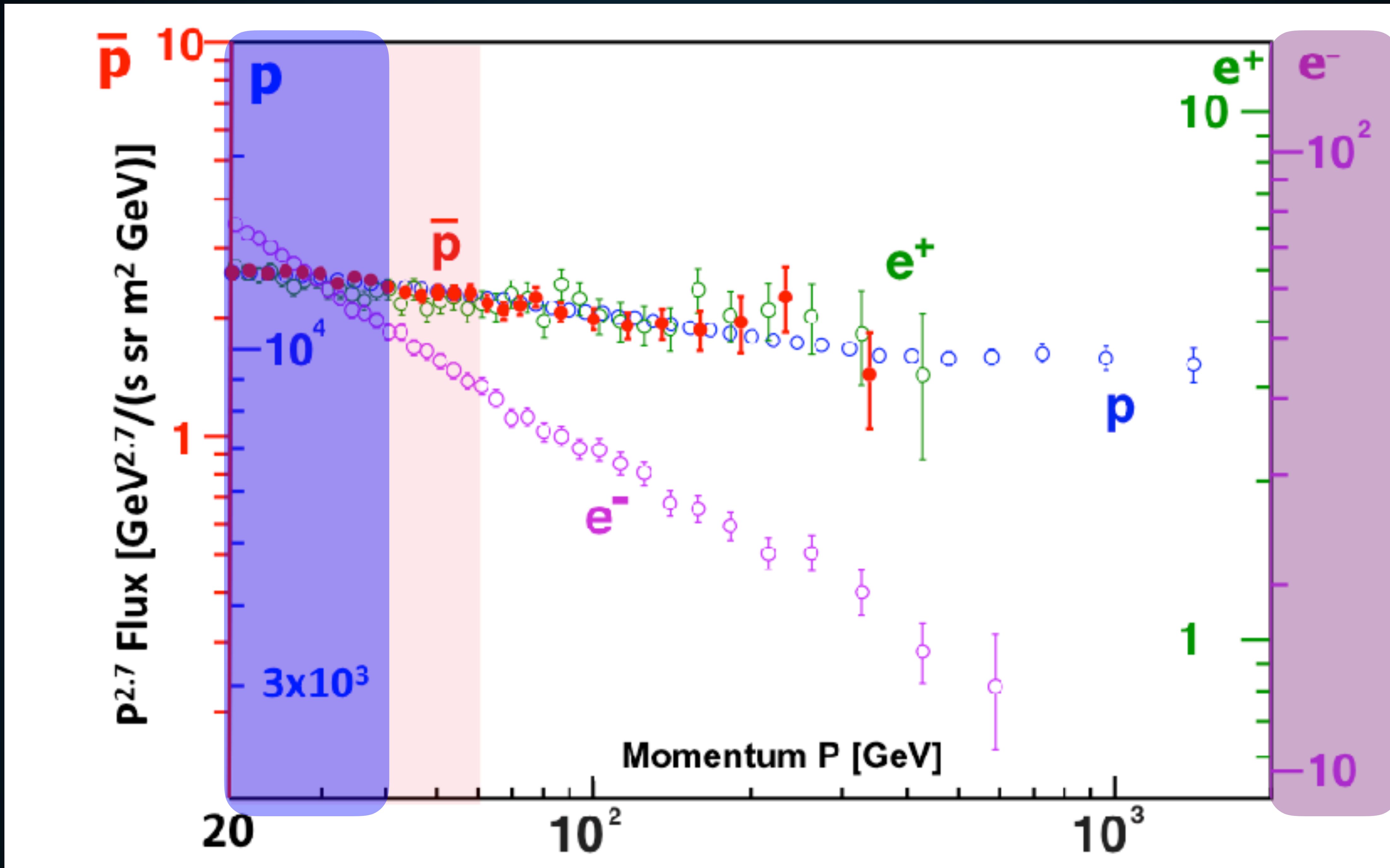

- Protons are approximately 2-3 orders of magnitude more prevalent near the solar position.

HADRONIC GAMMA RAYS

- Models of GeV galactic diffuse emission indicate that hadronic emission mechanisms are highlight dominant.
- Slightly less true at high energies - a hint!

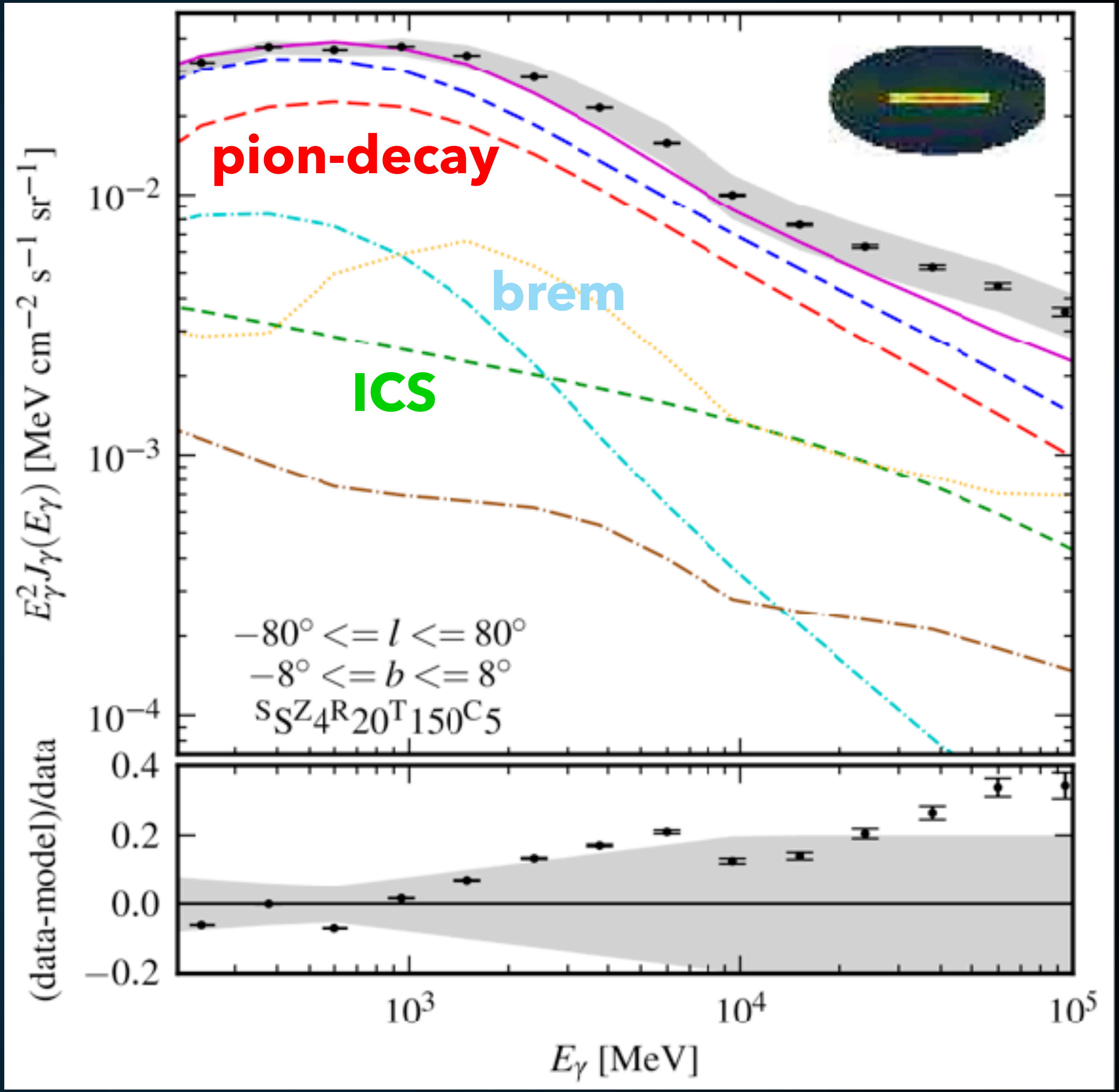

A NEW PICTURE

- In this talk, I will instead argue that electrons and positrons dominate the Milky Way's energetics at TeV energies:
  - 1.) Pulsars are responsible for the rising positron fraction observed by PAMELA/AMS-02
  - 2.) Pulsars produce the majority of the bright TeV sources observed by CTA/HAWC/HESS etc.
  - 3.) Pulsars produce the majority of the TeV gamma-ray emission observed from the Milky Way

A VERY SIMPLE MODEL OF PULSAR EMISSION

Pulsars as high-energy particle accelerators

PULSARS AS ASTROPHYSICAL ACCELERATORS

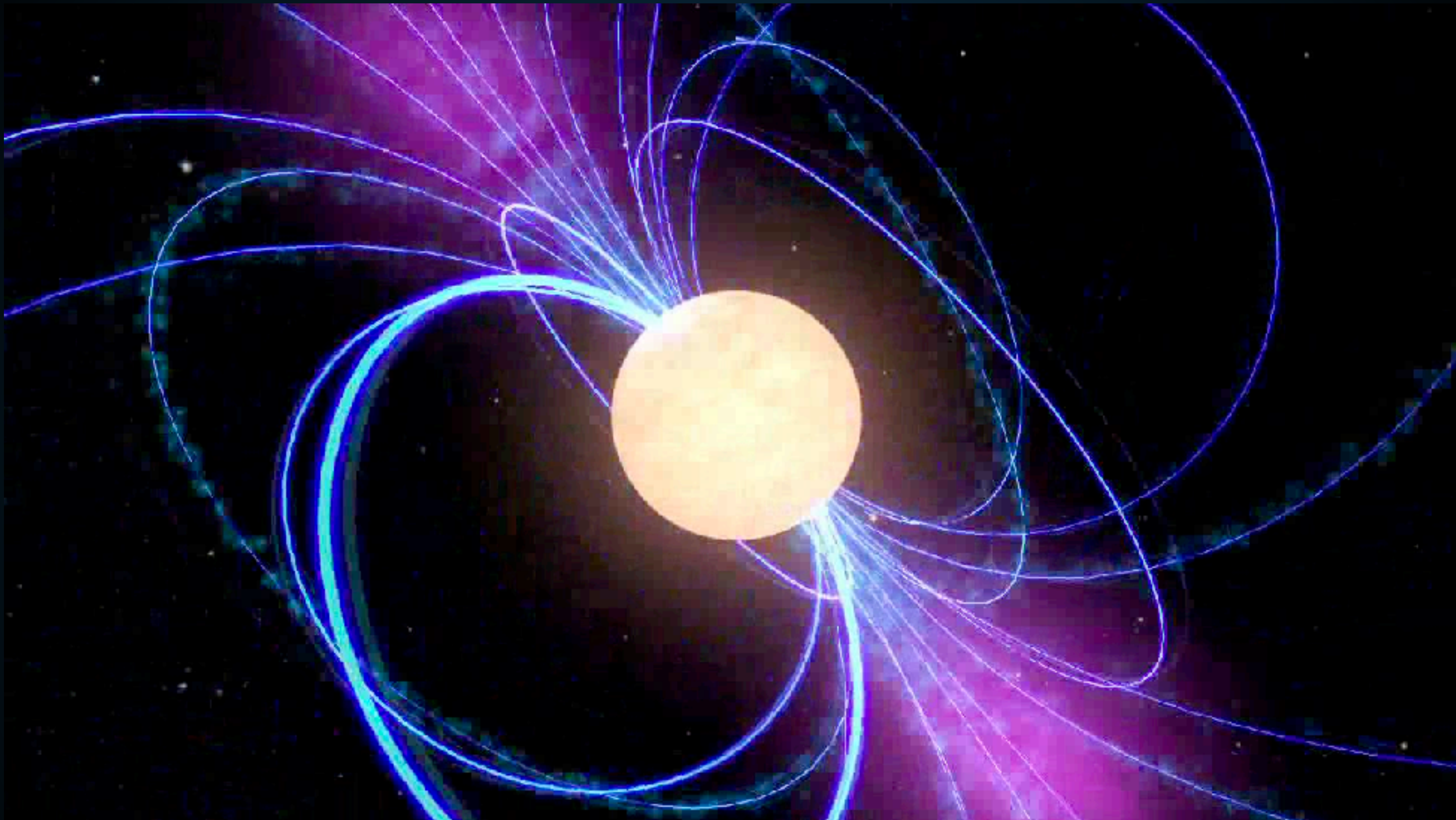

- **Rotational Kinetic Energy of the neutron star is the <u>ultimate power source</u> of all emission in this problem.**

PULSARS AS ASTROPHYSICAL ACCELERATORS

- radio beam
- gamma-ray beam
- e^+e^- acceleration in pulsar magnetosphere
- e^+e^- acceleration at termination shock

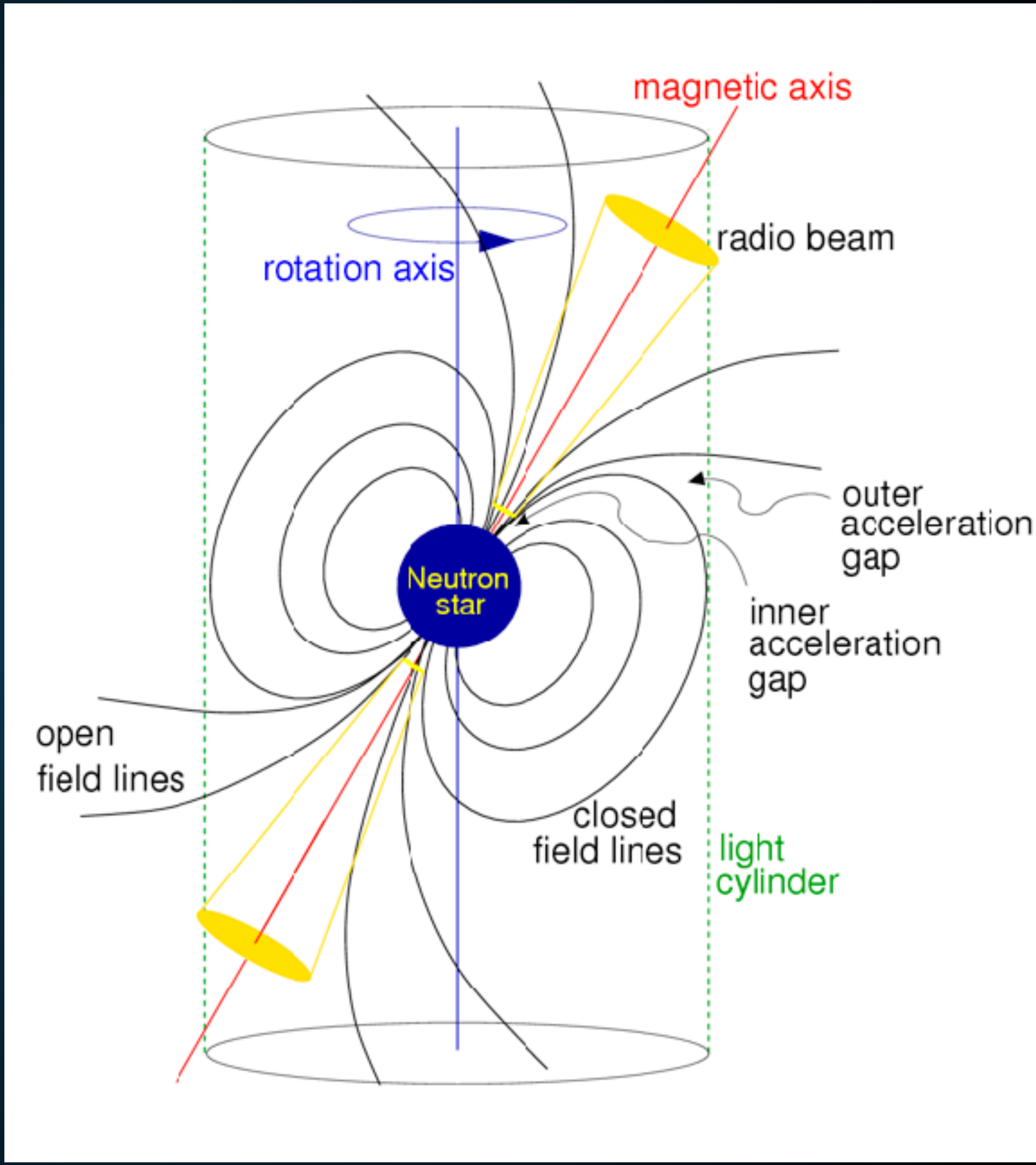

PRODUCTION OF ELECTRON AND POSITRON PAIRS

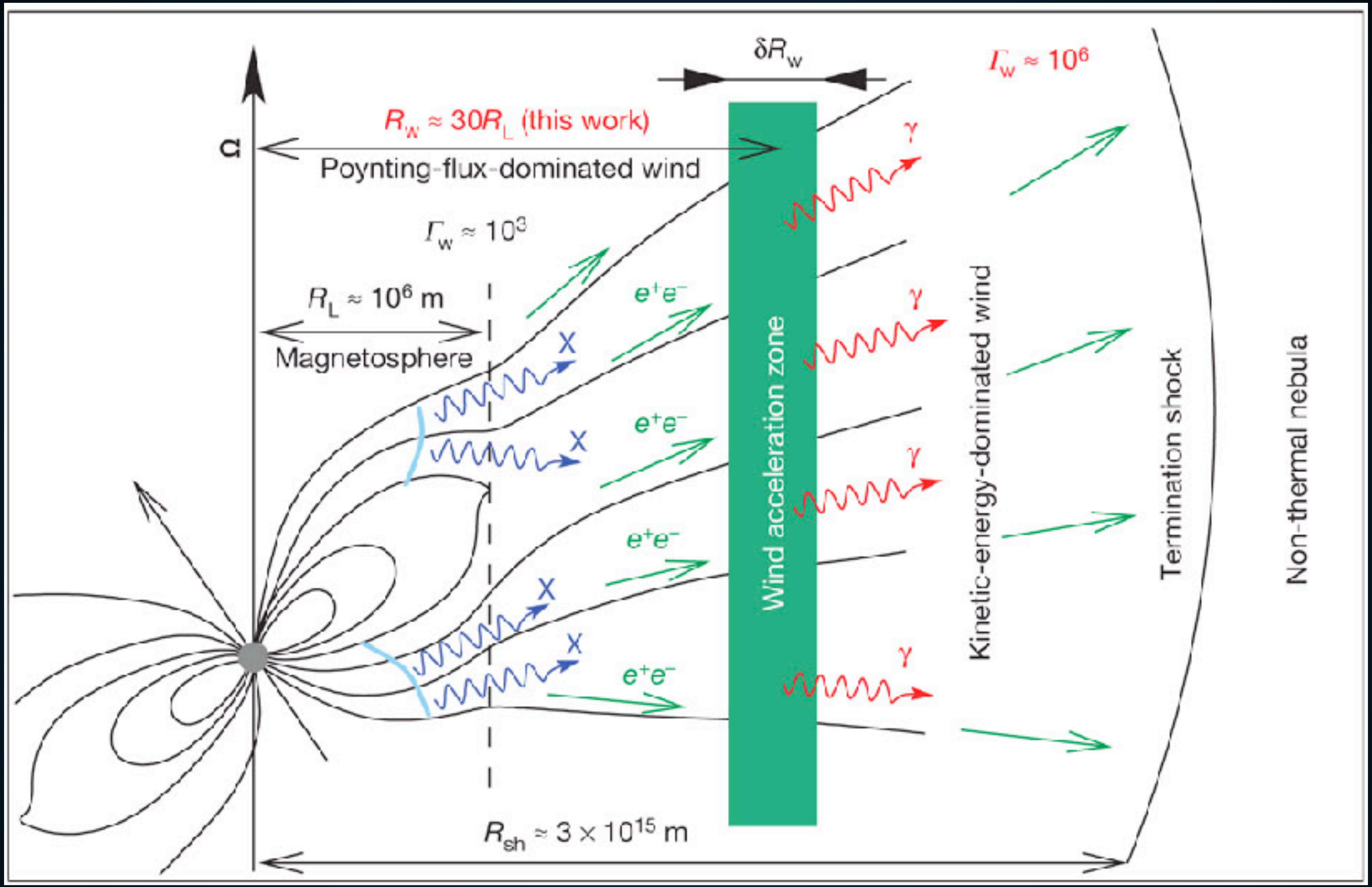

- **Electrons boiled off the pulsar surface produce e^+e^- pairs**
- **Pair multiplicity is high, but model dependent.**

PRODUCTION OF ELECTRON AND POSITRON PAIRS

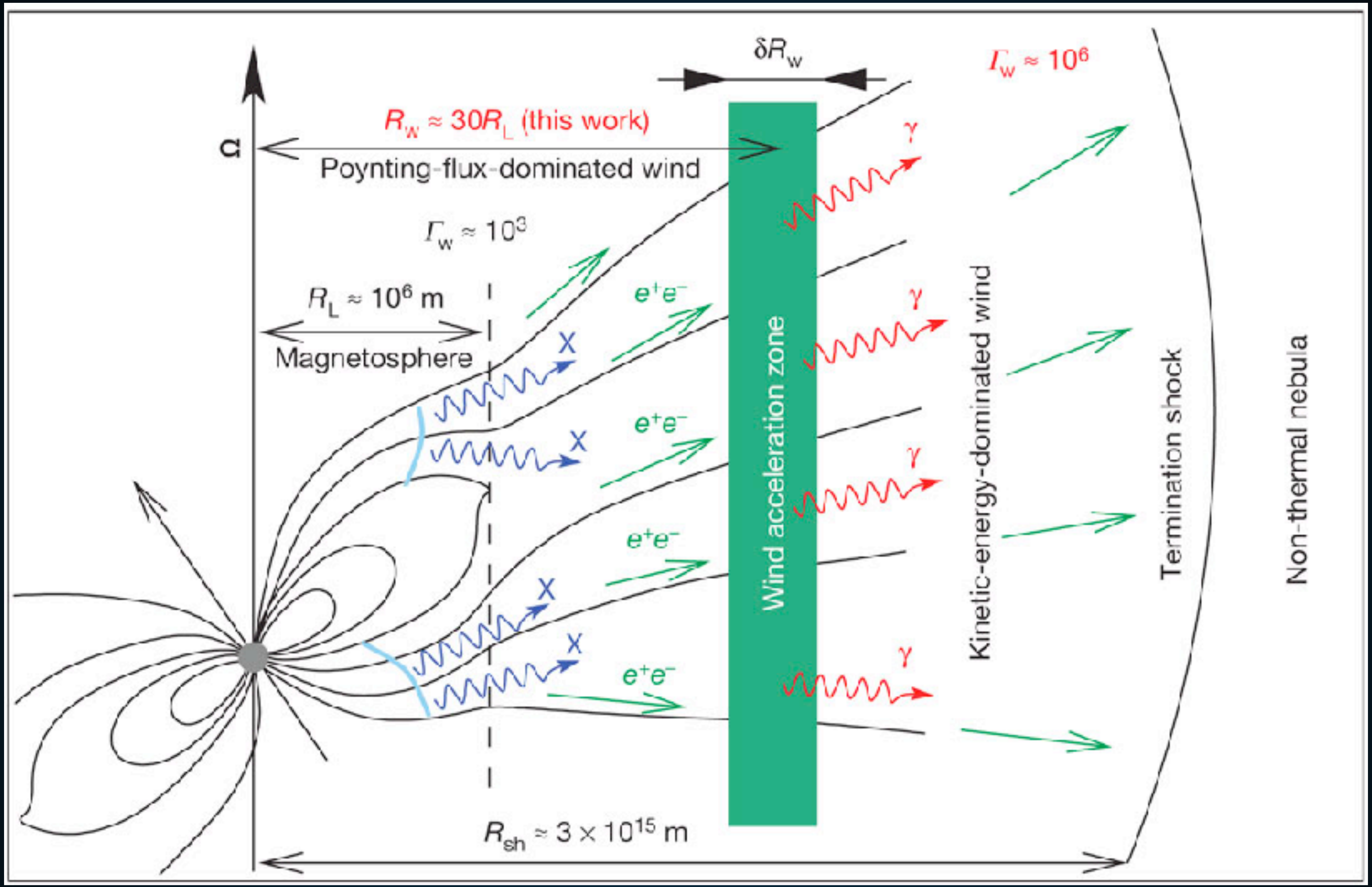

- Final e^+e^- spectrum is model dependent.
- Understanding this is important for MSPs.

REACCELERATION IN THE PULSAR WIND NEBULA

- PWN termination shock:
  - Voltage Drop > 30 PV
  - e^+e^- energy > 1 PeV (known from synchrotron)
- Resets e^+e^- spectrum.
- Many Possible Models:
  - 1st Order Fermi-Acceleration
  - Magnetic Reconnection
  - Shock-Driven Reconnection

IN THIS TALK

- **Will remain agnostic to source of relativistic e+e-**
- **Will assume a simple power-law spectrum with an exponential cutoff:**

$$\frac{dN}{dE} = E^{-\alpha} \exp(-E/E_{\mathrm{cut}})$$

1611.03496
astro-ph/0202232

LOW-ENERGY OBSERVATIONS OF PULSAR WIND NEBULAE

- **Extent of radio and X-Ray PWN is approximately 1 pc.**
- **Termination shock produced when ISM energy density overwhelms and stops the relativistic pulsar wind.**

$$R_{\rm PWN} \simeq 1.5 \left(\frac{\dot{E}}{10^{35}\,{\rm erg/s}}\right)^{1/2} \times \left(\frac{n_{\rm gas}}{1\,{\rm cm}^{-3}}\right)^{-1/2} \left(\frac{v}{100\,{\rm km/s}}\right)^{-3/2} {\rm pc}$$

- **NOTE: The radial extent of PWN is explained by a known physical mechanism.**

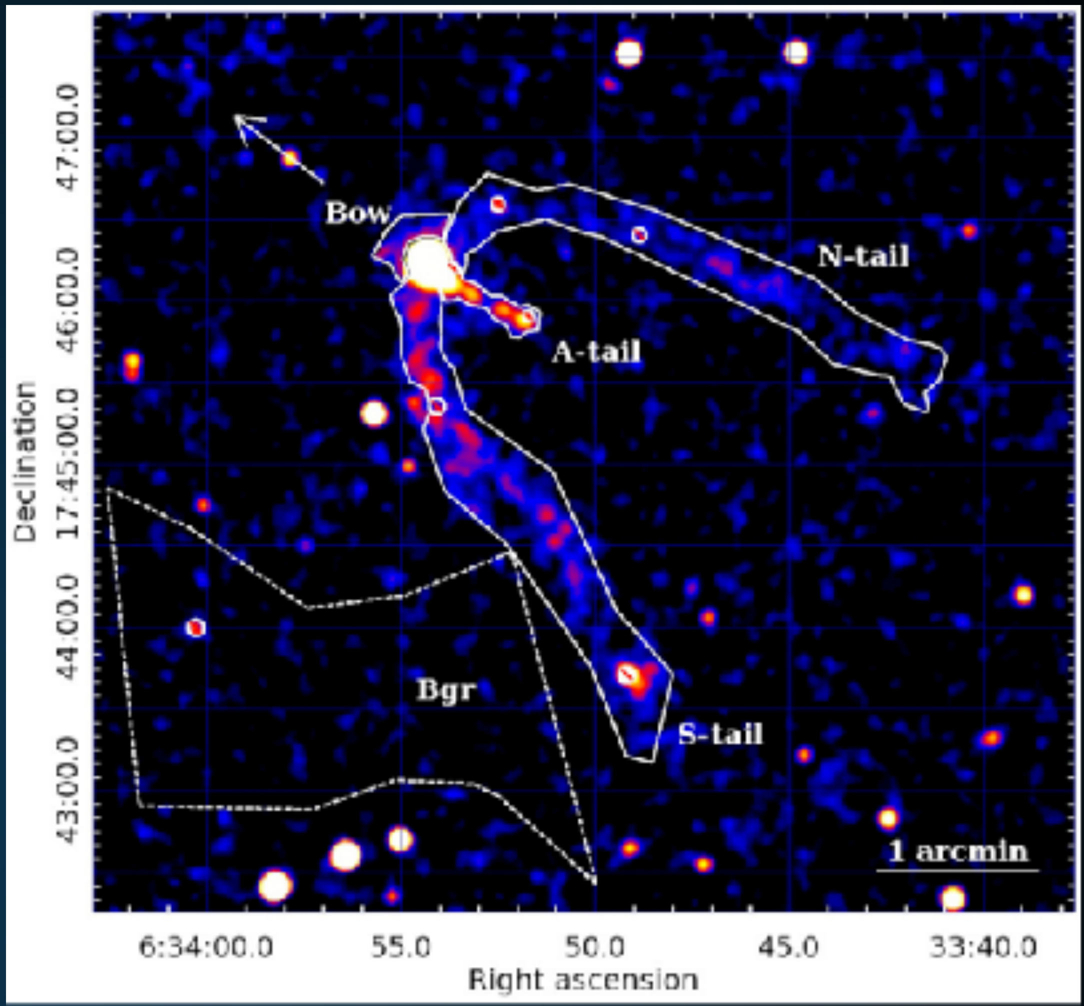

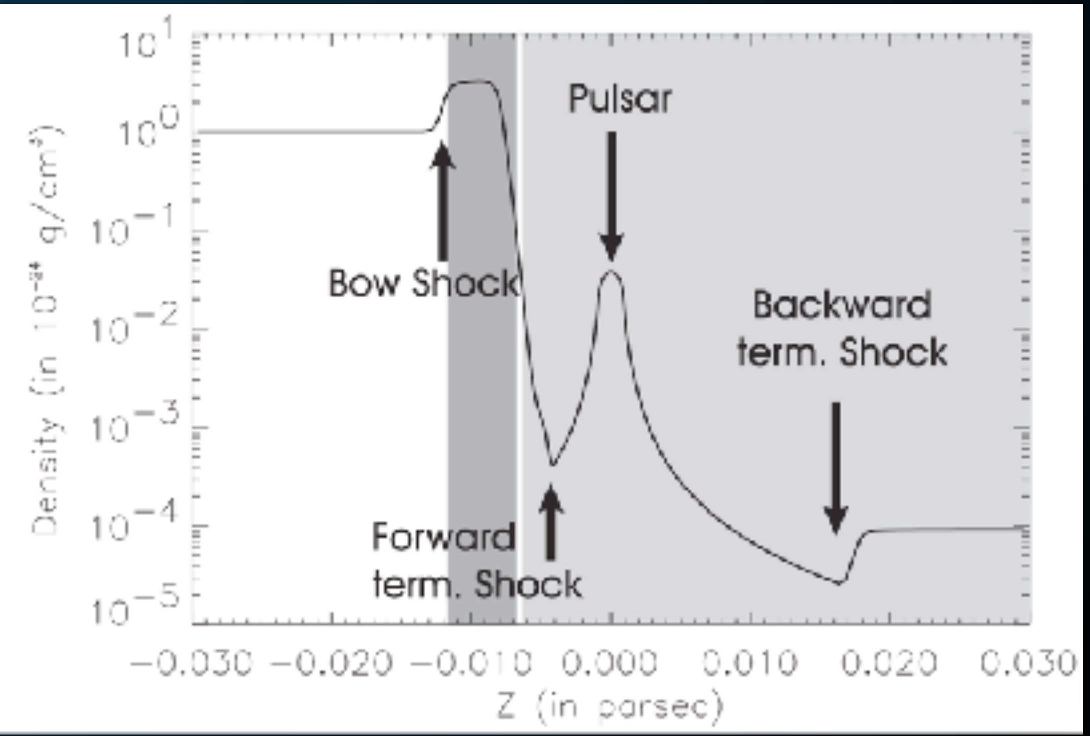

TeV observations inform pulsar models

TEV OBSERVATIONS OF PULSARS

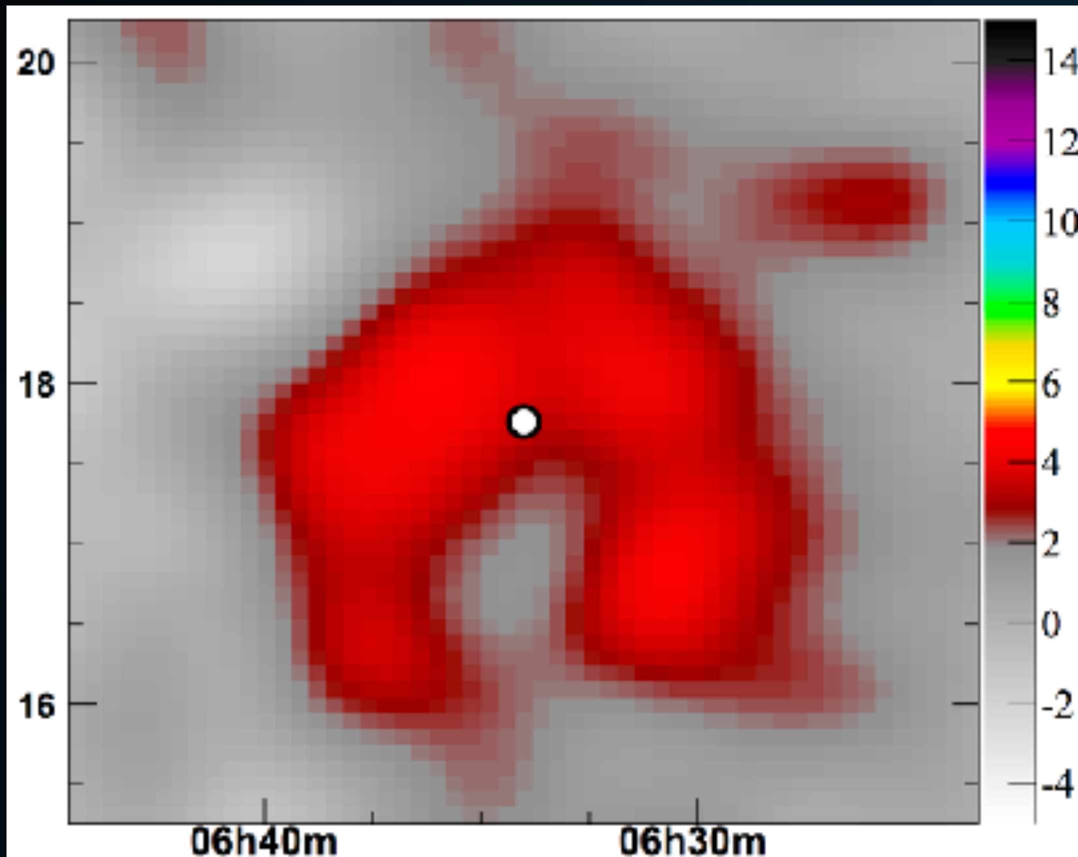

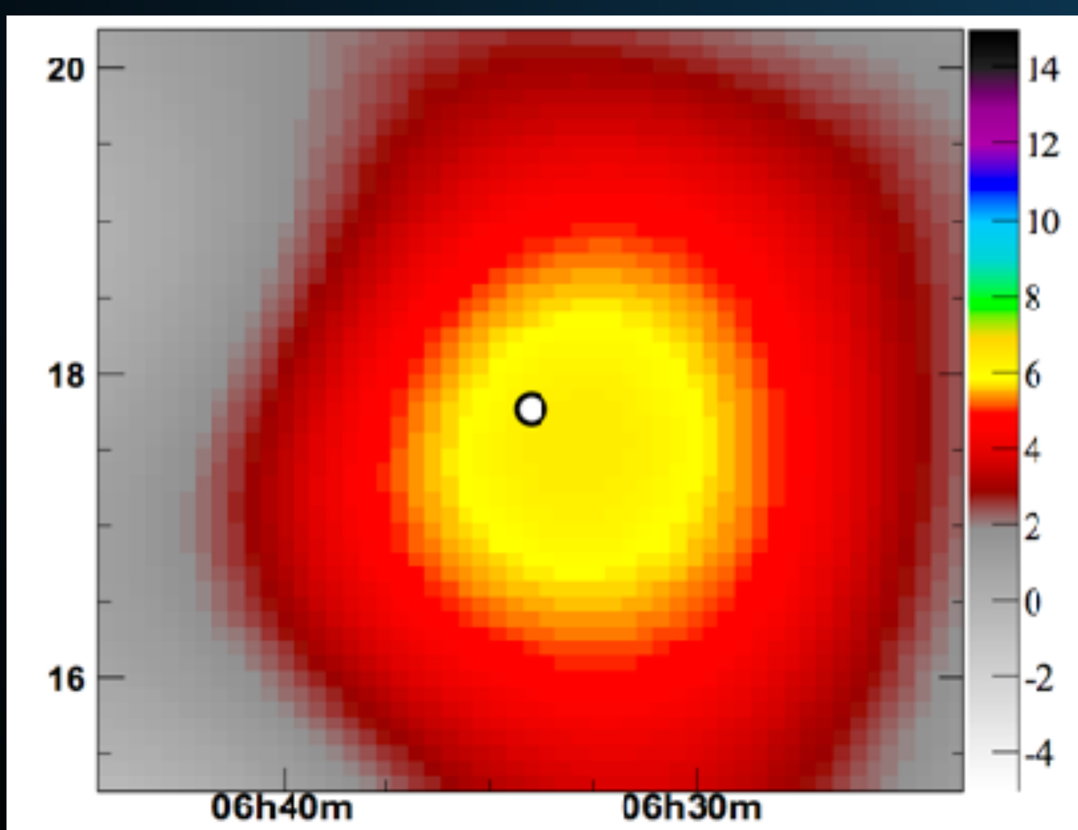

- Milagro observes very extended emission from Geminga ($2.6^{+0.7}_{-0.9}$°)
- Corresponds to ~10 pc assuming Geminga distance is 250 pc.
- Note: Large distance uncertainty on Geminga:
  - 250^{+230}_{-80} pc

HAWC OBSERVATIONS OF GEMINGA AND MONOGEM

Name	Tested radius [°]	Index	$F_7 \times 10^{15}$ [$\mathrm{TeV^{-1}cm^{-2}s^{-1}}$]	TeVCat
2HWC J0534+220	-	-2.58 ± 0.01	184.7 ± 2.4	Crab
2HWC J0631+169	-	-2.57 ± 0.15	6.7 ± 1.5	Geminga
"	2.0	-2.23 ± 0.08	48.7 ± 6.9	Geminga
2HWC J0635+180	-	-2.56 ± 0.16	6.5 ± 1.5	Geminga
2HWC J0700+143	1.0	-2.17 ± 0.16	13.8 ± 4.2	-
"	2.0	-2.03 ± 0.14	23.0 ± 7.3	-

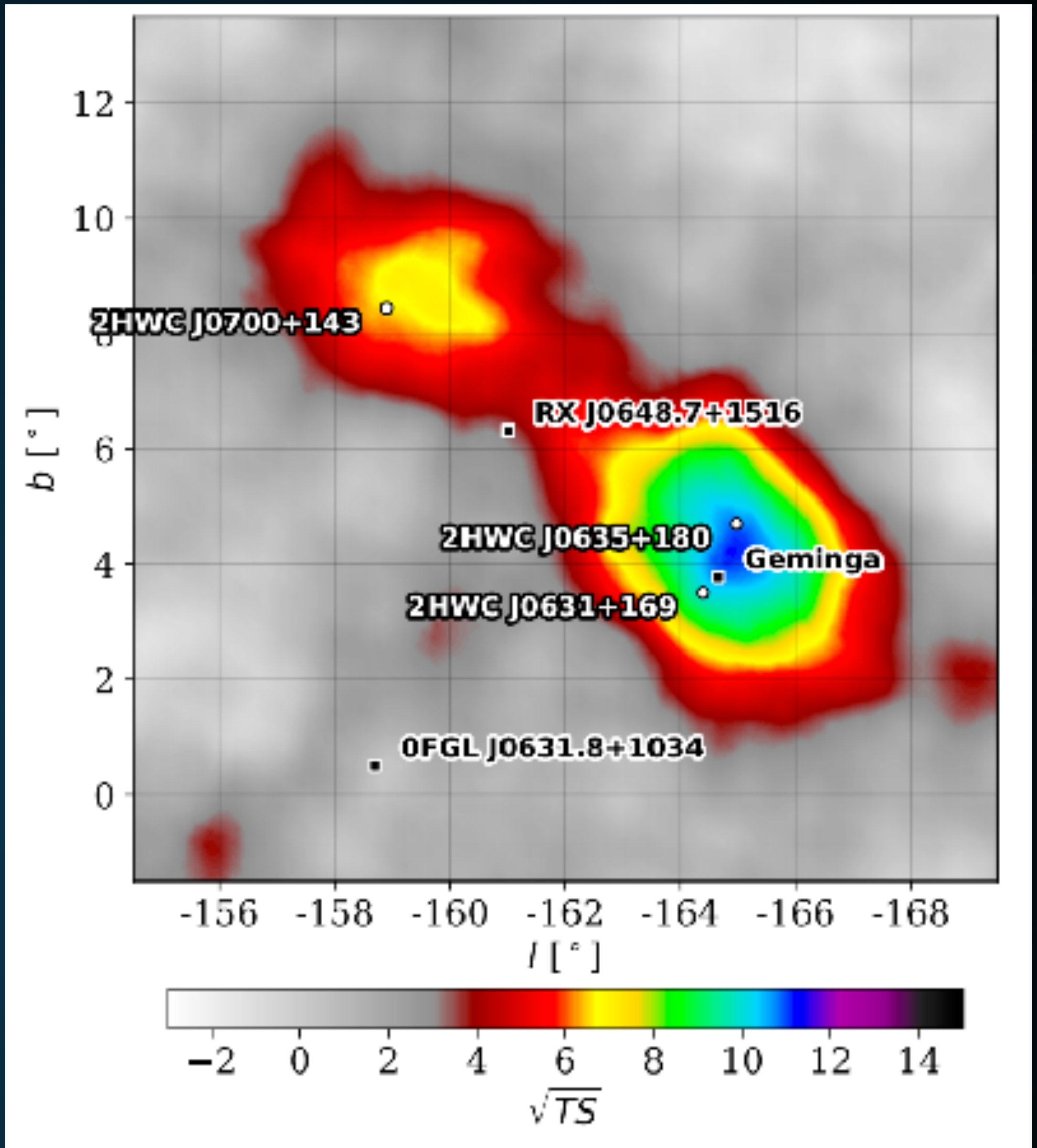

- HAWC confirms Geminga observation.
- Also sees Monogem at high significance and spatial extension.
- Spatial extension for both systems is ~2°.

1702.08280

Table 1 HGPS sources considered as firmly identified pulsar wind nebulae in this paper.

HGPS name	ATNF name	Canonical name	lg $\dot{E}$	τ_c (kyr)	d (kpc)	PSR offset (pc)	Γ	R_{PWN} (pc)	$L_{1-10\,TeV}$ (10^{33} erg s^{-1})
J1813−178[1]	J1813−1749		37.75	5.60	4.70	< 2	2.07 ± 0.05	4.0 ± 0.3	19.0 ± 1.5
J1833−105	J1833−1034	G21.5−0.9[2]	37.53	4.85	4.10	< 2	2.42 ± 0.19	< 4	2.6 ± 0.5
J1514−591	B1509−58	MSH 15−52[3]	37.23	1.56	4.40	< 4	2.26 ± 0.03	11.1 ± 2.0	52.1 ± 1.8
J1930+188	J1930+1852	G54.1+0.3[4]	37.08	2.89	7.00	< 10	2.6 ± 0.3	< 9	5.5 ± 1.8
J1420−607	J1420−6048	Kookaburra (K2)[5]	37.00	13.0	5.61	5.1 ± 1.2	2.20 ± 0.05	7.9 ± 0.6	44 ± 3
J1849−000	J1849−0001	IGR J18490−0000[6]	36.99	42.9	7.00	< 10	1.97 ± 0.09	11.0 ± 1.9	12 ± 2
J1846−029	J1846−0258	Kes 75[2]	36.91	0.728	5.80	< 2	2.41 ± 0.09	< 3	6.0 ± 0.7
J0835−455	B0833−45	Vela X[7]	36.84	11.3	0.280	2.37 ± 0.18	1.89 ± 0.03	2.9 ± 0.3	0.83 ± 0.11*
J1837−069[8]	J1838−0655		36.74	22.7	6.60	17 ± 3	2.54 ± 0.04	41 ± 4	204 ± 8
J1418−609	J1418−6058	Kookaburra (Rabbit)[5]	36.69	10.3	5.00	7.3 ± 1.5	2.26 ± 0.05	9.4 ± 0.9	31 ± 3
J1356−645[9]	J1357−6429		36.49	7.31	2.50	5.5 ± 1.4	2.20 ± 0.08	10.1 ± 0.9	14.7 ± 1.4
J1825−137[10]	B1823−13		36.45	21.4	3.93	33 ± 6	2.38 ± 0.03	32 ± 2	116 ± 4
J1119−614	J1119−6127	G292.2−0.5[11]	36.36	1.61	8.40	< 11	2.64 ± 0.12	14 ± 2	23 ± 4
J1303−631[12]	J1301−6305		36.23	11.0	6.65	20.5 ± 1.8	2.33 ± 0.02	20.6 ± 1.7	96 ± 5

- HESS finds a large population of "TeV PWN"
- HESS systems have a higher spin down power, but are more distant.

HESS OBSERVATIONS OF PULSAR WIND NEBULAE

1702.08280

Table 4 Candidate pulsar wind nebulae from the pre-selection.

HGPS name	ATNF name	$\lg \dot{E}$	τ_c (kyr)	d (kpc)	PSR offset (pc)	Γ	R_{PWN} (pc)	$L_{1-10\,\mathrm{TeV}}$ (10^{33} erg s^{-1})
J1616−508 (1)	J1617−5055	37.20	8.13	6.82	< 26	2.34 ± 0.06	28 ± 4	162 ± 9
J1023−575	J1023−5746	37.04	4.60	8.00	< 9	2.36 ± 0.05	23.2 ± 1.2	67 ± 5
J1809−193 (1)	J1811−1925	36.81	23.3	5.00	29 ± 7	2.38 ± 0.07	35 ± 4	53 ± 3
J1857+026	J1856+0245	36.66	20.6	9.01	21 ± 6	2.57 ± 0.06	41 ± 9	118 ± 13
J1640−465	J1640−4631 (1)	36.64	3.35	12.8	< 20	2.55 ± 0.04	25 ± 8	210 ± 12
J1641−462	J1640−4631 (2)	36.64	3.35	12.8	50 ± 5	2.50 ± 0.11	< 14	17 ± 4
J1708−443	B1706−44	36.53	17.5	2.60	17 ± 3	2.17 ± 0.08	12.7 ± 1.4	6.6 ± 0.9
J1908+063	J1907+0602	36.45	19.5	3.21	21 ± 3	2.26 ± 0.06	27.2 ± 1.5	28 ± 2
J1018−589A	J1016−5857 (1)	36.41	21.0	8.00	47.5 ± 1.6	2.24 ± 0.13	< 4	8.1 ± 1.4
J1018−589B	J1016−5857 (2)	36.41	21.0	8.00	25 ± 7	2.20 ± 0.09	21 ± 4	23 ± 5
J1804−216	B1800−21	36.34	15.8	4.40	18 ± 5	2.69 ± 0.04	19 ± 3	42.5 ± 2.0
J1809−193 (2)	J1809−1917	36.26	51.3	3.55	< 17	2.38 ± 0.07	25 ± 3	26.9 ± 1.5
J1616−508 (2)	B1610−50	36.20	7.42	7.94	60 ± 7	2.34 ± 0.06	32 ± 5	220 ± 12
J1718−385	J1718−3825	36.11	89.5	3.60	5.4 ± 1.6	1.77 ± 0.06	7.2 ± 0.9	4.6 ± 0.8
J1026−582	J1028−5819	35.92	90.0	2.33	9 ± 2	1.81 ± 0.10	5.3 ± 1.6	1.7 ± 0.5
J1832−085	B1830−08 (1)	35.76	147	4.50	23.3 ± 1.5	2.38 ± 0.14	< 4	1.7 ± 0.4
J1834−087	B1830−08 (2)	35.76	147	4.50	32.3 ± 1.9	2.61 ± 0.07	17 ± 3	25.8 ± 2.0
J1858+020	J1857+0143	35.65	71.0	5.75	38 ± 3	2.39 ± 0.12	7.9 ± 1.6	7.1 ± 1.5
J1745−303	B1742−30 (1)	33.93	546	0.200	1.42 ± 0.15	2.57 ± 0.06	0.62 ± 0.07	0.014 ± 0.003
J1746−308	B1742−30 (2)	33.93	546	0.200	< 1.1	3.3 ± 0.2	0.56 ± 0.12	0.009 ± 0.003

- HESS finds a large population of “TeV PWN”
- HESS systems have a higher spin down power, but are more distant.

SPATIAL EXTENSION OF “TEV PWN”

1702.08280

- **TeV PWN are much larger.**
- **Particularly true in low-energy systems.**

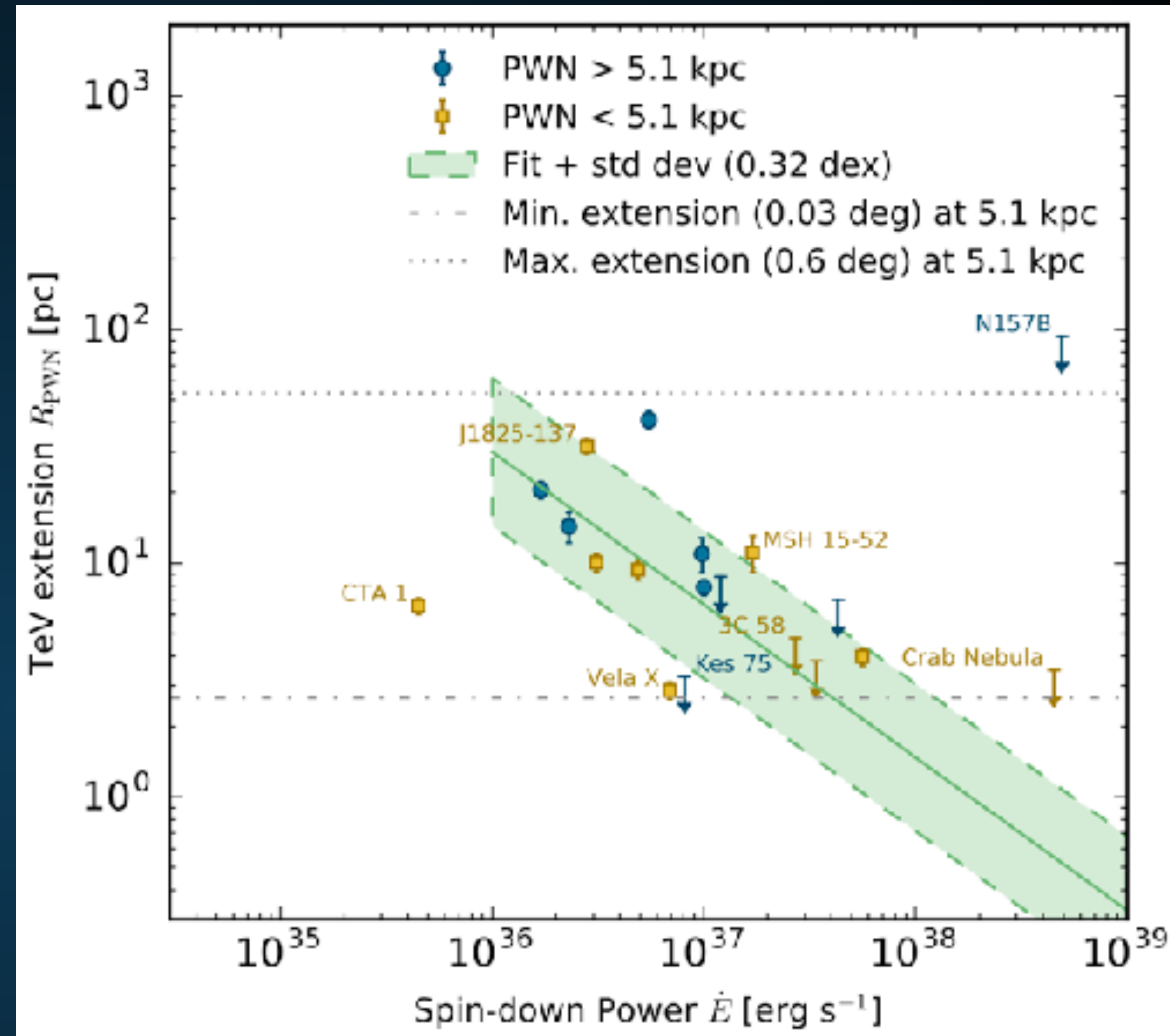

NOTE: This has the opposite energy dependence as the X-Ray PWN.

$$R_{\rm PWN} \simeq 1.5 \left(\frac{\dot{E}}{10^{35}\,{\rm erg/s}}\right)^{1/2} \times \left(\frac{n_{\rm gas}}{1\,{\rm cm}^{-3}}\right)^{-1/2} \left(\frac{v}{100\,{\rm km/s}}\right)^{-3/2} {\rm pc}$$

TEV HALOS

- TeV halos are a new feature
  - 3 orders of magnitude larger than PWN in volume
  - Opposite energy dependence

- PWN are morphologically connected to the physics of the termination shock

- TeV halos need a similar morphological description.

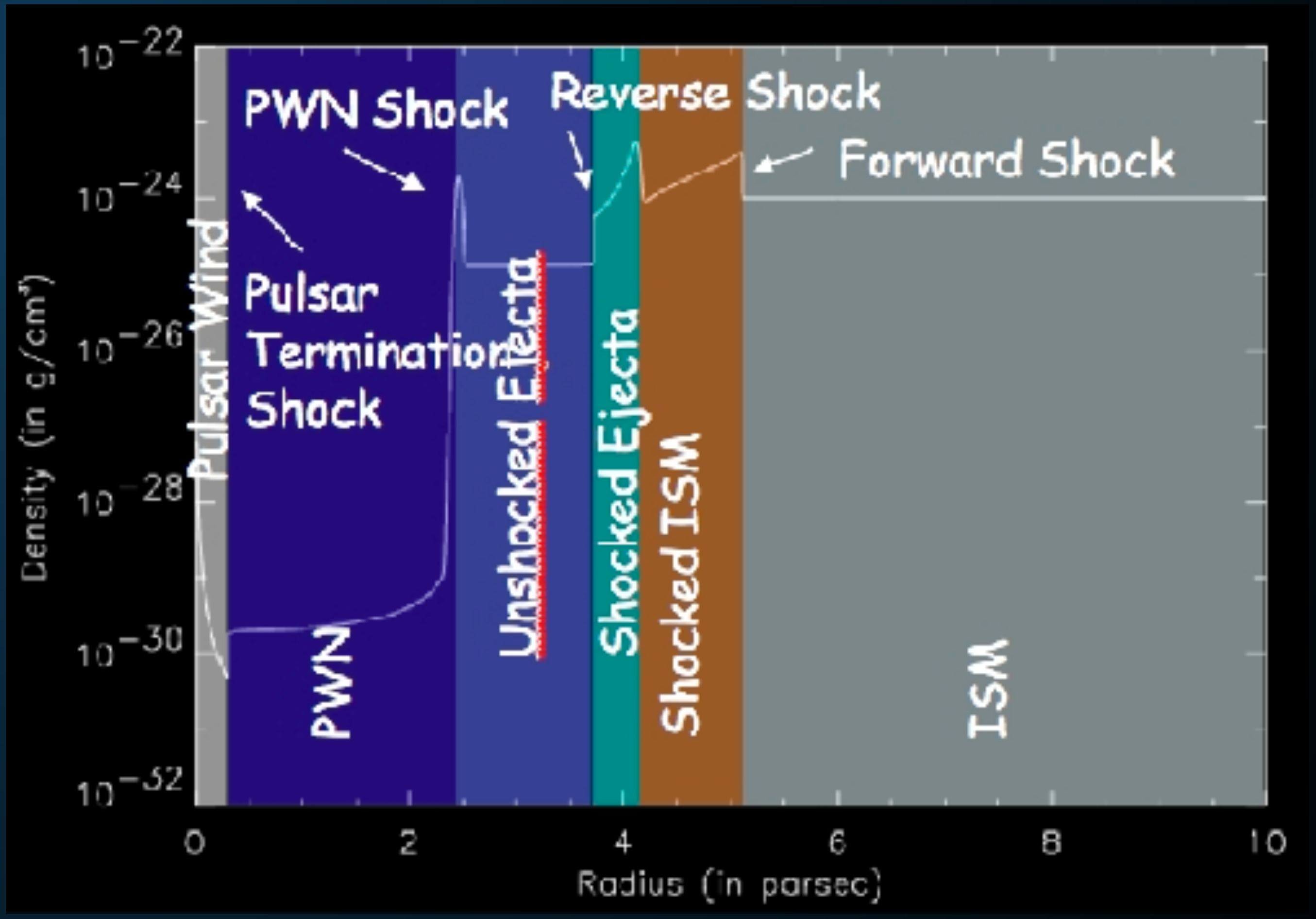

AN ALTERNATIVE EXPLANATION

- Maybe TeV electrons propagate farther?
- Energy loss time-scale: E^{-1}.
- Propagation Distance in t: $E^{0.16}$.
- Size of Halo: $E^{-0.33}$.
- Moving from PeV to ~50 TeV electrons leads to 10x larger radius.

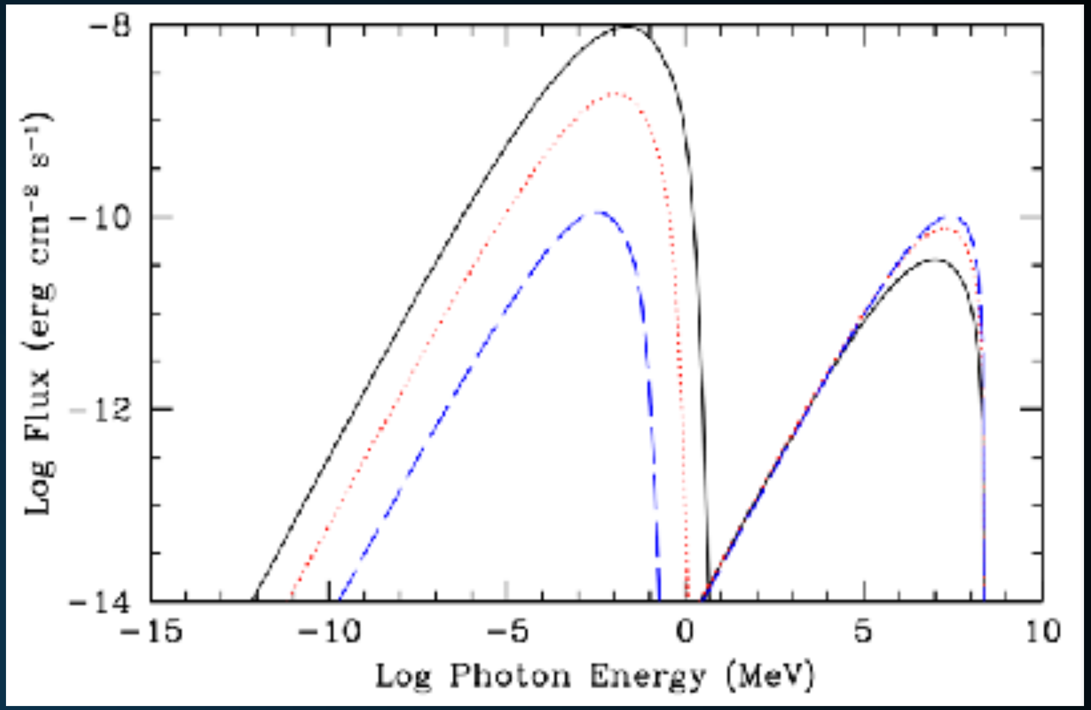

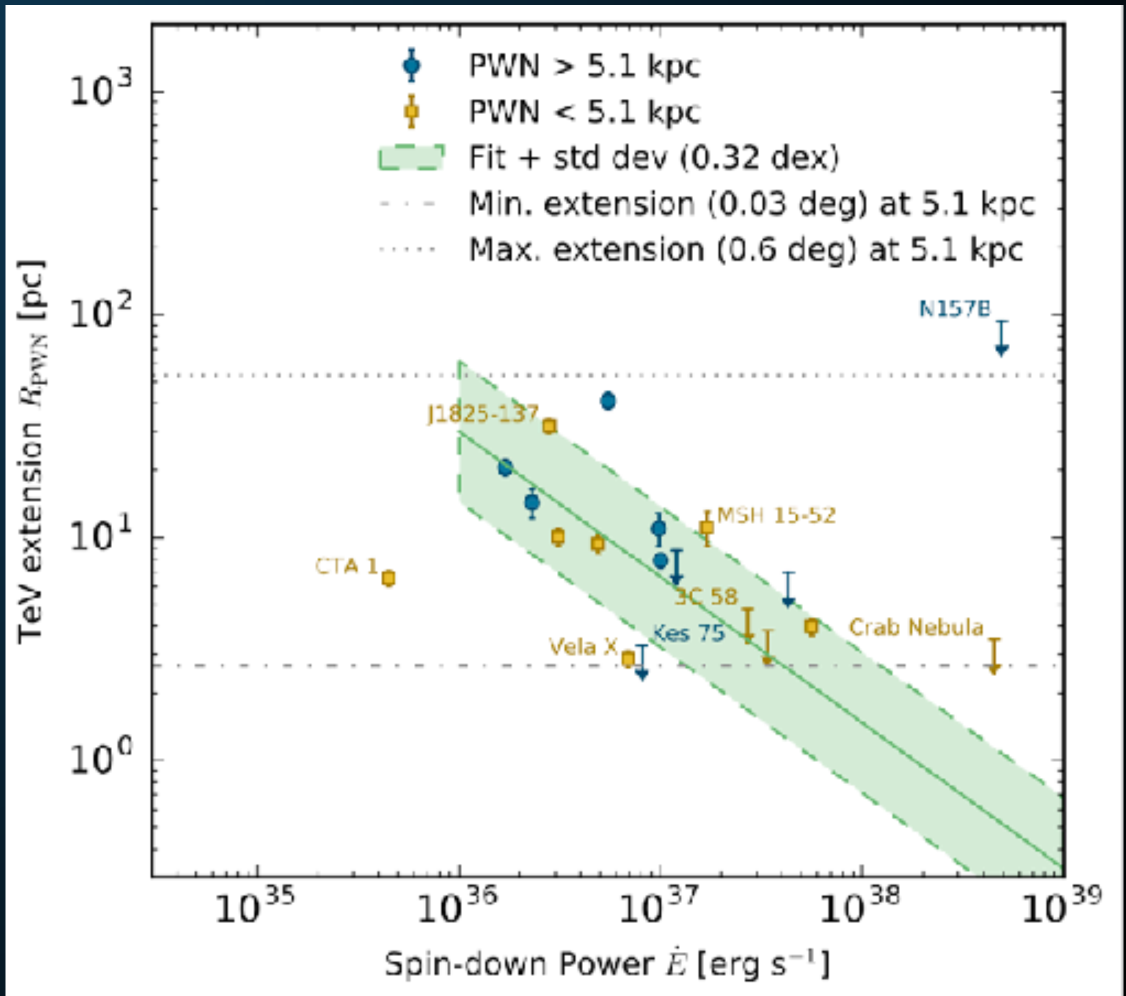

GEMINGA - A TEMPLATE FOR TEV HALOS

- Will now use Geminga as a standard template for TeV halos.
    - Bright (nearby)
    - High latitude (low background)
    - Middle-Aged (no associated SNR)
- Would get same (actually slightly better) results if we used Monogem.

INVERSE COMPTON SCATTERING WITH THE ISM

- **It is not energetically possible for Geminga to produce the magnetic field or ISRF that these electrons interact with.**

$$U = \frac{1}{8\pi} B^2 = \frac{(10\mu G)^2}{8\pi}$$
$$= 4\times10^{-12} \frac{erg}{cm^3}$$
$$\int_0^{10pc} U\, dV = 5\times10^{47}\, erg$$
$$\hookrightarrow \text{Magnetic Flux} \simeq 5\times10^{38} \frac{erg}{s}$$

$$ISRF = 1 \frac{eV}{cm^3}$$
$$\int ISRF\, dV = 8\times10^{47}\, erg$$
$$\hookrightarrow \text{Flux} = 8\times10^{38} \frac{erg}{s}$$

- **We can use typical ISM values (5 μG; 1 eV cm^{-3}) to characterize interactions.**

- **Nearly equal energy to synchrotron and ICS.**

TWO CONTRASTING OBSERVABLES

Geminga is Bright

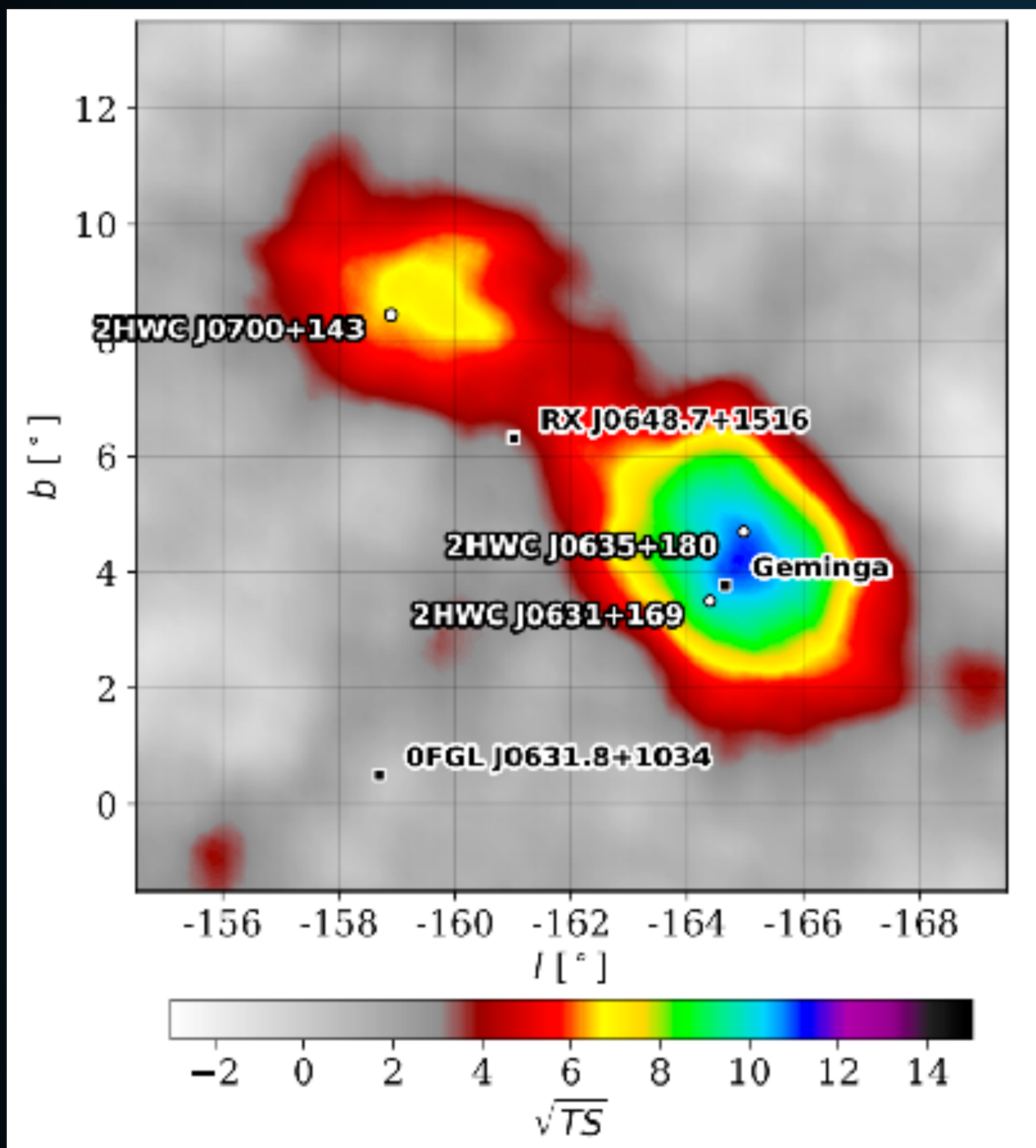

Indicative of significant electron cooling

Geminga has a hard-spectrum

Name	Tested radius	Index	$F_\gamma \times 10^{15}$	TeVCat
	[°]		[TeV^{-1}cm^{-2}s^{-1}]	
2HWC J0631+169	-	-2.57 ± 0.15	6.7 ± 1.5	Geminga
"	2.0	-2.23 ± 0.08	48.7 ± 6.9	Geminga
2HWC J0635+180	-	-2.56 ± 0.16	6.5 ± 1.5	Geminga

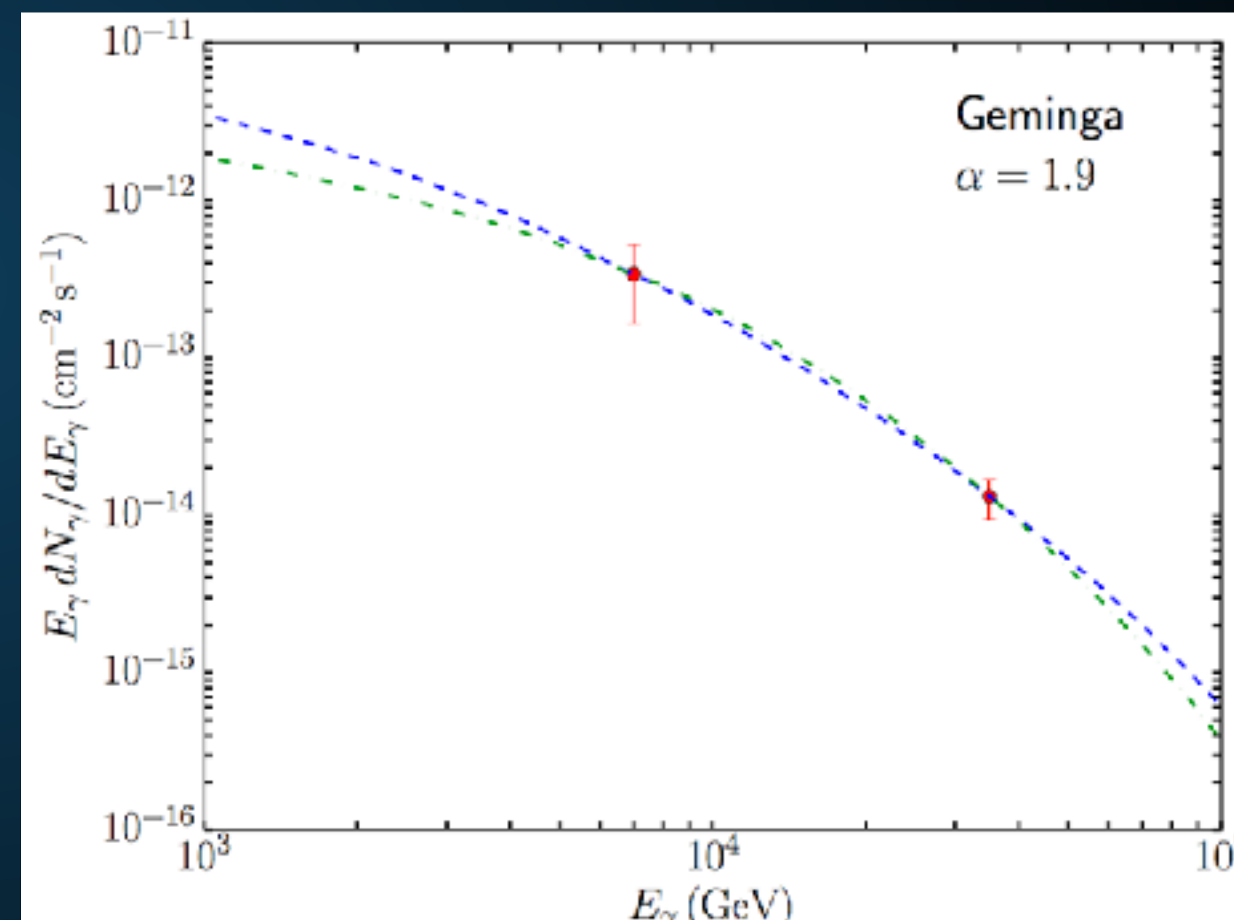

Indicative of minimal electron cooling

TOTAL POWER OF TEV HALOS

- **Measured Geminga flux translates to an intensity:**

2.86×10^{31} erg s^{-1} at 7 TeV

- **For the best-fit spectrum, this requires an e^+e^- injection:**

3.8×10^{33} erg s^{-1}

- **Total Spindown Power of Geminga is:**

3.4×10^{34} erg s^{-1}

- **Roughly 10% conversion efficiency to e^+e^- !**

COSMIC-RAY DIFFUSION IN A TEV HALO

- **Energy constraints demand that ~30 TeV electrons lose the majority of their energy before exiting TeV halo.**

$$\tau = 3.1 \times 10^{4}\,\text{yr} \left(\frac{E_e}{10\,\text{TeV}}\right)^{-1}$$

- **This strongly constrains the efficiency of particle propagation near the halo.**

$$D = \frac{L^2}{6\tau} = \frac{(10\,\text{pc})^2}{6(3.1\times10^{4}\,\text{yr})} = \frac{(3.08\times10^{19}\,\text{cm})^2}{5.86\times10^{12}\,\text{s}}$$

$$\boxed{D = 1.6\times10^{26}\,\frac{\text{cm}^2}{\text{s}}}$$

- **Provides strong evidence for new morphological feature.**

COSMIC-RAY DIFFUSION IN A TEV HALO

- Actual source of particle propagation is unknown:
  - Diffusion
  - Advection

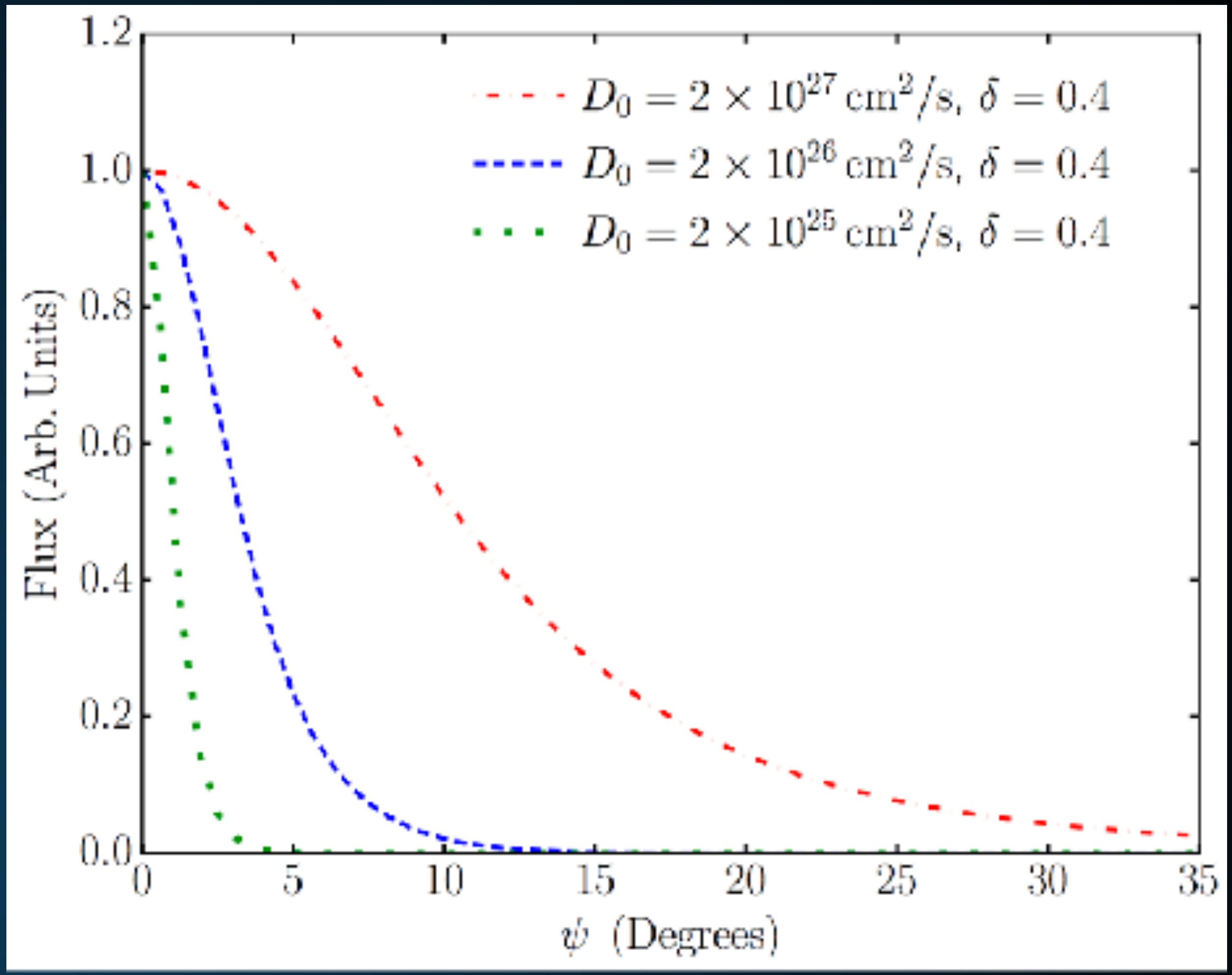

- **Particle propagation near pulsars must be orders of magnitude less efficient than typical for the ISM.**
- **Continues far outside the termination shock of a pulsar with no SNR.**

- **Geminga has a hard gamma-ray spectrum**

Name	Tested radius [°]	Index	$F_7 \times 10^{15}$ [$\mathrm{TeV^{-1}cm^{-2}s^{-1}}$]	TeVCat
2HWC J0631+169	-	-2.57 ± 0.15	6.7 ± 1.5	Geminga
"	2.0	-2.23 ± 0.08	48.7 ± 6.9	Geminga
2HWC J0635+180	-	-2.56 ± 0.16	6.5 ± 1.5	Geminga

- **Electrons cannot be completely cooled, or else gamma-ray spectrum would be too soft (Klein-Nishina effects)**
- **Combined with Milagro observation at 30 TeV, this requires:**
  - **$-1.9 < \alpha < -1.5$**
  - **$E_{cut} \cong 50$ TeV**

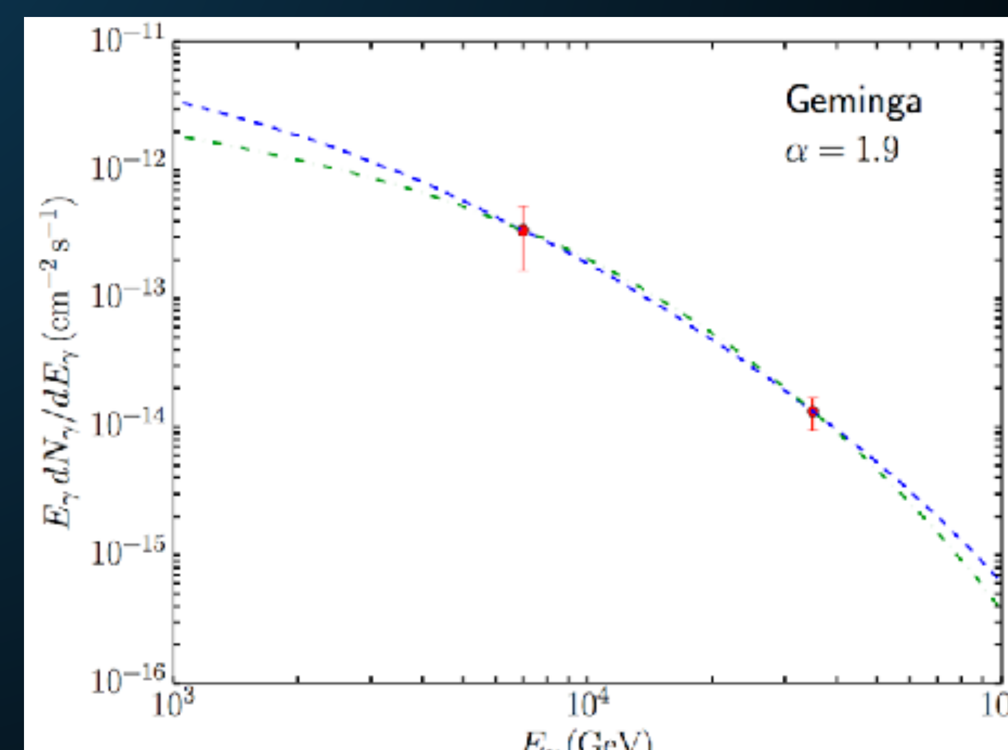

WHAT ABOUT THE LOW-ENERGY ELECTRONS?

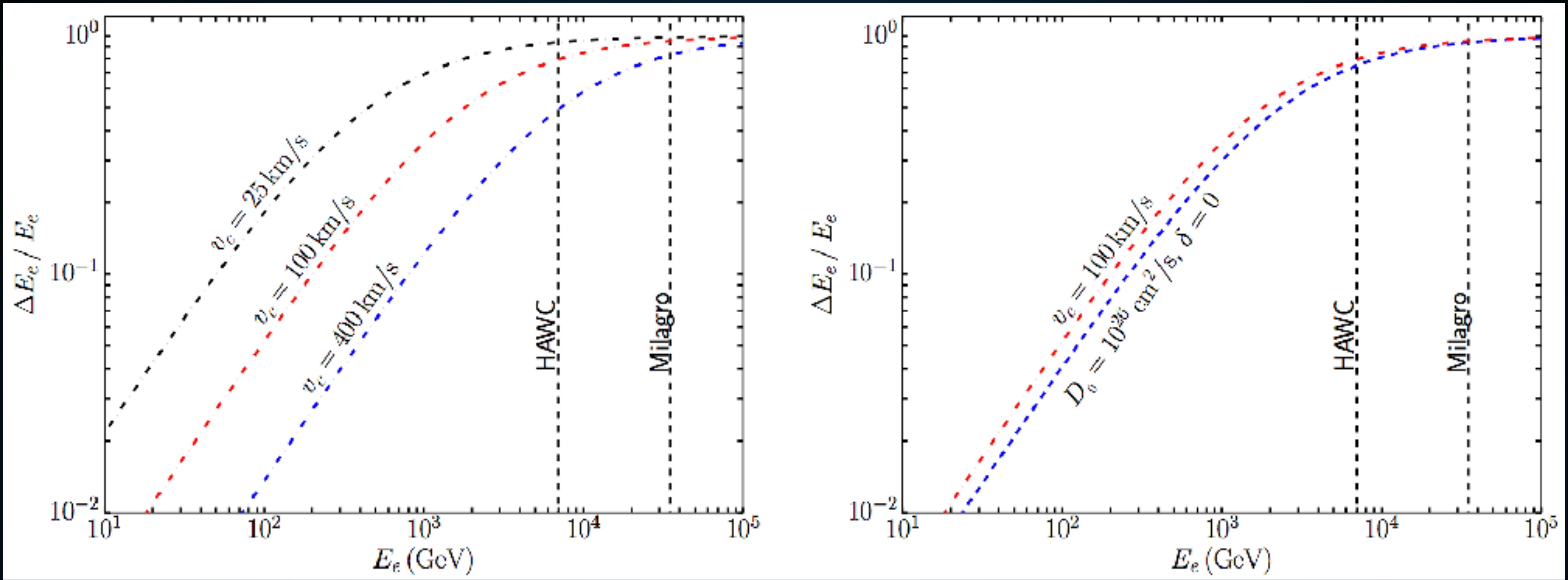

- Low-energy electrons lose energy slower, must escape.
- This is true in both convective and most diffusive (Kolmogorov, Kraichnian) scenarios.

BOHMIAN DIFFUSION

$$\tau_{Diff} \propto \frac{L^2}{D_0 E^{\delta}} \qquad \tau_{loss} \propto E^{-1}$$

$$\left(\frac{\Delta E}{E}\right) \tilde{\propto} \frac{\tau_{Diff}}{\tau_{loss}} \propto E^{1-\delta}$$

- **More generically, low-energy electrons can only be confined if the diffusion is Bohmian (diffusion coefficient scales as E^1.)**

GEMINGA SPECTRUM INDICATIVE OF CONVECTION

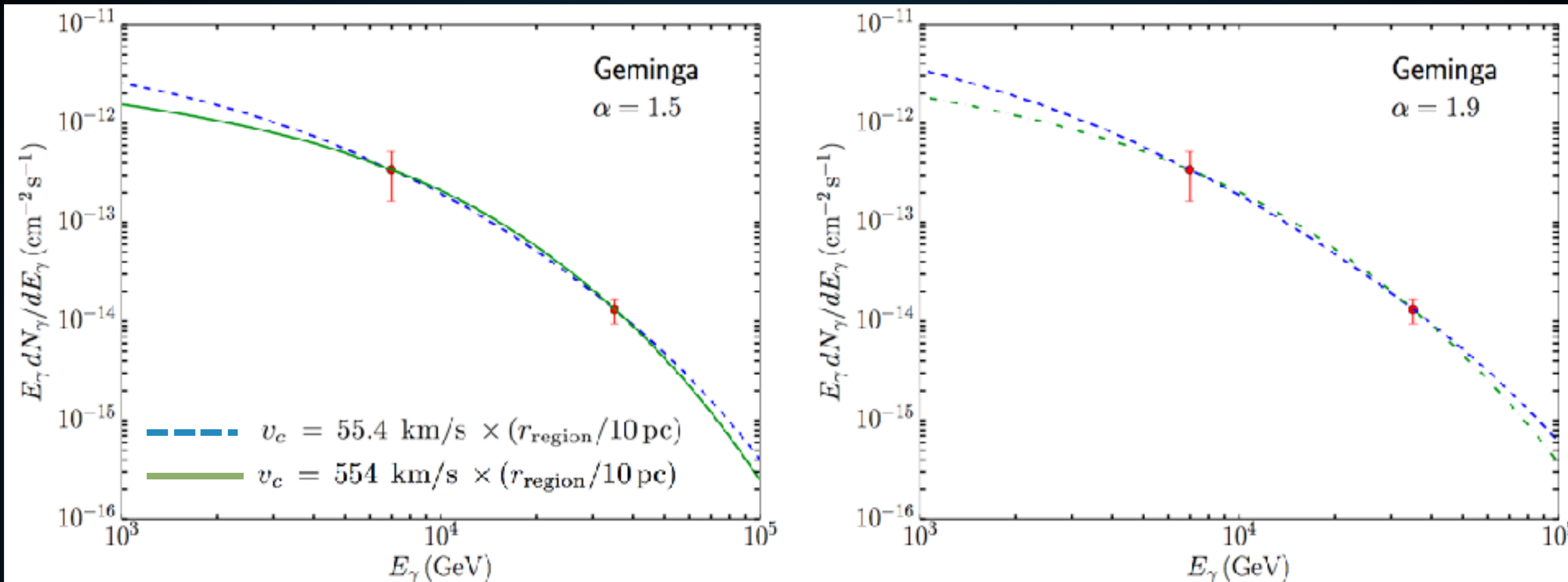

- **However, Bohmian diffusion is incompatible with the gamma-ray spectrum.**
- **If low-energy electrons are cooled, the spectrum at 7 TeV should be significantly softer.**

AN UPPER LIMIT ON THE TEV HALO SIZE

- These arguments only set a lower limit on the TeV halo size.
- What if TeV halos are much larger, but the TeV electrons die at ~10 pc?
- Will need to answer this question on the population level.

A GLOBAL FOCUS

- **New Assumption: Geminga is typical of a 100-400 kyr pulsar.**

- **Two Nearest Systems Observed: Geminga, Monogem**

- **Indications of many similar HESS sources.**

EFFECT OF TEV HALOS ON ISM PROPAGATION

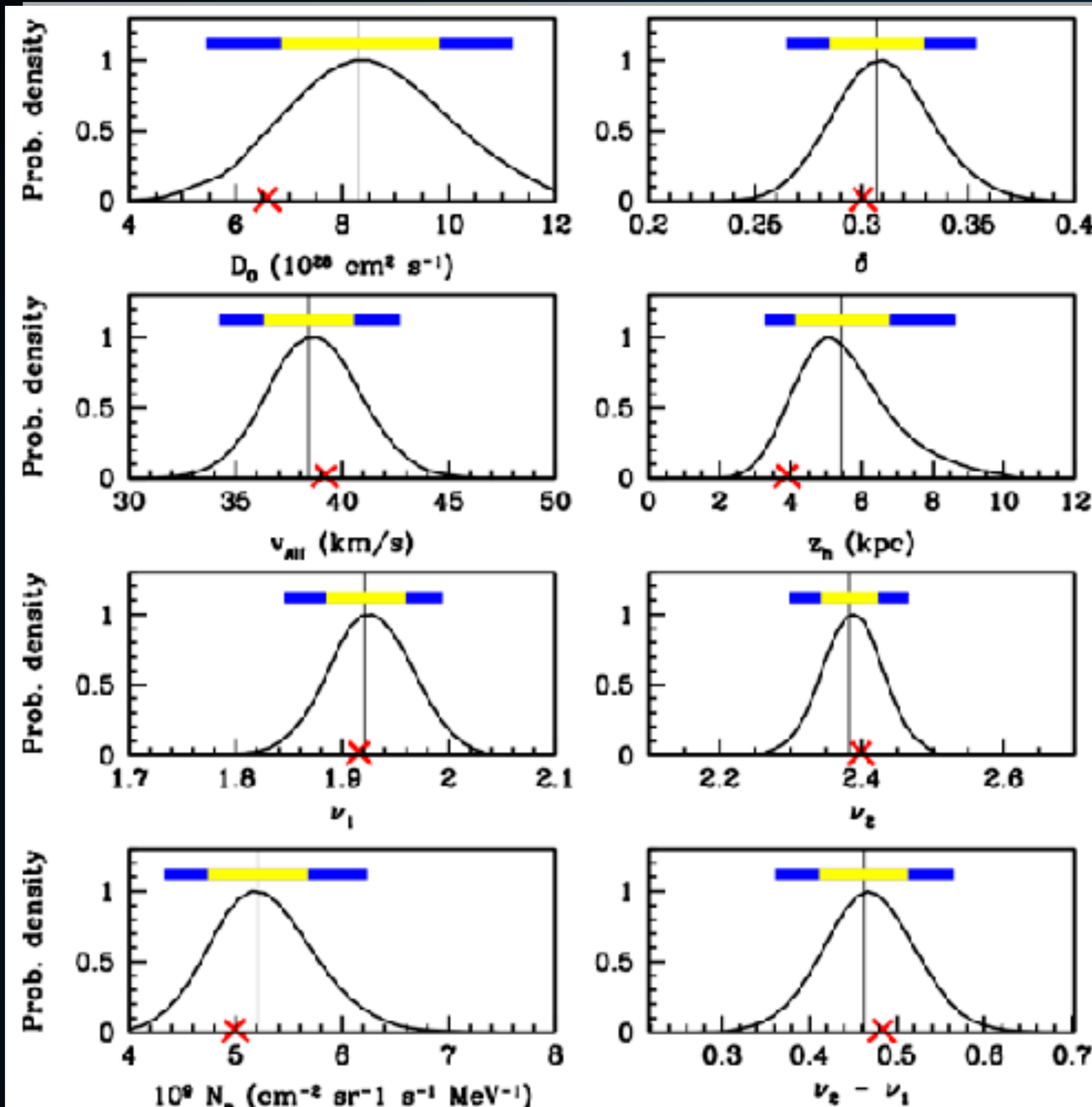

- Multiple cosmic-ray observations indicate that the average diffusion constant is ~5×10^{28} cm^{2}s^{-1}
- Inhibited cosmic-ray propagation in TeV halos must not substantially affect this number.

$$
\begin{aligned}
f &\sim \frac{N_{\rm region} \times \frac{4\pi}{3} r_{\rm region}^3}{\pi R_{\rm MW}^2 \times 2 z_{\rm MW}} \\
&\sim 0.25 \times \left(\frac{r_{\rm region}}{100\,{\rm pc}}\right)^3 \left(\frac{\dot{N}_{\rm SN}}{0.03\,{\rm yr}^{-1}}\right) \left(\frac{\tau_{\rm region}}{10^6\,{\rm yr}}\right) \left(\frac{20\,{\rm kpc}}{R_{\rm MW}}\right)^2 \left(\frac{200\,{\rm pc}}{z_{\rm MW}}\right)
\end{aligned}
$$

CAN WE BE INSIDE A TEV HALO?

- We probably cannot be inside a TeV halo without affecting cosmic-ray anisotropies.
- If we are at the center of a TeV halo, it must be huge.
- Would make understanding the e^+e^- flux even more difficult.

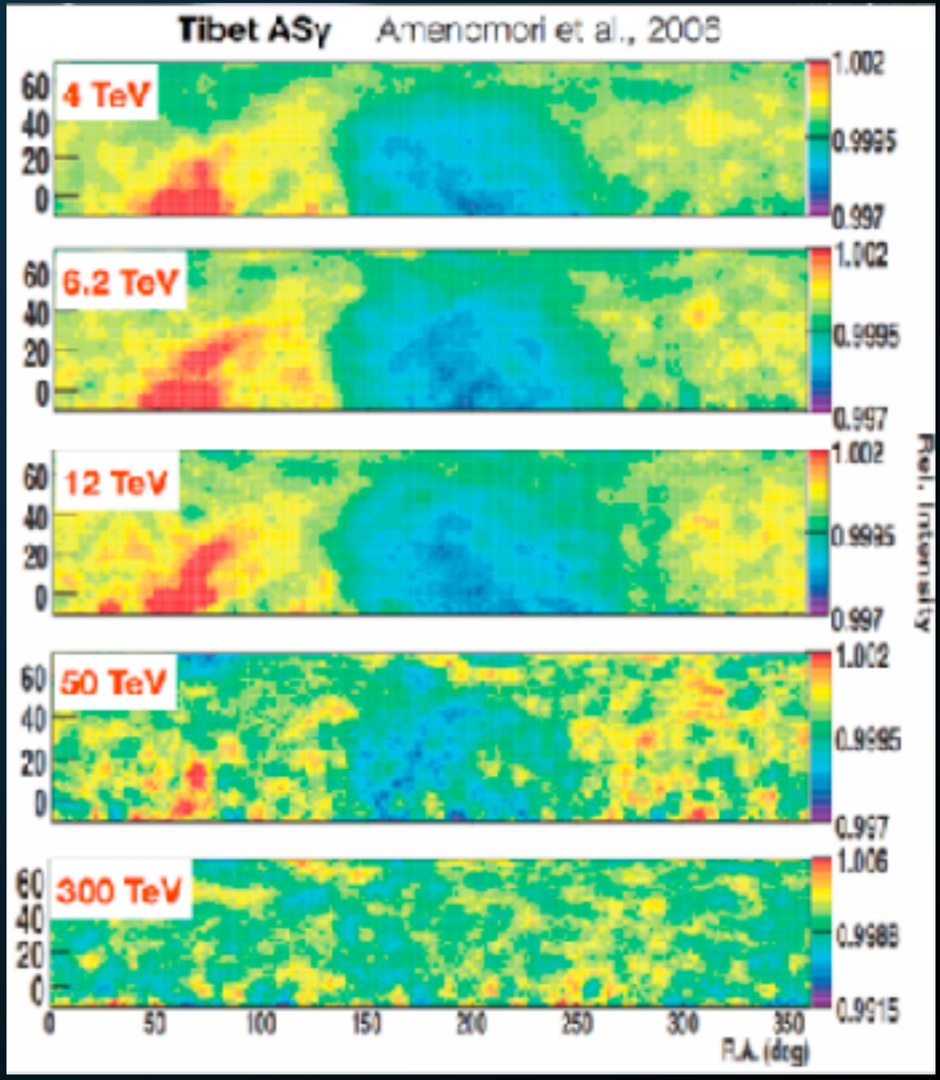

Implication I:

Most TeV gamma-ray sources are TeV halos.

TEV HALOS ARE A GENERIC FEATURE OF PULSARS

2HWC Name	ATNF Name	Distance (kpc)	Angular Separation	Projected Separation	Expected Flux ($\times 10^{-15}$)	Actual Flux ($\times 10^{-15}$)	Flux Ratio	Expected Extension	Actual Extension	Age (kyr)	Chance Overlap
J0700+143	B0656+14	0.29	0.18°	0.91 pc	43.0	23.0	1.87	2.0°	1.73°	111	0.0
J0631+169	J0633+1746	0.25	0.89°	3.88 pc	48.7	48.7	1.0	2.0°	2.0°	342	0.0
J1912+099	J1913+1011	4.61	0.34°	27.36 pc	13.0	36.6	0.36	0.11°	0.7°	169	0.30
J2031+415	J2032+4127	1.70	0.11°	3.26 pc	5.59	61.6	0.091	0.29°	0.7°	181	0.002
J1831-098	J1831-0952	3.68	0.04°	2.57 pc	7.70	95.8	0.080	0.14°	0.9°	128	0.006

- 5 / 39 sources in the 2HWC catalog are correlated with bright, middle-aged (100 – 400 kyr) pulsars.

2HWC Name	ATNF Name	Distance (kpc)	Angular Separation	Projected Separation	Expected Flux ($\times 10^{-15}$)	Actual Flux ($\times 10^{-15}$)	Flux Ratio	Expected Extension	Actual Extension	Age (kyr)	Chance Overlap
J1930+188	J1930+1852	7.0	0.03°	3.67 pc	23.2	9.8	2.37	0.07°	0.0°	2.89	0.002
J1814-173	J1813-1749	4.7	0.54°	44.30 pc	243	152	1.60	0.11°	1.0°	5.6	0.61
J2019+367	J2021+3651	1.8	0.27°	8.48 pc	99.8	58.2	1.71	0.28°	0.7°	17.2	0.04
J1928+177	J1928+1746	4.34	0.03°	2.27 pc	8.08	10.0	0.81	0.11°	0.0°	82.6	0.002
J1908+063	J1907+0602	2.58	0.36°	16.21 pc	40.0	85.0	0.47	0.2°	0.8°	19.5	0.26
J2020+403	J2021+4026	2.15	0.18°	6.75 pc	2.48	18.5	0.134	0.23°	0.0°	77	0.01
J1857+027	J1856+0245	6.32	0.12°	13.24 pc	11.0	97.0	0.11	0.08°	0.9°	20.6	0.06
J1825-134	J1826-1334	3.61	0.20°	12.66 pc	20.5	249	0.082	0.14°	0.9°	21.4	0.14
J1837-065	J1838-0655	6.60	0.38°	43.77 pc	12.0	341	0.035	0.08°	2.0°	22.7	0.48
J1837-065	J1837-0604	4.78	0.50°	41.71 pc	8.3	341	0.024	0.10°	2.0°	33.8	0.68
J2006+341	J2004+3429	10.8	0.42°	80.07 pc	0.48	24.5	0.019	0.04°	0.9°	18.5	0.08

- 12 others with young pulsars (2.36 chance overlaps)
- Young pulsars may be contaminated by SNR.

STEP I: TEV HALOS ARE A GENERIC FEATURE OF PULSARS

2HWC Name	ATNF Name	Distance (kpc)	Angular Separation	Projected Separation	Expected Flux ($\times 10^{-15}$)	Actual Flux ($\times 10^{-15}$)	Flux Ratio	Expected Extension	Actual Extension	Age (kyr)	Chance Overlap
J0700+143	B0656+14	0.29	0.18°	0.91 pc	43.0	23.0	1.87	2.0°	1.73°	111	0.0
J0631+169	J0633+1746	0.25	0.89°	3.88 pc	48.7	48.7	1.0	2.0°	2.0°	342	0.0
J1912+099	J1913+1011	4.61	0.34°	27.36 pc	13.0	36.6	0.36	0.11°	0.7°	169	0.30
J2031+415	J2032+4127	1.70	0.11°	3.26 pc	5.59	61.6	0.091	0.29°	0.7°	181	0.002
J1831-098	J1831-0952	3.68	0.04°	2.57 pc	7.70	95.8	0.080	0.14°	0.9°	128	0.006

- There are 57 middle-aged pulsars in the HAWC field of view.
- Can produce a ranked list of the spin-down flux of these systems (spin-down luminosity divided by distance squared).
- If TeV halo luminosity is correlated to spin-down power, these should be among the brightest systems.

STEP I: TEV HALOS ARE A GENERIC FEATURE OF PULSARS

ATNF Name	Dec. (°)	Distance (kpc)	Age (kyr)	Spindown Lum. (erg s^{-1})	Spindown Flux (erg s^{-1} kpc^{-2})	2HWC
J0633+1746	17.77	0.25	342	3.2e34	4.1e34	2HWC J0631+169
B0656+14	14.23	0.29	111	3.8e34	3.6e34	2HWC J0700+143
B1951+32	32.87	3.00	107	3.7e36	3.3e34	—
J1740+1000	10.00	1.23	114	2.3e35	1.2e34	—
J1913+1011	10.18	4.61	169	2.9e36	1.1e34	2HWC J1912+099
J1831-0952	-9.86	3.68	128	1.1e36	6.4e33	2HWC J1831-098
J2032+4127	41.45	1.70	181	1.7e35	4.7e33	2HWC J2031+415
B1822-09	-9.58	0.30	232	4.6e33	4.1e33	—
B1830-08	-8.45	4.50	147	5.8e35	2.3e33	—
J1913+0904	9.07	3.00	147	1.6e35	1.4e33	—
B0540+23	23.48	1.56	253	4.1e34	1.4e33	—

- **The five pulsars associated with TeV emission are among the seven brightest sources.**
- **Private communication with the HAWC collaboration reveals that the missing two sources are currently 2-3σ excesses!**

TEV HALOS: THE FIRST ORDER MODEL

$$\phi_{\mathrm{TeV\ halo}} = \left(\frac{\dot{E}_{\mathrm{psr}}}{\dot{E}_{\mathrm{Geminga}}}\right)\left(\frac{d^2_{\mathrm{Geminga}}}{d^2_{\mathrm{psr}}}\right)\phi_{\mathrm{Geminga}}$$

$$\theta_{\mathrm{TeV\ halo}} = \left(\frac{d_{\mathrm{Geminga}}}{d_{\mathrm{psr}}}\right)\theta_{\mathrm{Geminga}}$$

- **Assume that every pulsar converts an equivalent fraction of its spin-down power into the TeV halo flux.**
- **Can then calculate the TeV flux and extension of every TeV halo based on its spin-down power, and the observations of Geminga.**
- **Note: Using Monogem would increases fluxes by nearly a factor of 2.**

HAWC SENSITIVITY AFTER 10 YEARS

ATNF Name	Dec. (°)	Distance (kpc)	Age (kyr)	Spindown Lum. (erg s^{-1})	Spindown Flux (erg s^{-1} kpc^{-2})	2HWC
J0633+1746	17.77	0.25	342	3.2e34	4.1e34	2HWC J0631+169
B0656+14	14.23	0.29	111	3.8e34	3.6e34	2HWC J0700+143
B1951+32	32.87	3.00	107	3.7e36	3.3e34	—
J1740+1000	10.00	1.23	114	2.3e35	1.2e34	—
J1913+1011	10.18	4.61	169	2.9e36	1.1e34	2HWC J1912+099
J1831-0952	-9.86	3.68	128	1.1e36	6.4e33	2HWC J1831-098
J2032+4127	41.45	1.70	181	1.7e35	4.7e33	2HWC J2031+415
B1822-09	-9.58	0.30	232	4.6e33	4.1e33	—
B1830-08	-8.45	4.50	147	5.8e35	2.3e33	—
J1913+0904	9.07	3.00	147	1.6e35	1.4e33	—
B0540+23	23.48	1.56	253	4.1e34	1.4e33	—

- **HAWC will eventually reach a flux sensitivity of 0.02 Geminga**

- **Will observe**
  - **TeV halos from a dozen middle-aged ATNF pulsars.**
  - **TeV halos from ~40 additional young pulsars.**

A PLETHORA OF (RADIO) PULSARS

- **Pulsations detected from 2613 systems.**

- **Vast majority in radio.**

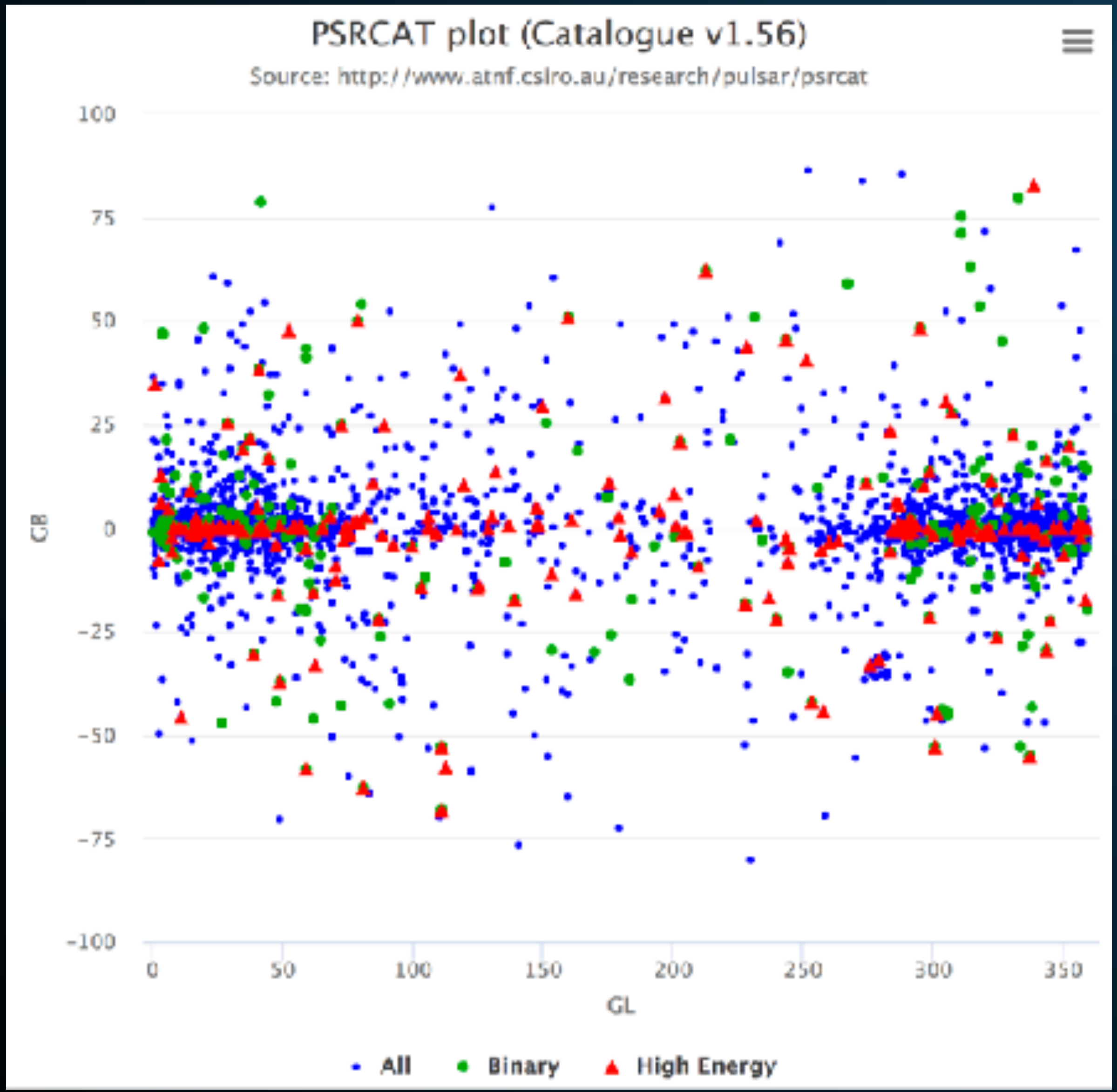

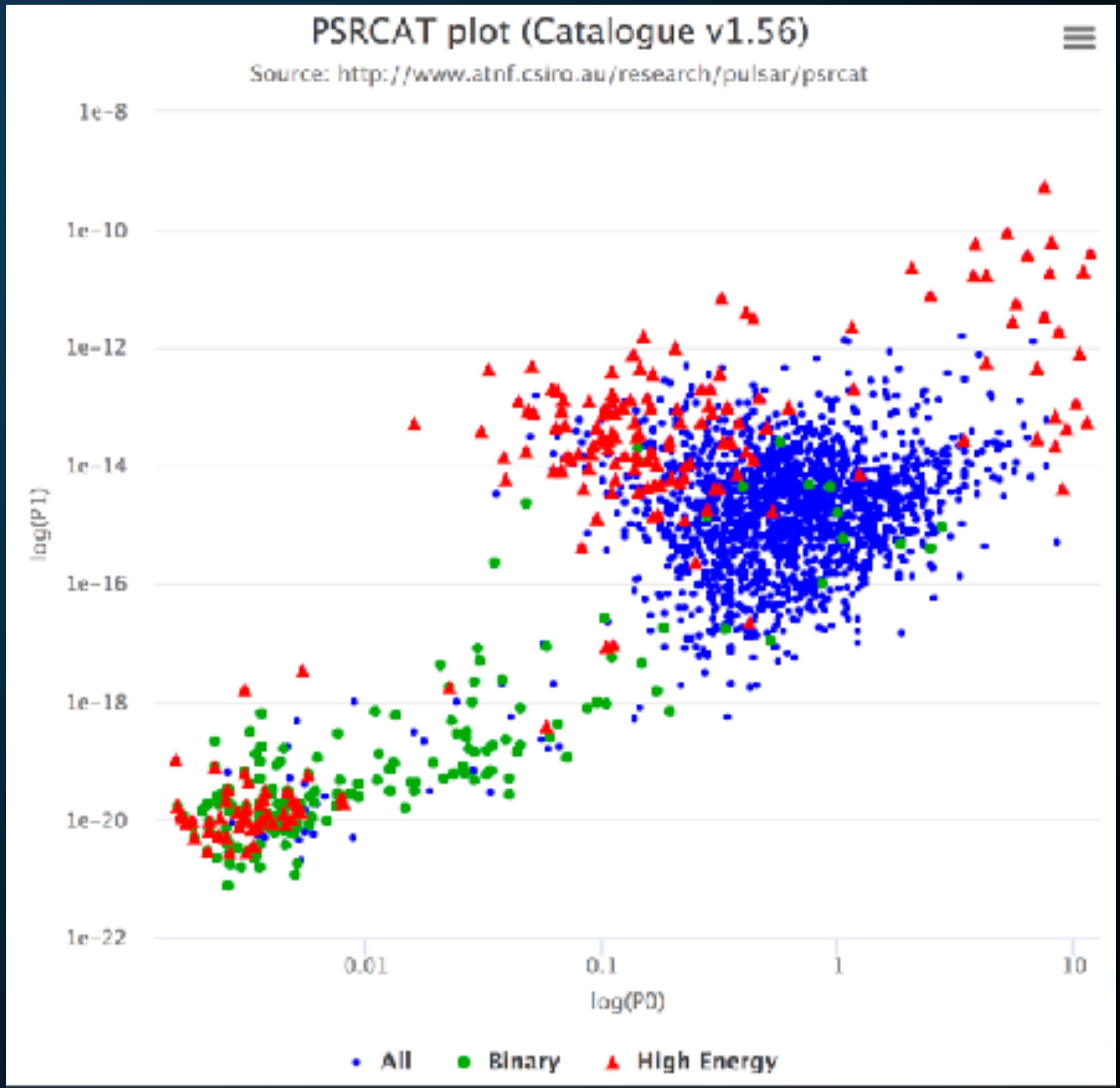

USING TEV HALOS TO DISCOVER PULSARS

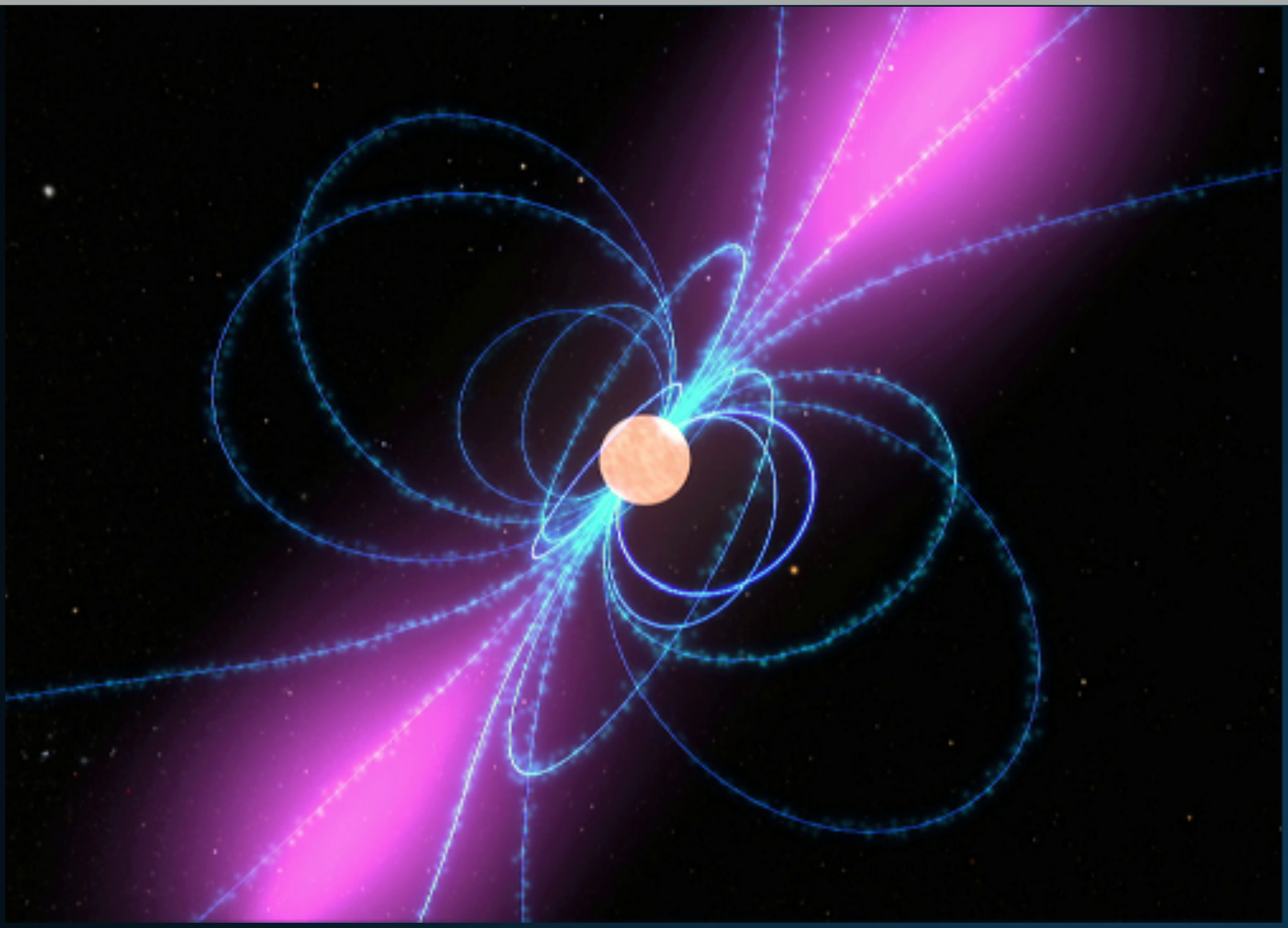

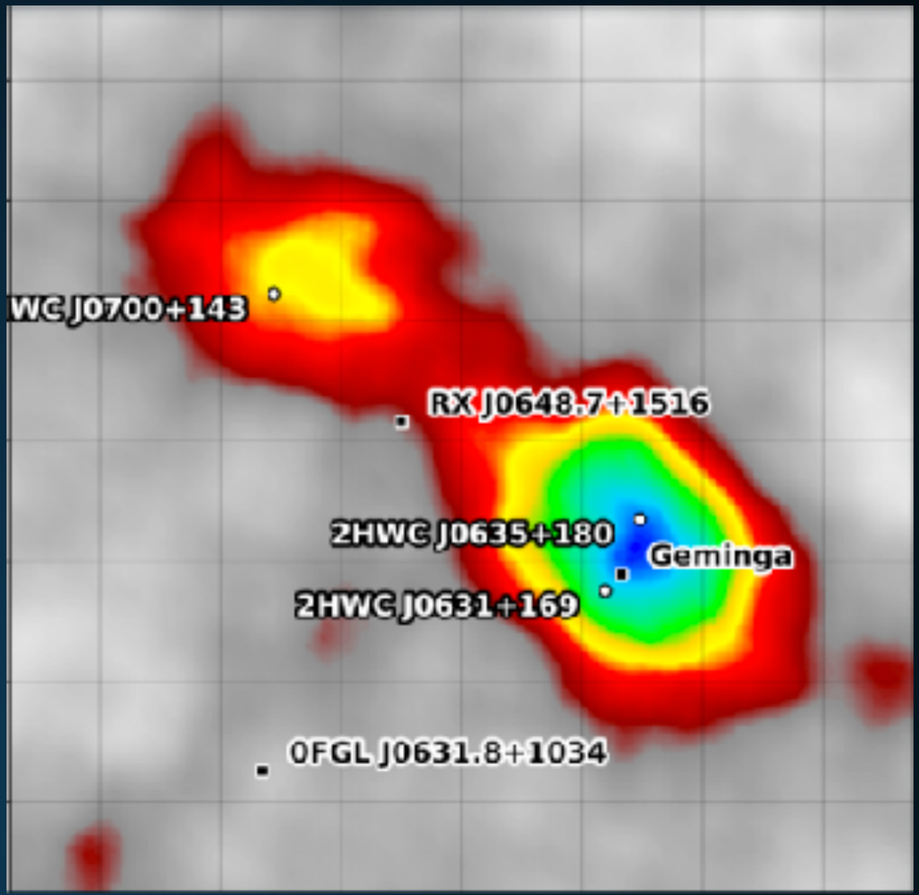

- **Multi-wavelength emission from pulsar is beamed.**
- **30 kyr propagation time of TeV halo implies the emission is isotropic.**
- **Can find off-beam pulsars by detecting the TeV halo.**

- **Tauris and Manchester (1998) calculated the beaming angle from a population of young and middle-aged pulsars.**

$$f = \left[1.1\left(\log_{10}\left(\frac{\tau}{100\ \mathrm{Myr}}\right)\right)^2 + 15\right]\%$$

- **This varies between 15-30%.**

- **1/f pulsars are unseen in radio surveys.**

MISSING TEV HALOS

2HWC Name	ATNF Name	Distance (kpc)	Angular Separation	Projected Separation	Expected Flux ($\times 10^{-15}$)	Actual Flux ($\times 10^{-15}$)	Flux Ratio	Expected Extension	Actual Extension	Age (kyr)	Chance Overlap
J0700+143	B0656+14	0.29	0.18°	0.91 pc	43.0	23.0	1.87	2.0°	1.73°	111	0.0
J0631+169	J0633+1746	0.25	0.89°	3.88 pc	48.7	48.7	1.0	2.0°	2.0°	342	0.0
J1912+099	J1913+1011	4.61	0.34°	27.36 pc	13.0	36.6	0.36	0.11°	0.7°	169	0.30
J2031+415	J2032+4127	1.70	0.11°	3.26 pc	5.59	61.6	0.091	0.29°	0.7°	181	0.002
J1831-098	J1831-0952	3.68	0.04°	2.57 pc	7.70	95.8	0.080	0.14°	0.9°	128	0.006

2HWC Name	ATNF Name	Distance (kpc)	Angular Separation	Projected Separation	Expected Flux ($\times 10^{-15}$)	Actual Flux ($\times 10^{-15}$)	Flux Ratio	Expected Extension	Actual Extension	Age (kyr)	Chance Overlap
J1930+188	J1930+1852	7.0	0.03°	3.67 pc	23.2	9.8	2.37	0.07°	0.0°	2.89	0.002
J1814-173	J1813-1749	4.7	0.54°	44.30 pc	243	152	1.60	0.11°	1.0°	5.6	0.61
J2019+367	J2021+3651	1.8	0.27°	8.48 pc	99.8	58.2	1.71	0.28°	0.7°	17.2	0.04
J1928+177	J1928+1746	4.34	0.03°	2.27 pc	8.08	10.0	0.81	0.11°	0.0°	82.6	0.002
J1908+063	J1907+0602	2.58	0.36°	16.21 pc	40.0	85.0	0.47	0.2°	0.8°	19.5	0.26
J2020+403	J2021+4026	2.15	0.18°	6.75 pc	2.48	18.5	0.134	0.23°	0.0°	77	0.01
J1857+027	J1856+0245	6.32	0.12°	13.24 pc	11.0	97.0	0.11	0.08°	0.9°	20.6	0.06
J1825-134	J1826-1334	3.61	0.20°	12.66 pc	20.5	249	0.082	0.14°	0.9°	21.4	0.14
J1837-065	J1838-0655	6.60	0.38°	43.77 pc	12.0	341	0.035	0.08°	2.0°	22.7	0.48
J1837-065	J1837-0604	4.78	0.50°	41.71 pc	8.3	341	0.024	0.10°	2.0°	33.8	0.68
J2006+341	J2004+3429	10.8	0.42°	80.07 pc	0.48	24.5	0.019	0.04°	0.9°	18.5	0.08

- **The beaming fractions predicts that 56^{+15}_{-11} TeV halos are currently observed by HAWC.**
- **However, only 39 total HAWC sources**
- **Chance overlaps, SNR contamination must be taken into account.**

EVENTUAL TEV HALO DETECTIONS

ATNF Name	Dec. (°)	Distance (kpc)	Age (kyr)	Spindown Lum. (erg s^{-1})	Spindown Flux (erg s^{-1} kpc^{-2})	2HWC
J0633+1746	17.77	0.25	342	3.2e34	4.1e34	2HWC J0631+169
B0656+14	14.23	0.29	111	3.8e34	3.6e34	2HWC J0700+143
B1951+32	32.87	3.00	107	3.7e36	3.3e34	—
J1740+1000	10.00	1.23	114	2.3e35	1.2e34	—
J1913+1011	10.18	4.61	169	2.9e36	1.1e34	2HWC J1912+099
J1831-0952	-9.86	3.68	128	1.1e36	6.4e33	2HWC J1831-098
J2032+4127	41.45	1.70	181	1.7e35	4.7e33	2HWC J2031+415
B1822-09	-9.58	0.30	232	4.6e33	4.1e33	—
B1830-08	-8.45	4.50	147	5.8e35	2.3e33	—
J1913+0904	9.07	3.00	147	1.6e35	1.4e33	—
B0540+23	23.48	1.56	253	4.1e34	1.4e33	—

- **10 year HAWC observations should detect 37^{+17}_{-13} TeV halos surrounding middle-aged pulsars.**
- **These numbers correspond to most of the TeV sources detectable by HAWC.**

HOW MANY OF THESE SOURCES ARE NEW?

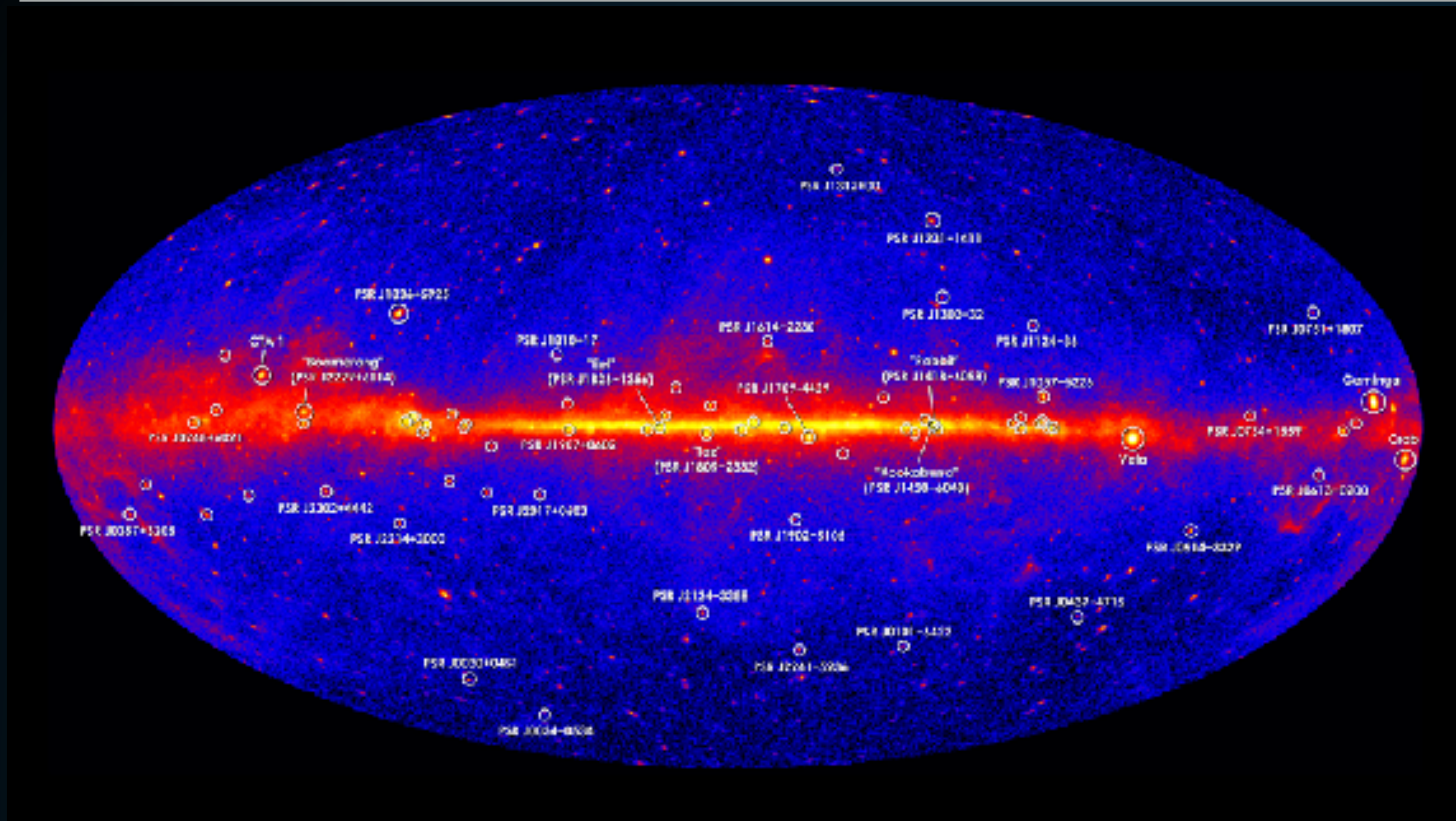

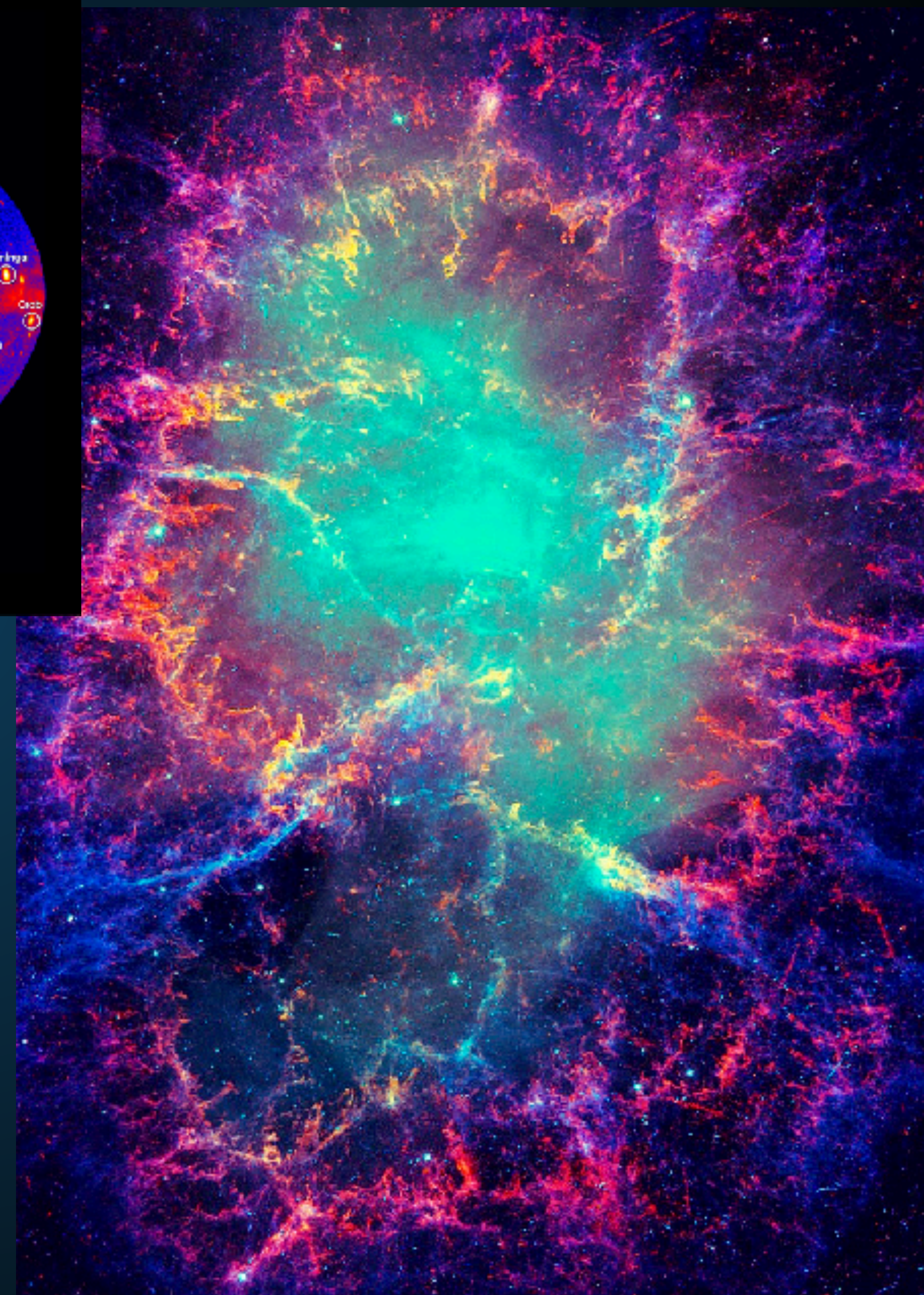

- How many of these sources have been discovered?
  - gamma-ray pulsars
  - X-Ray PWN
  - Current ACTs

FERMI-LAT DETECTIONS

- **Fermi-LAT has detected 54 new pulsars**
  - **35 younger than 100 kyr**
  - **Only 5/35 in HAWC field of view**

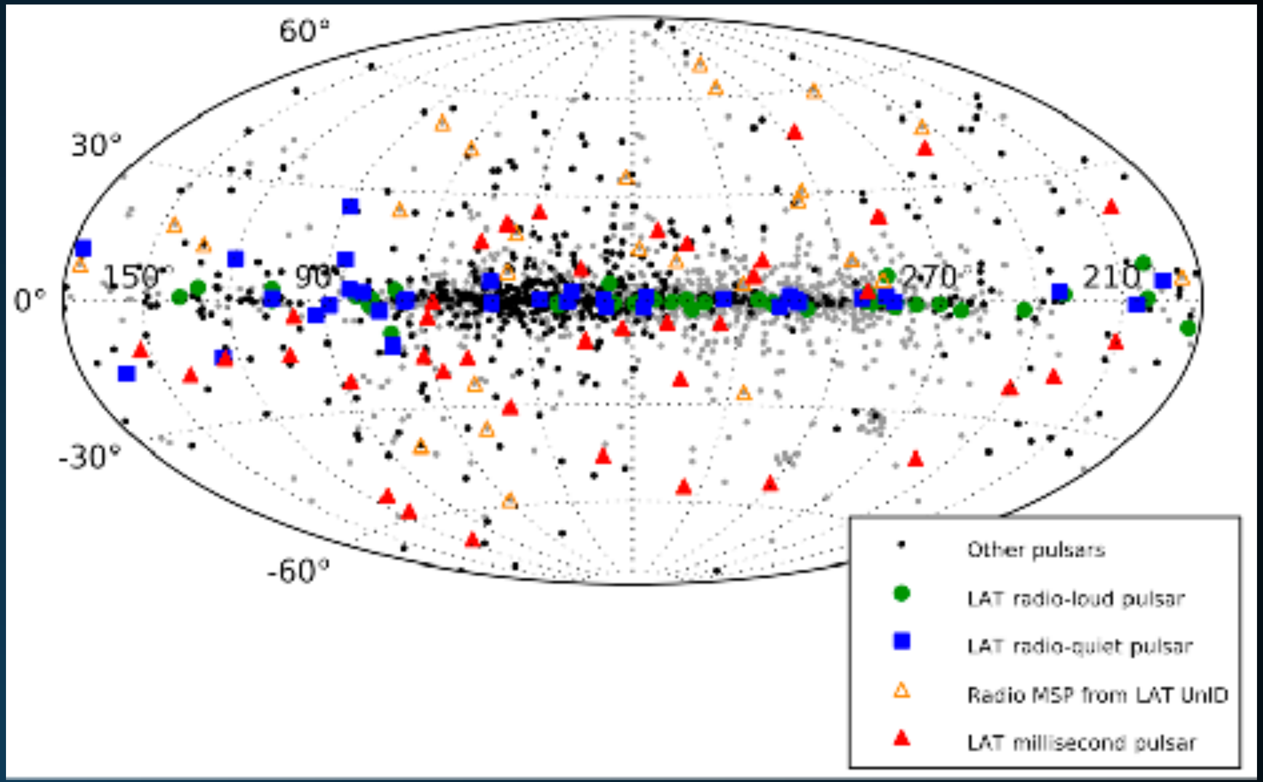

- **Fermi-LAT has detected only ~5 of these 37 systems.**

https://confluence.slac.stanford.edu/display/GLAMCOG/Public+List+of+LAT-Detected+Gamma-Ray+Pulsars

X-RAY PWN DETECTIONS

PWNe With No Detected Pulsar

Gname	other name(s)	R	X	O	G	
G0.13-0.11					?	notes
G0.9+0.1					N	notes
G7.4-2.0	GeV J1809-2327, Tazzie				Y	notes
G16.7+0.1					N	notes
G18.5-0.4	GeV J1825-1310, Eel				Y	notes
G20.0-0.2					N	notes
G24.7+0.6					N	notes
G27.8+0.6					N	notes
G39.2-0.3	3C 396				Y	notes
G63.7+1.1					N	notes
G74.9+1.2	CTB 87				Y	notes
G119.5+10.2	CTA 1				Y	notes
G189.1+3.0	IC 443				?	notes
G279.8-35.8	B0453-685				N	notes
G291.0-0.1	MSH 11-62				Y	notes
G293.8+0.6					N	notes
G313.3+0.1	Rabbit				Y	notes
G318.9+0.4					N	notes
G322.5-0.1					N	notes
G326.3-1.8	MSH 15-56				N	notes
G327.1-1.1					N	notes
G328.4+0.2	MSH 15-57				N	notes
G358.6-17.2	RX J1856.5-3754	N	N		N	notes
G359.89-0.08					Y	notes

- X-Ray PWN have detected only ~6 of these 37 systems.

HESS/VERITAS DETECTIONS

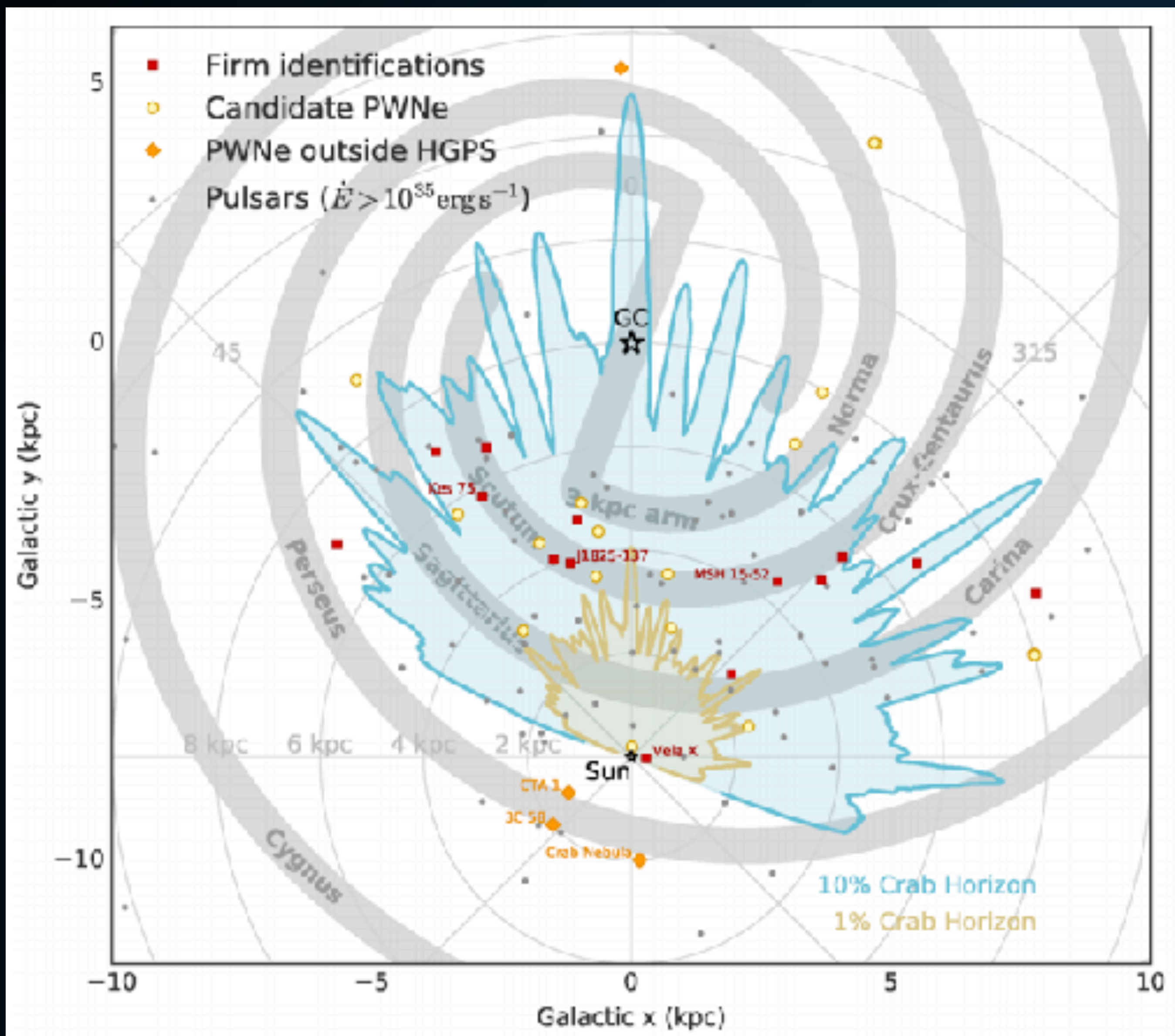

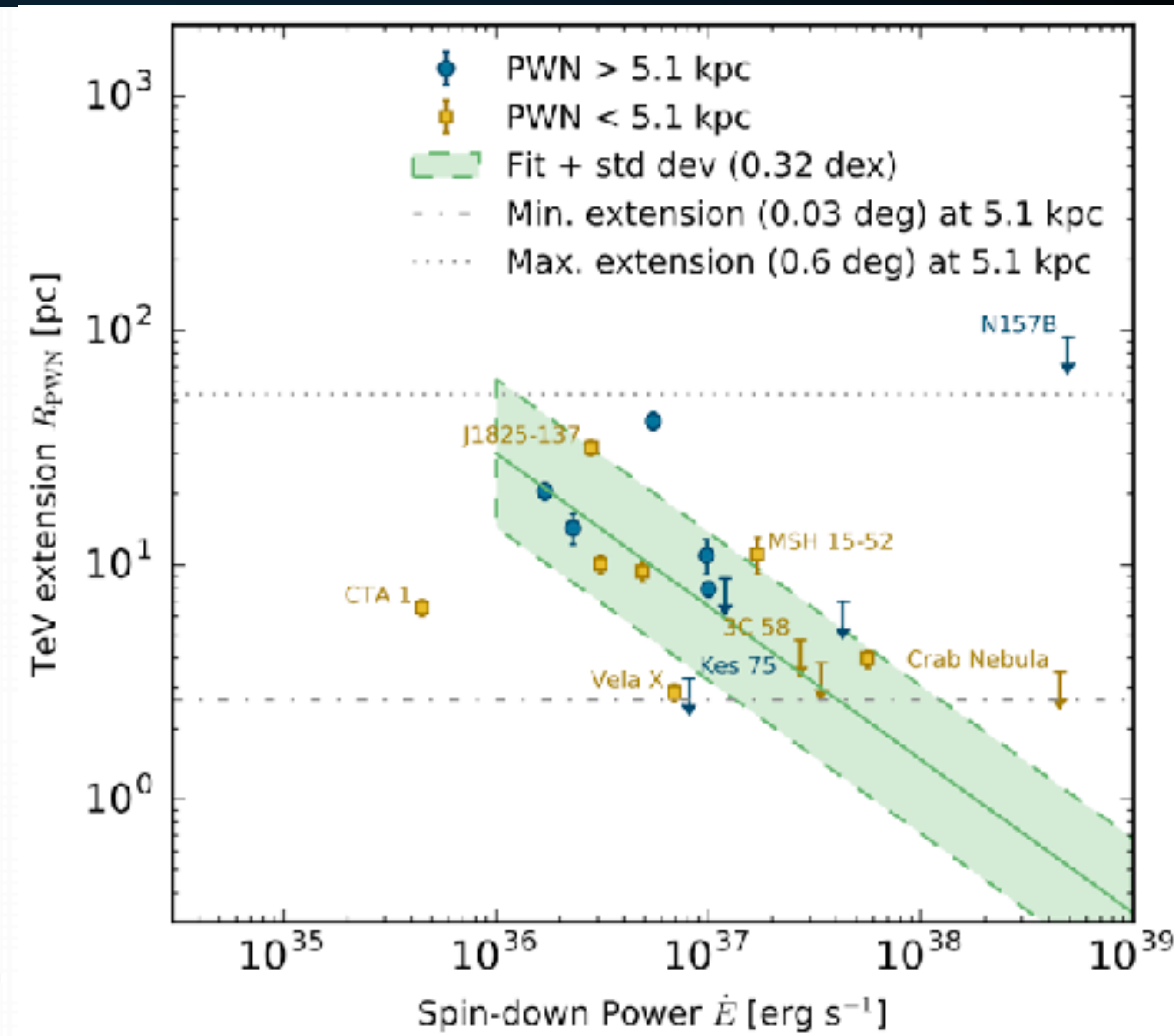

- **Targeted ACTs are sensitive to the flux from TeV halos.**
- **ACTs are not sensitive to sources extended >0.5°.**
- **Large parameter space available only to HAWC.**

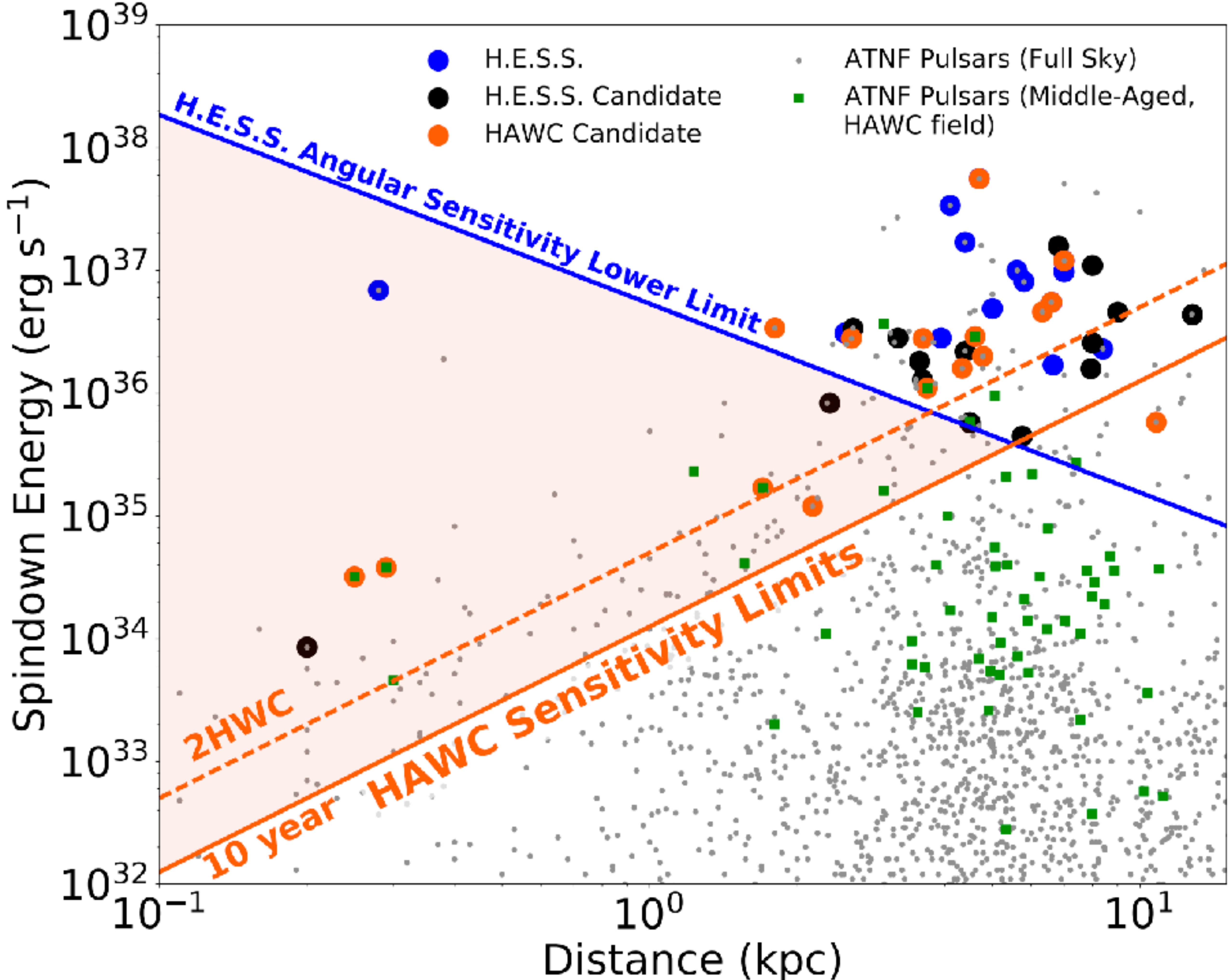

H.E.S.S.
H.E.S.S. Candidate
HAWC Candidate
ATNF Pulsars (Full Sky)
ATNF Pulsars (Middle-Aged, HAWC field)
H.E.S.S. Angular Sensitivity Lower Limit
2HWC
10 year HAWC Sensitivity Limits
Spindown Energy (erg s^{-1})
Distance (kpc)
10^{39}
10^{38}
10^{37}
10^{36}
10^{35}
10^{34}
10^{33}
10^{32}
10^{-1}
10^{0}
10^{1}

CONFIRMING TEV HALOS

- Several Methods to confirm TeV halo detections:
  - X-Ray halos
  - X-Ray PWN

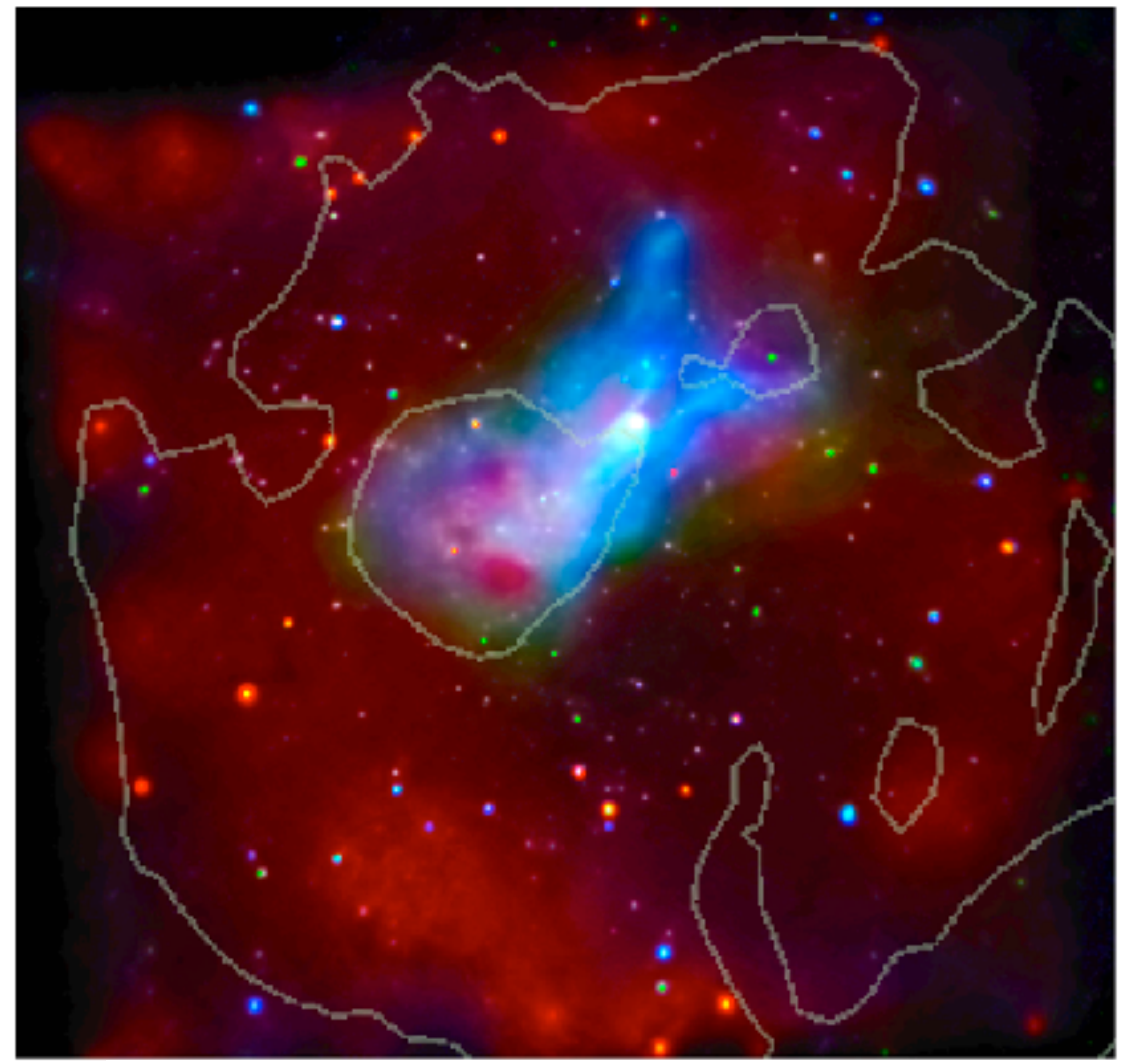

- Possible Detection! (G327-1.1)
- Young Pulsar (17.4 kyr)
- Two PWN
  - Diffuse PWN has significantly softer spectrum

	Region	Area (arcsec^2)	Cts (1000)	N_H (10^{22} cm^{-2})	Photon Index	Amplitude (10^{-4})	kT (keV)	τ (10^{12} s cm^{-3})	Norm. (10^{-3})	F_1 (10^{-12})	F_2 (10^{-12})	Red. χ^2
1	Compact Source	84.657	6.34	$1.93^{+0.08}_{-0.08}$	$1.61^{+0.08}_{-0.07}$	$1.05^{+0.11}_{-0.10}$	...	...	...	0.45	...	0.80
2	Cometary PWN	971.22	7.75	1.93	$1.62^{+0.08}_{-0.07}$	$1.47^{+0.16}_{-0.14}$	...	...	...	1.09	...	...
3	Trail East	537.42	2.13	1.93	$1.84^{+0.12}_{-0.12}$	$0.44^{+0.07}_{-0.06}$	...	...	...	0.27	...	...
4	Trail West	766.56	3.12	1.93	$1.80^{+0.11}_{-0.11}$	$0.61^{+0.09}_{-0.08}$	...	...	...	0.39	...	...
5	Trail 1	424.45	1.98	1.93	$1.76^{+0.12}_{-0.12}$	$0.39^{+0.05}_{-0.05}$	...	...	...	0.26	...	...
6	Trail 2	588.19	2.13	1.93	$1.95^{+0.11}_{-0.11}$	$0.49^{+0.07}_{-0.06}$	...	...	...	0.28	...	...
7	Trail 3	994.92	2.99	1.93	$2.09^{+0.10}_{-0.10}$	$0.78^{+0.09}_{-0.08}$	...	...	...	0.42	...	...
8	Trail 4	839.48	2.38	1.93	$2.28^{+0.12}_{-0.12}$	$0.74^{+0.09}_{-0.09}$	...	...	...	0.37	...	...
9	Prong East	828.58	1.66	1.93	$1.72^{+0.14}_{-0.14}$	$0.30^{+0.06}_{-0.05}$	...	...	...	0.27	...	...
10	Prong West	971.22	2.06	1.93	$1.85^{+0.14}_{-0.14}$	$0.44^{+0.08}_{-0.07}$	...	...	...	1.09	...	...
11	Diffuse PWN*	20007	27.7	1.93	$2.11^{+0.04}_{-0.05}$	$6.91^{+0.37}_{-0.74}$	$0.23^{+0.14}_{-0.05}$	$0.21^{+0.88}_{-0.16}$	$6.0^{+16}_{-4.0}$	3.68	17.7	0.82
12	Relic PWN*	26787	17.2	1.93	$2.58^{+0.07}_{-0.10}$	$6.51^{+0.53}_{-0.71}$	0.23	0.21	$6.9^{+18}_{-5.5}$	3.14	20.3	...

Implication II:

The Positron Excess

THE POSITRON EXCESS

- Rising fraction of cosmic-ray positrons at energies above 10 GeV

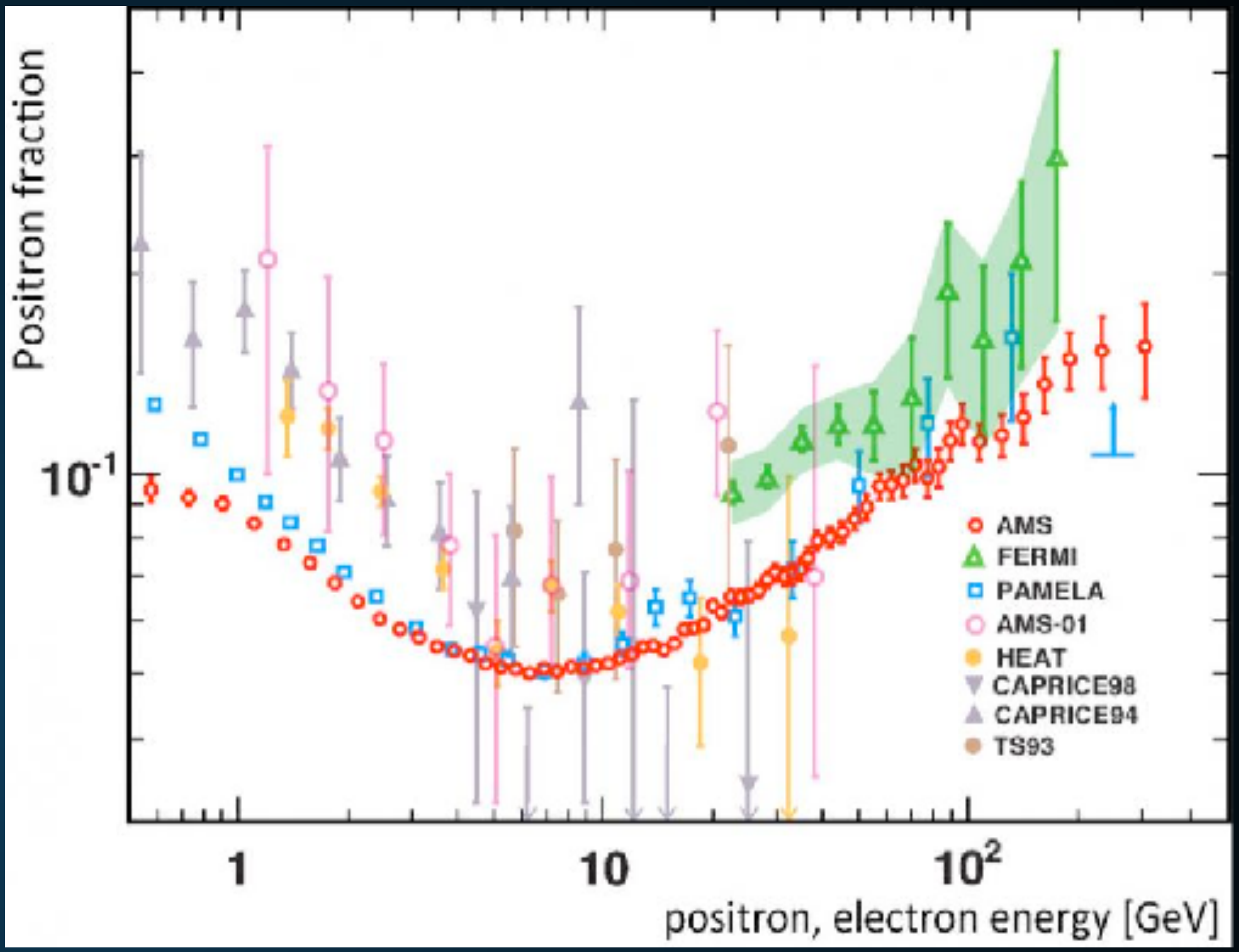

- Standard Cosmic-Ray Secondary Production predicts the positron fraction falls as $\sim E^{-0.4}$.

- Indicates a new primary source of high energy e^+e^- pairs.

IMPLICATION I: THE POSITRON EXCESS

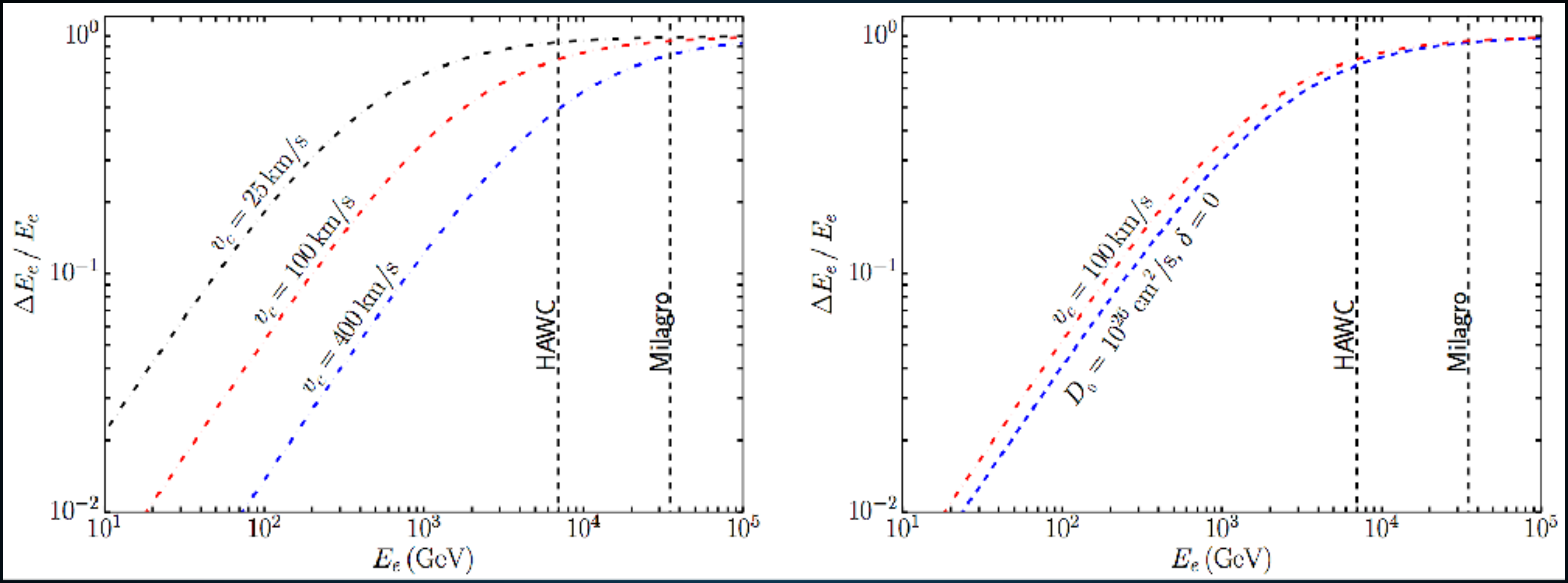

- What do the low-energy e^+e^- do?
  - Large flux (10% of spin-down power)
  - Hard Spectrum
  - Most escape

THE POSITRON FRACTION FROM TEV HALOS

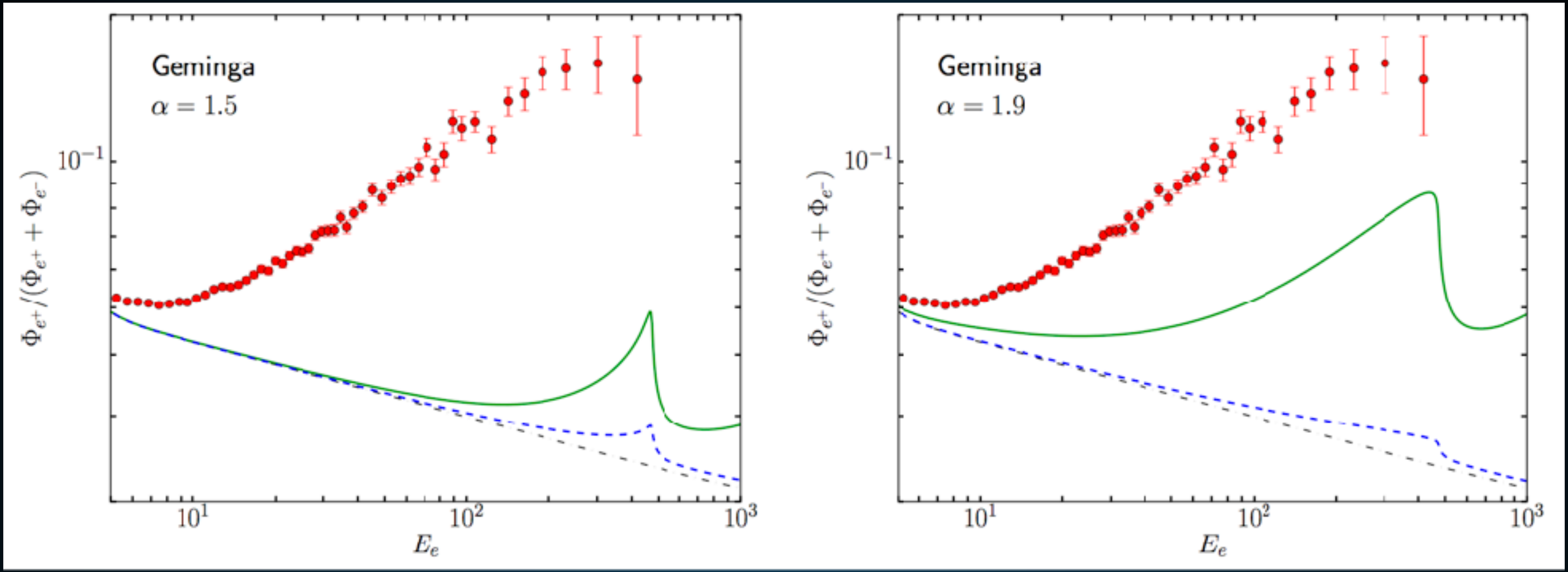

- **Geminga can individually produce nearly half of the positron excess.**
- **Models not fit to the data - this contribution must exist.**

THE POSITRON FRACTION FROM TEV HALOS

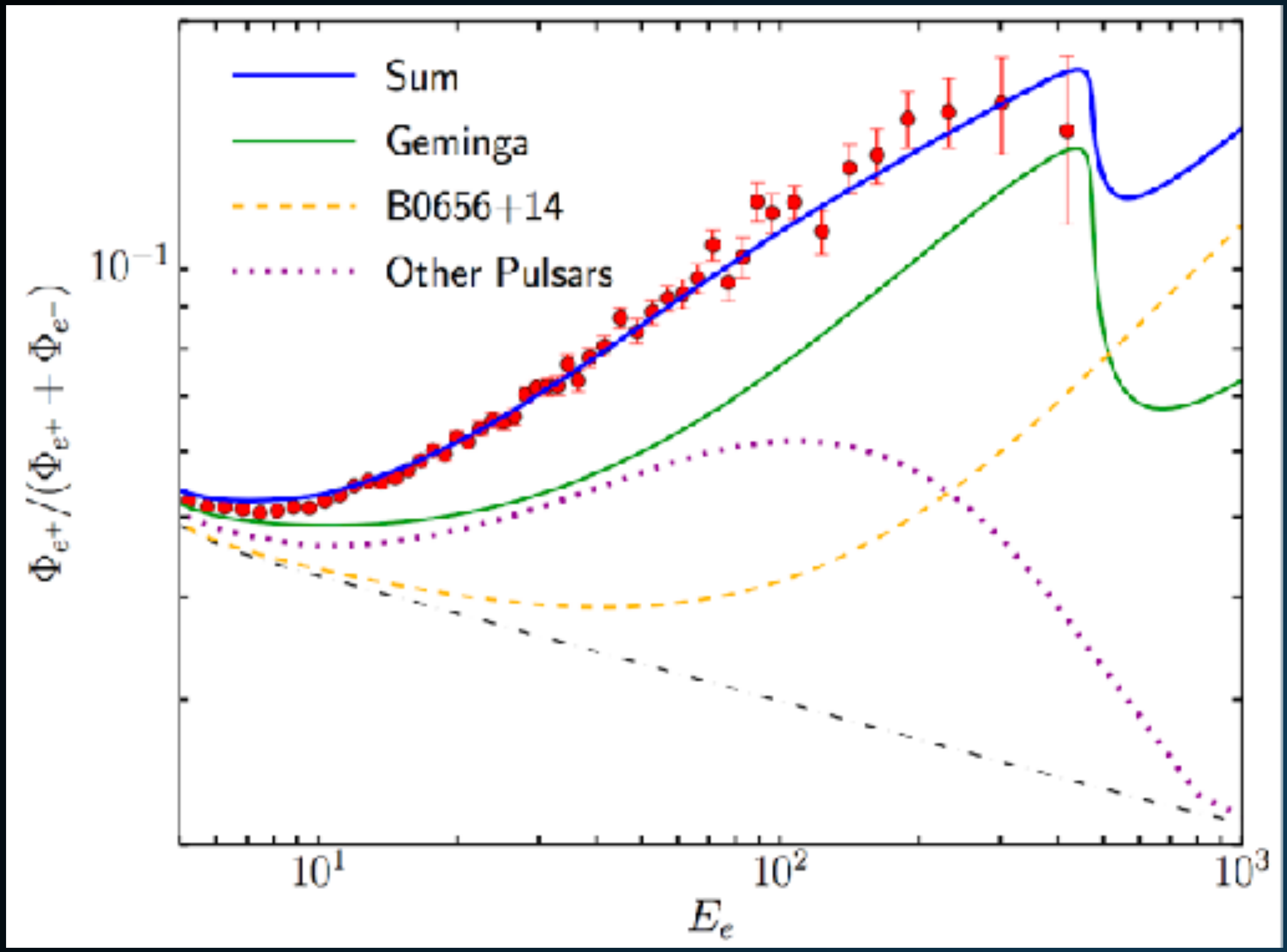

- Total Contribution from:
  - Geminga
  - Monogem
  - Average of other young pulsars

*Braking index slightly changed to fit model to data.

- Reasonable models can be exactly fit to the excess.

Implication III:

Most TeV gamma-rays are leptonic

Hadronic Emission

$$E_{p,SN} = 10^{50}\ \text{erg}$$

$$\frac{dN_{p,SN}}{dE} = 4\times 10^{51}\, E^{-2}\, e^{-E/1\,\text{PeV}}\ \text{GeV}^{-1}$$

$$\phi_{\gamma,\pi_0} \propto E^{-2.7} \rightarrow 4\times 10^{51}\, E^{-2.7}\, e^{-E/1\,\text{PeV}}$$

Leptonic Emission

$$KE_{pulsar} = 10^{49}\ \text{erg}$$

$$e^{+}e^{-}_{pulsar} \simeq 10^{48}\ \text{erg}$$

$$\frac{dN_{e^+e^-,p}}{dE} = 1.1\times 10^{48}\, E^{-1.5}\, e^{-E/100\,\text{TeV}}$$

$$\phi_{\gamma,ICS} = 1.1\times 10^{48}\, E^{-1.5}\, e^{-E/100\,\text{TeV}}$$

- **Traditionally believe that hadronic cosmic-rays are dominant.**
- **Two effects at high energies:**
  - **Hard primary electron injection spectra**
  - **Milky Way is calorimetric to TeV leptons**

TOTAL HIGH-ENERGY EMISSION FROM SNR AND PULSAR

- **At high energies, leptonic gamma-rays become dominant.**

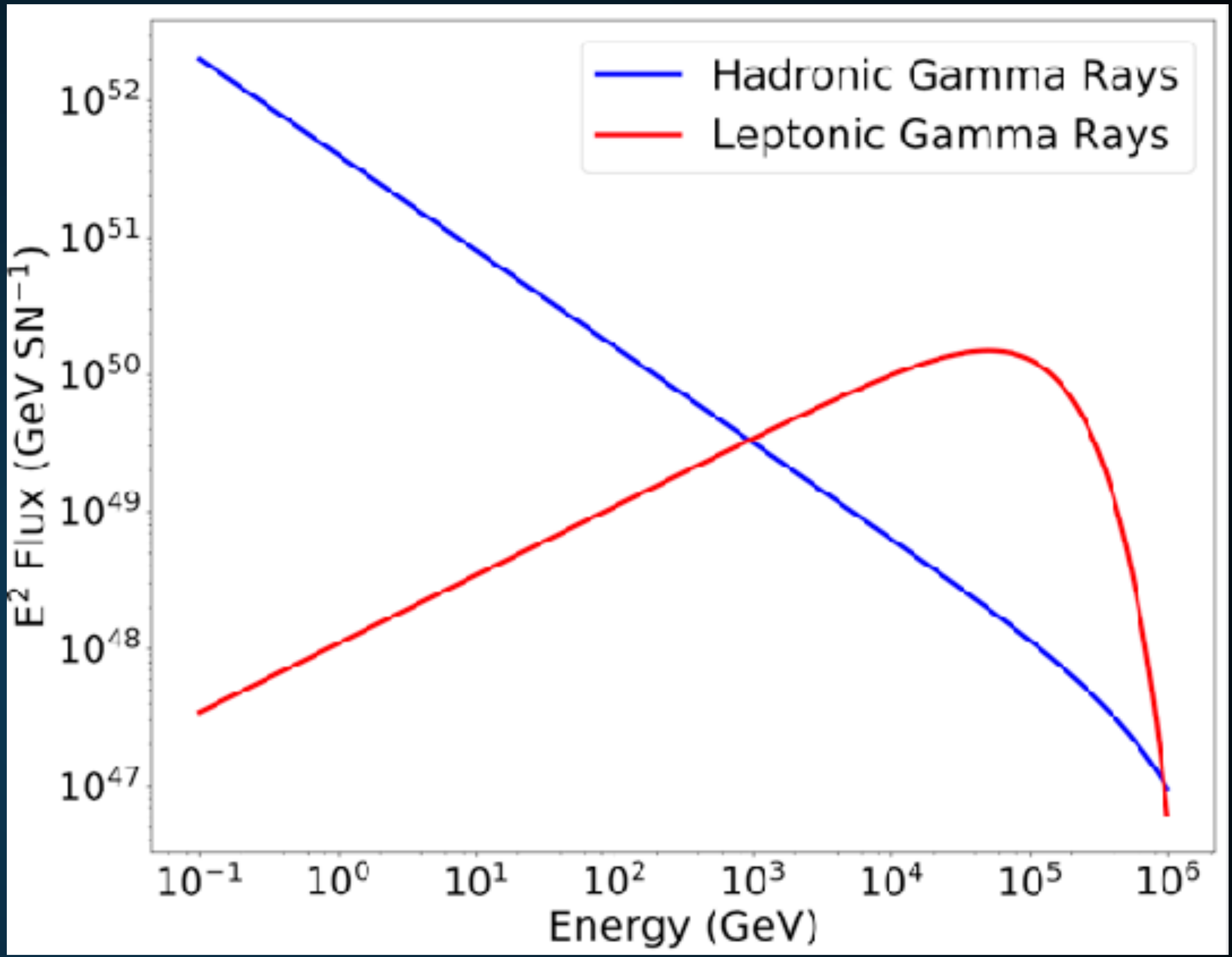

- **There are many TeV halos in the Milky Way**

- **Dim TeV halos will be observed as a new diffuse gamma-ray emission component.**

IMPLICATION IIIA: THE GALACTIC CENTER PEVATRON

- **HESS observations indicate diffuse ~50 TeV emission from the Galactic center**
- **If this emission is hadronic, it indicates PeV particle acceleration in the GC**
- **Spherical symmetry hints at Galactic Center source.**

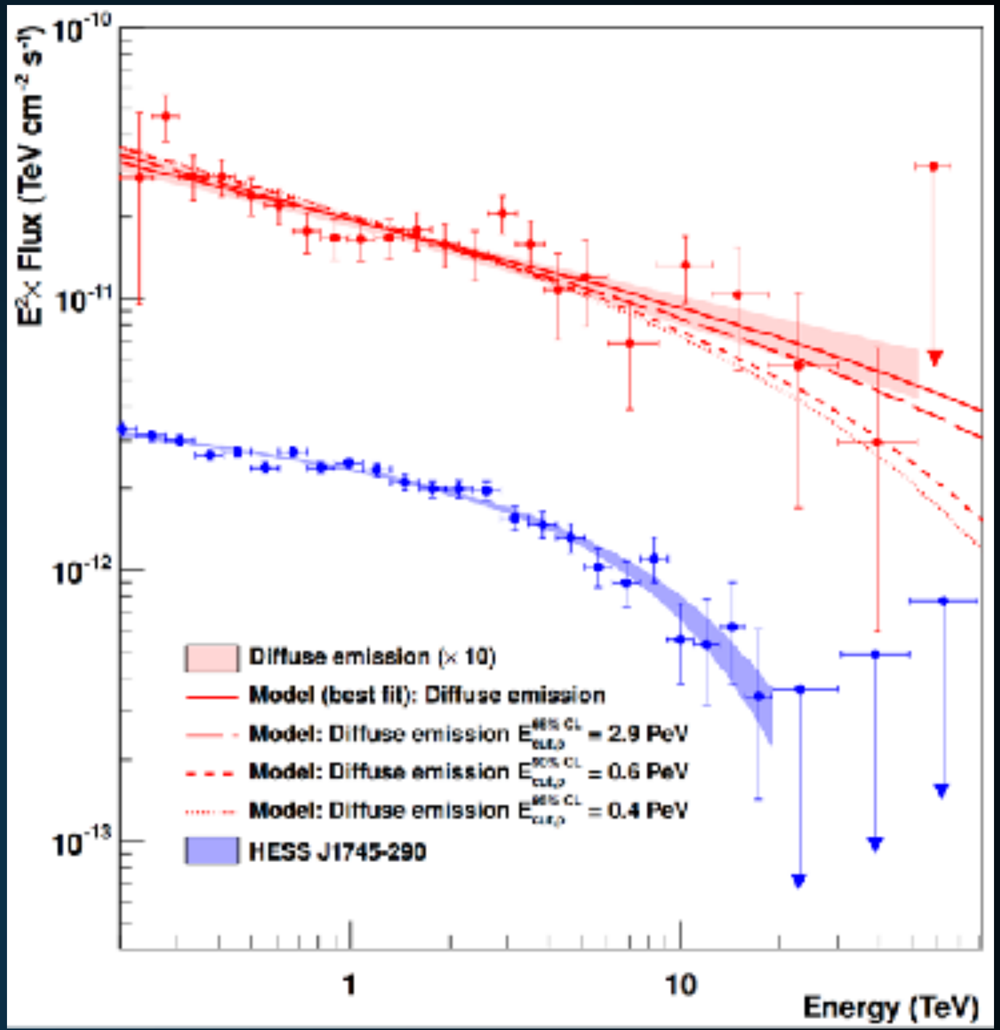

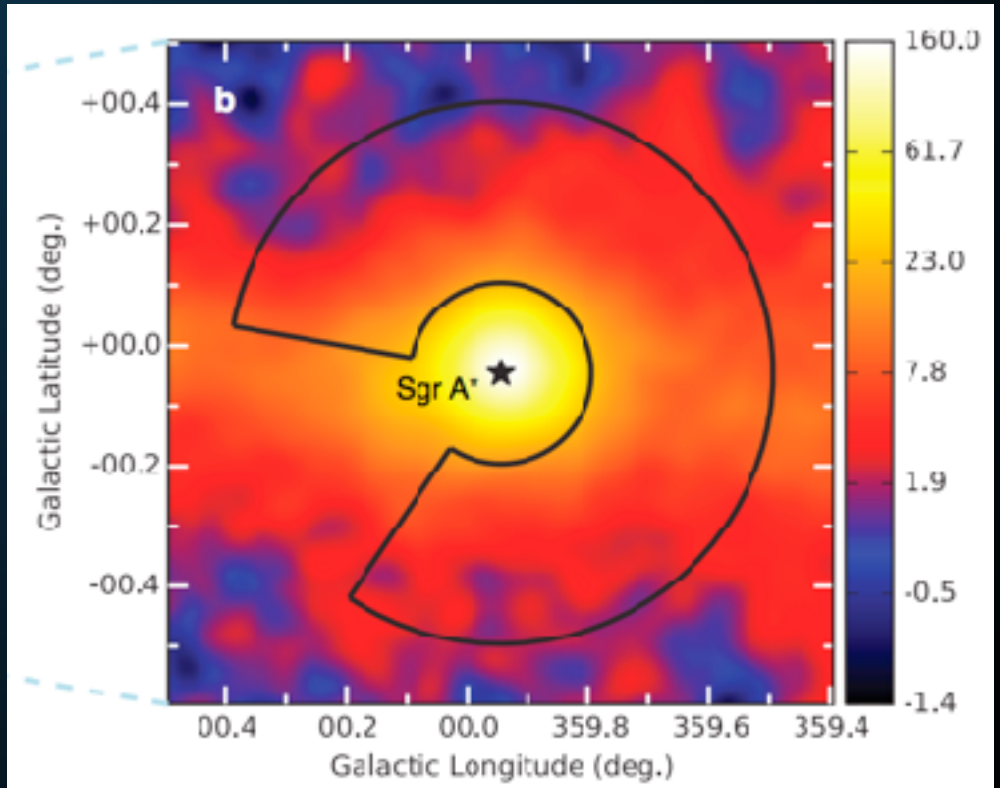

TEV HALOS PRODUCE THE PEVATRON SPECTRUM

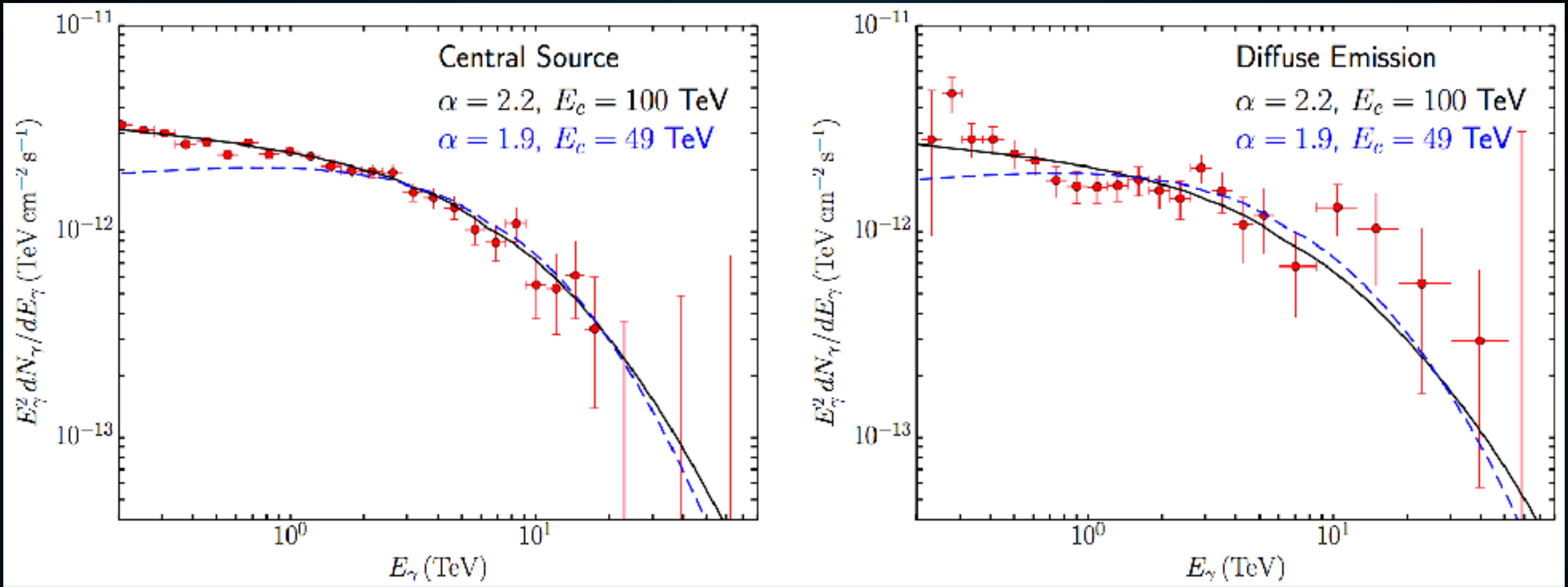

- The TeV halo spectrum from Geminga naturally reproduces the HESS observations.
- Slightly softer spectra preferred.
  - Some evidence that Geminga spectrum is particularly hard.
  - Hadronic diffuse background contamination?

DIFFUSE EMISSION FROM TEV HALOS

1705.09293

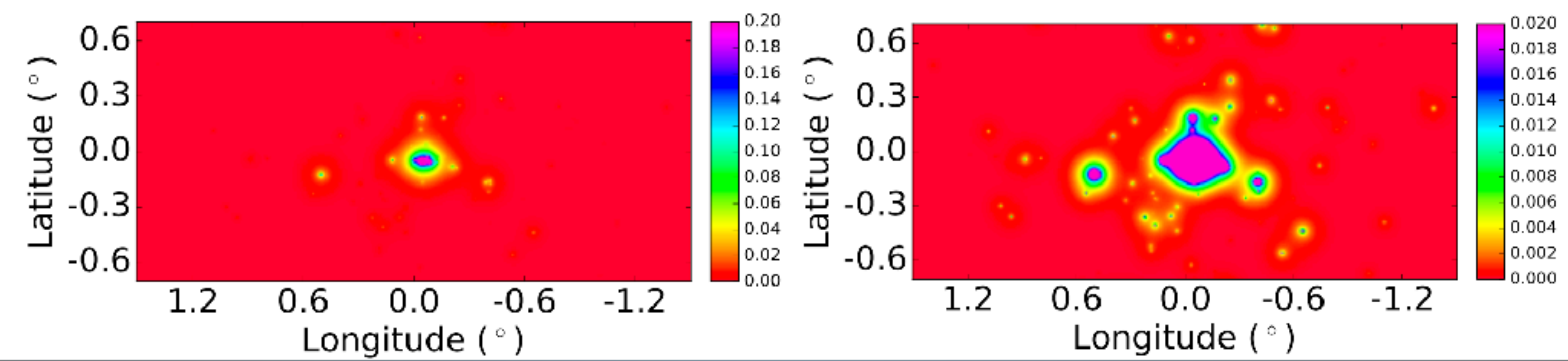

- **Significant star (pulsar) formation in the Galactic center**
- **Pulsars formed in the central parsec will be kicked into surrounding medium.**
- **Source of diffuse gamma-rays in the Galactic center.**

INTENSITY OF TEV HALO EMISSION IN GALACTIC CENTER

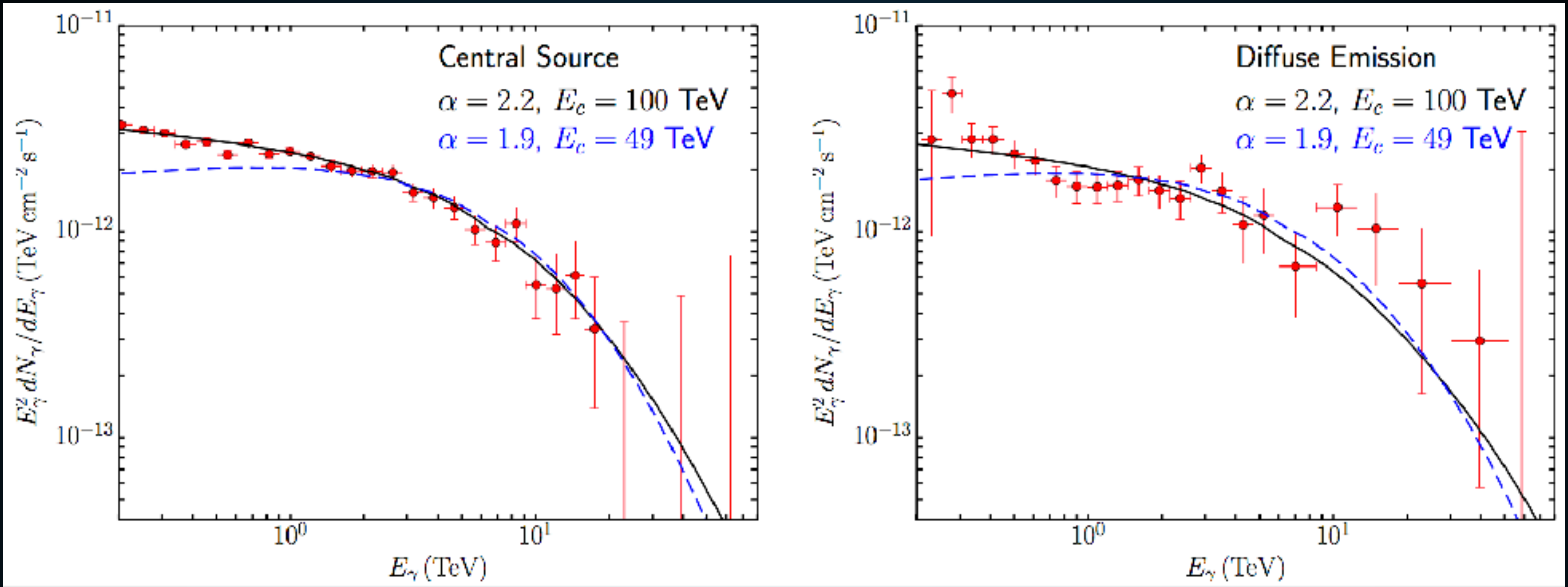

- Using standard values for the propagation of these sources:
  - TeV Halos survive 10 Myr (but become very dim)
  - Pulsar kicks ~ 400 km/s
  - Birth rate between 100-750 pulsars/Myr
- We reproduce the intensity and morphology of the HESS emission.

INTENSITY OF TEV HALO EMISSION IN GALACTIC CENTER

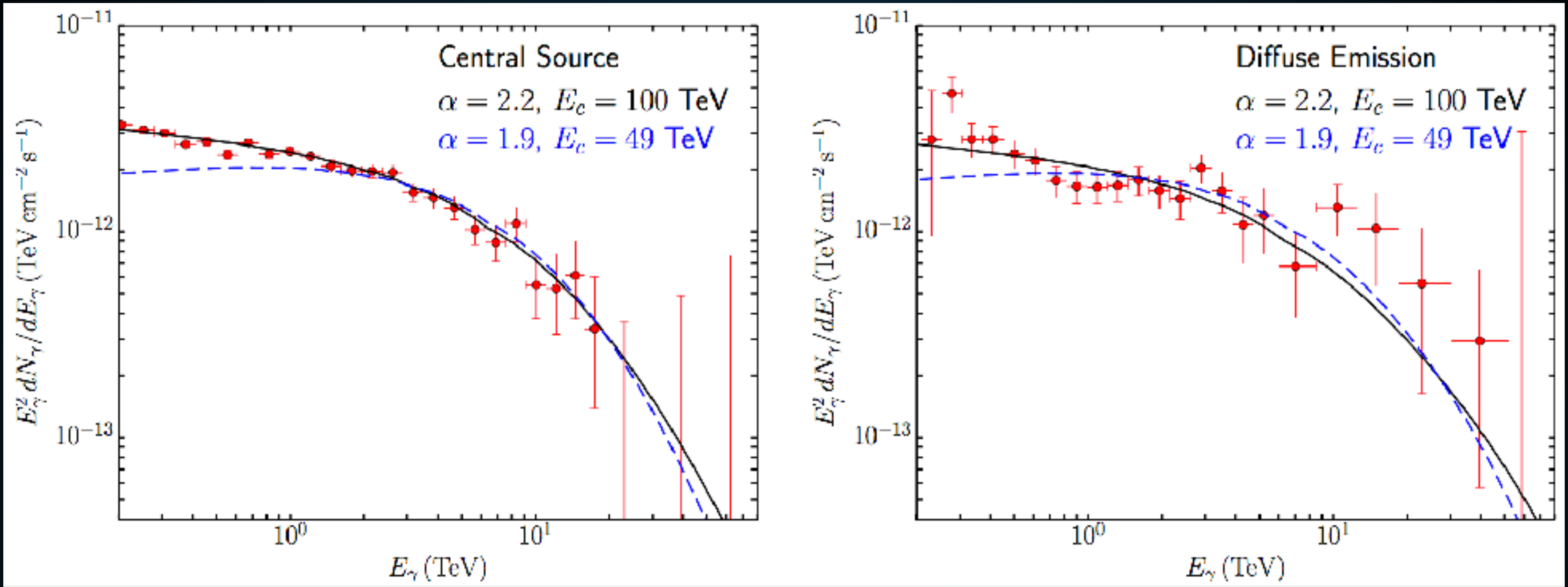

- **Our model implies that TeV halos must form a substantial fraction of the HESS Pevatron emission.**
- **Implies 100-300 observable pulsars in the Galactic center, providing a handle on the missing pulsar problem (1310.7022, 1311.4846).**

- **Milagro detects bright diffuse TeV emission along the Galactic plane.**

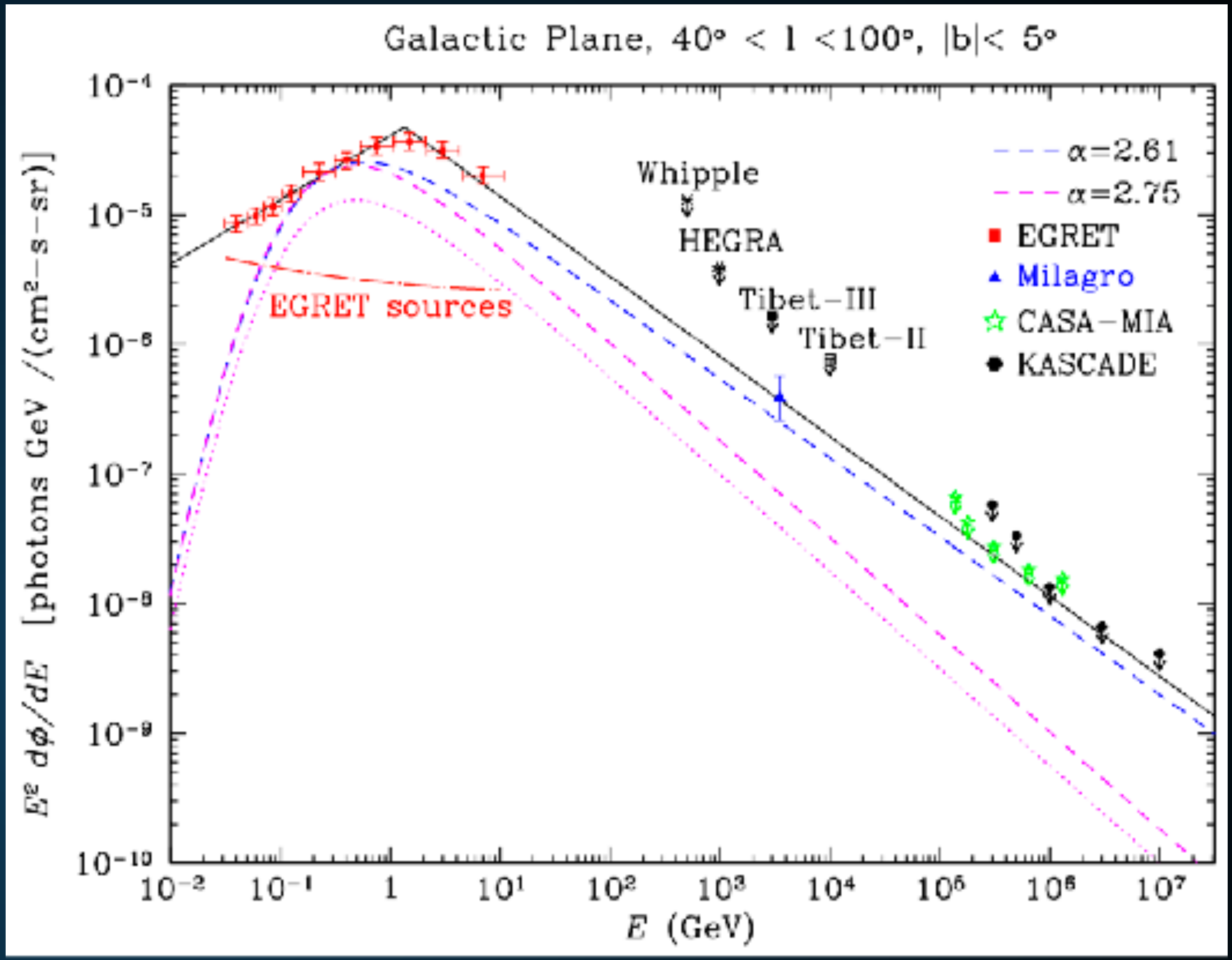

- **Difficult to explain with pion decay, due to steeply falling local hadronic CR spectrum.**

- **Can harden gamma-ray emission to some extent using radially dependent diffusion constants (1504.00227).**

IMPLICATION IIIB: THE TEV EXCESS

1507.06758

- Recent ARGO-YBJ observations are in tension with Milagro result.
- Tension can be alleviated if the gamma-ray spectrum in the region is very hard.
- TeV halos can produce this emission!

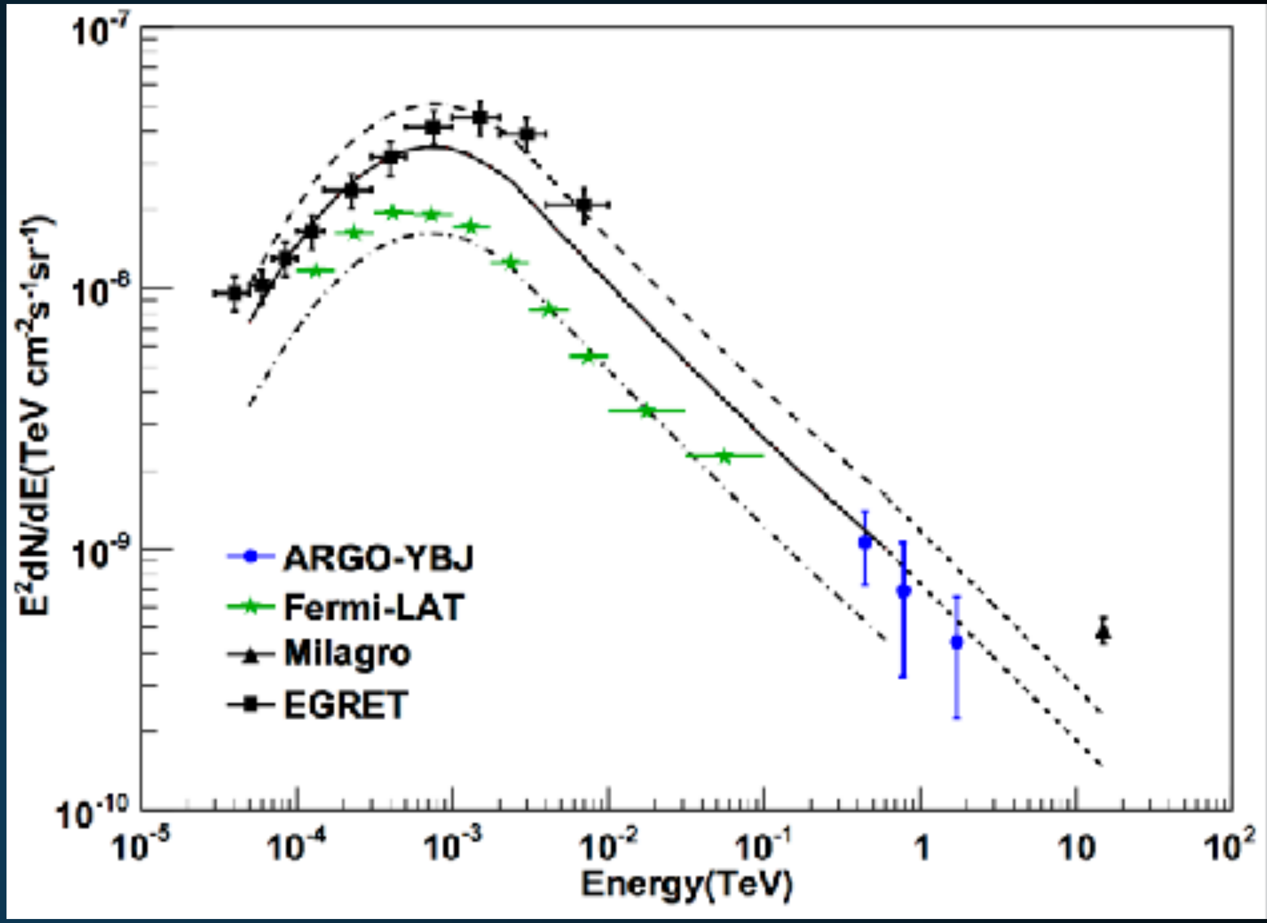

Linden et al. (TBS)

- Use a generic model for pulsar luminosities:
  - $B_0 = 10^{12.5}$ G ($10^{0.3}$ G)
  - $P_0 = 0.3$ s (0.15 s)
- Spindown Timescale of ~10^4 yr (depends on B_0)
- Galprop model for supernova distances

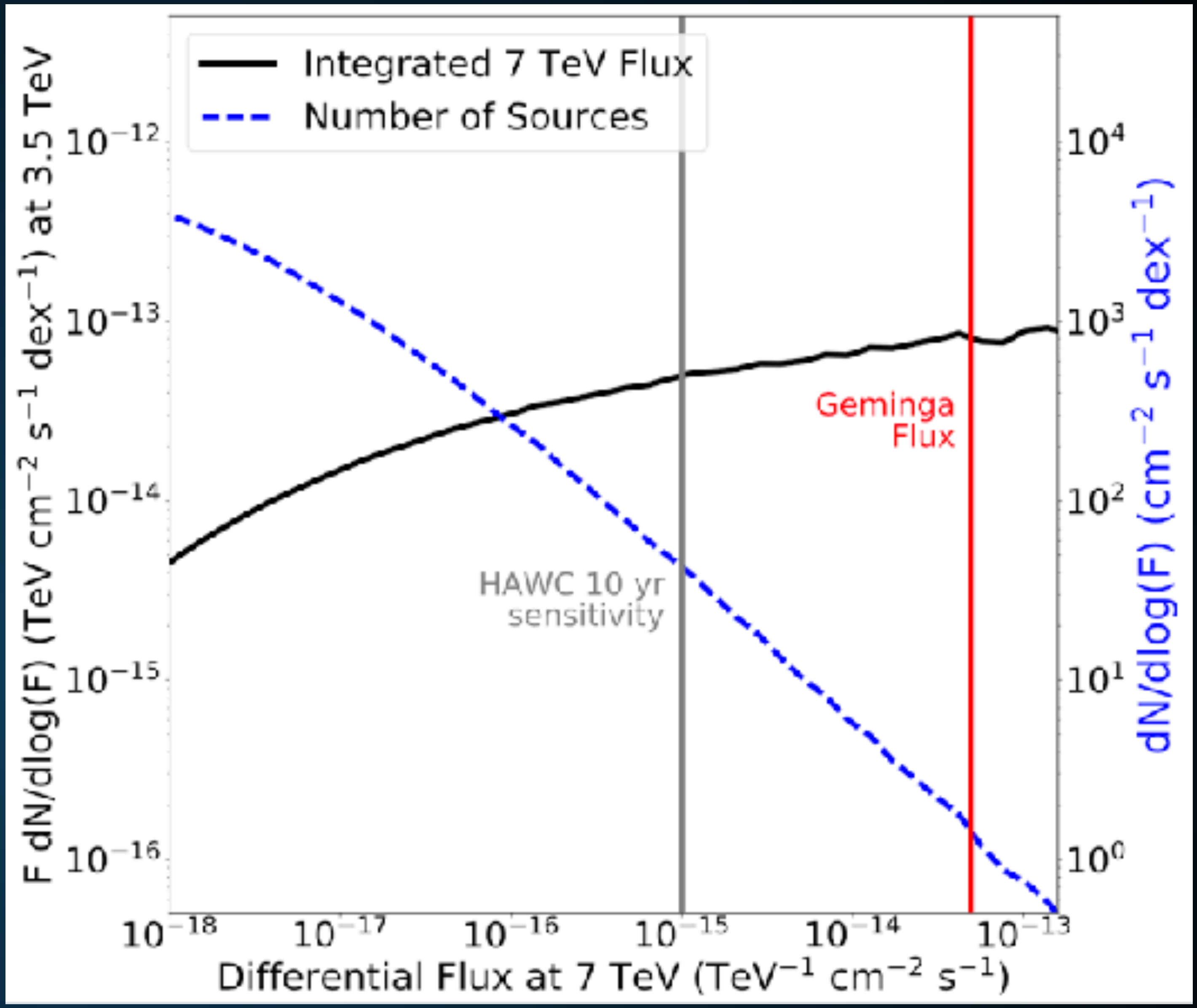

- <u>Naturally expect O(1) source as bright as Geminga</u>
- <u>HAWC eventually observes O(50) sources.</u>

Linden et al. (TBS)

- **Use Geminga as a template to calculate TeV halo intensity.**
- **Use Geminga spectrum with complete (diffuse) cooling.**
- **Hadronic background from Galprop models tuned to Fermi-LAT emission.**

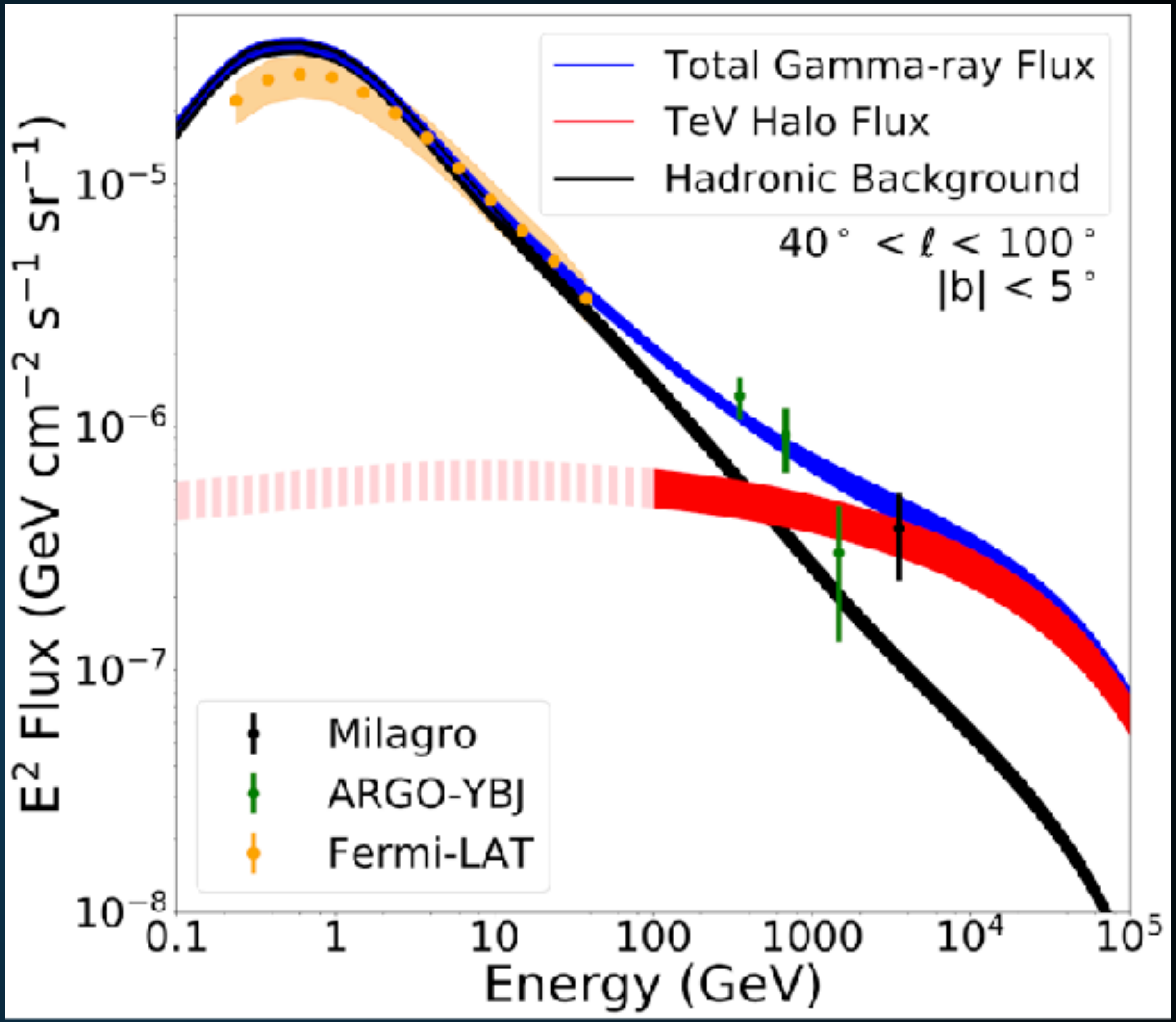

- **<u>TeV halos naturally explain the intensity and spectrum of the TeV excess.</u>**

TeVPA 2017

tevpa2017.osu.edu

- August 7–11, Columbus, OH
- Registration and abstract submission are open
- Pre-meeting mini-workshops on Sunday, August 6

- **TeV observations open up a new window into understanding Milky Way pulsars.**
- **Early indications:**
  - **Positron Excess is due to pulsar activity**
  - **TeV halos produce most of the TeV sources observed by ACTs and HAWC**
  - **TeV halos dominate the diffuse TeV emission in our galaxy.**

- **Additional implications:**
  - **Young pulsar braking index**
  - **Galactic cosmic-ray diffusion**
  - **Source of IceCube neutrinos**

Extra Slides

- **An X-Ray halo with an identical morphology as the TeV halo must exist.**

$$U = \frac{1}{8\pi} B^2 = \frac{(10\,\mu G)^2}{8\pi}$$
$$= 4\times10^{-12}\ \frac{\mathrm{erg}}{\mathrm{cm}^3}$$
$$\int_0^{10\,\mathrm{pc}} U\, dV = 5\times10^{47}\ \mathrm{erg}$$
$$\hookrightarrow \text{Magnetic Flux} \simeq 5\times10^{38}\ \frac{\mathrm{ers}}{\mathrm{s}}$$

$$\mathrm{ISRF} = 1\ \frac{\mathrm{eV}}{\mathrm{cm}^3}$$
$$\int \mathrm{ISRF}\, dV = 8\times10^{47}\ \mathrm{erg}$$
$$\hookrightarrow \text{Flux} = 8\times10^{38}\ \frac{\mathrm{ers}}{\mathrm{s}}$$

$$E_{\mathrm{sync,critical}} = 22\ \mathrm{eV}\left(\frac{B}{5\ \mu G}\right)\left(\frac{E_e}{10\ \mathrm{TeV}}\right)^2$$

- **However, the signal has a low surface brightness and peaks at a low energy.**

X-RAY PULSAR WIND NEBULAE

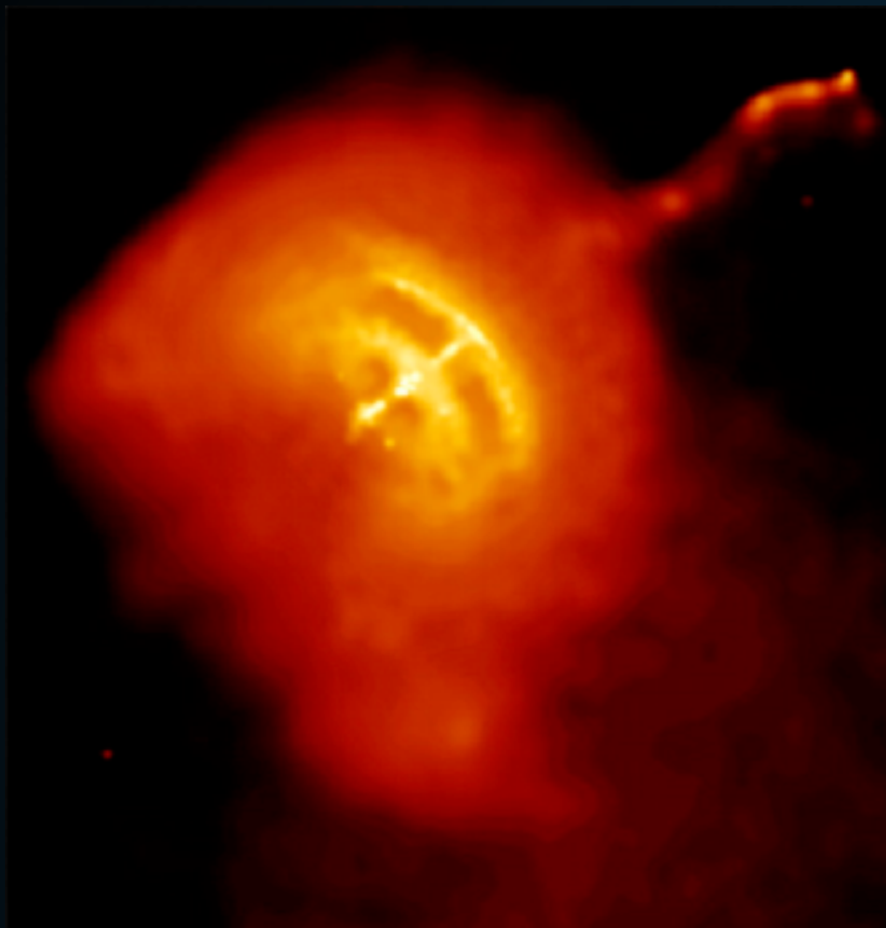

- Larger magnetic fields make compact PWN easier to observe
  - Synchrotron dominated
  - Higher energy peak
- More distant sources easier to see.
- Significant observation times require careful HAWC analysis.

GEMINGA SPECTRUM INDICATIVE OF CONVECTION

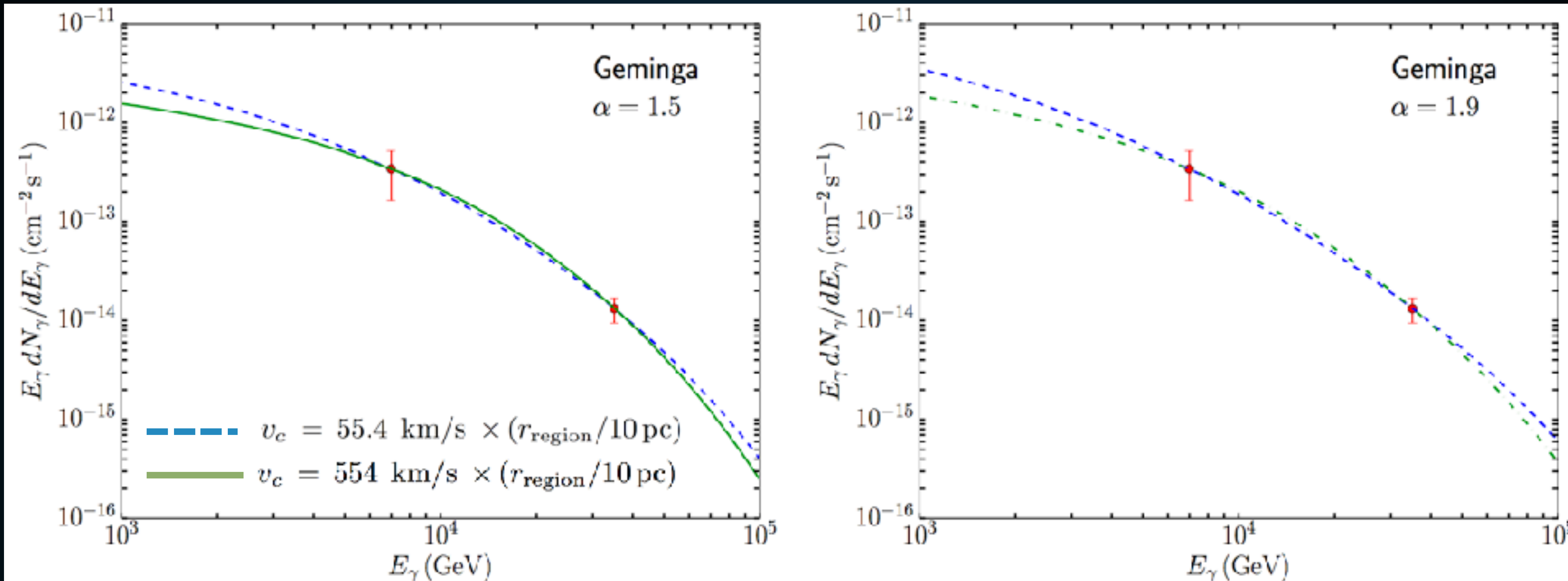

- **Geminga spectrum is fit better with convective models.**
- **Energy-independent diffusion provides identical results**
- **Best-fit spectral-index (-2.23 +/- 0.08) prefers high convection**

WHY ARE HIGH-ENERGY ELECTRONS TRAPPED?

- Cooling dominated by 20 μG magnetic field.
- Energy loss time: ~40 years
- Distance Traveled: ~6 pc for standard diffusion constant. Real diffusion must be slower.
- The spectrum changes as a function of distance and time.

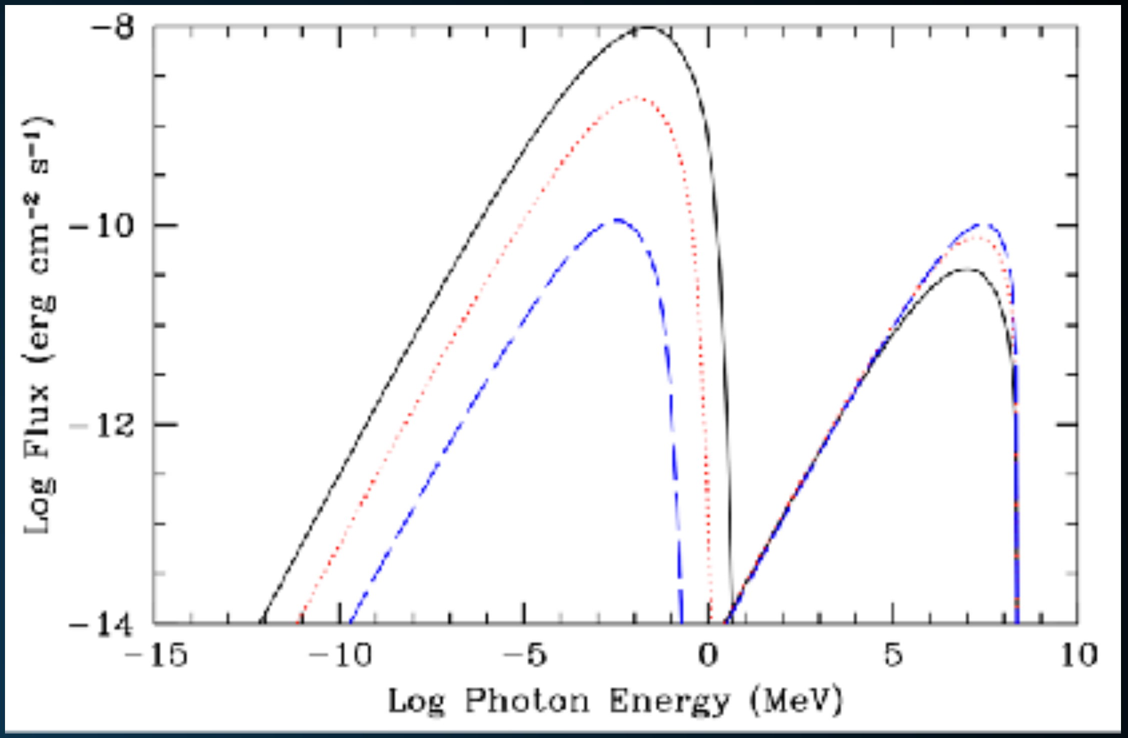

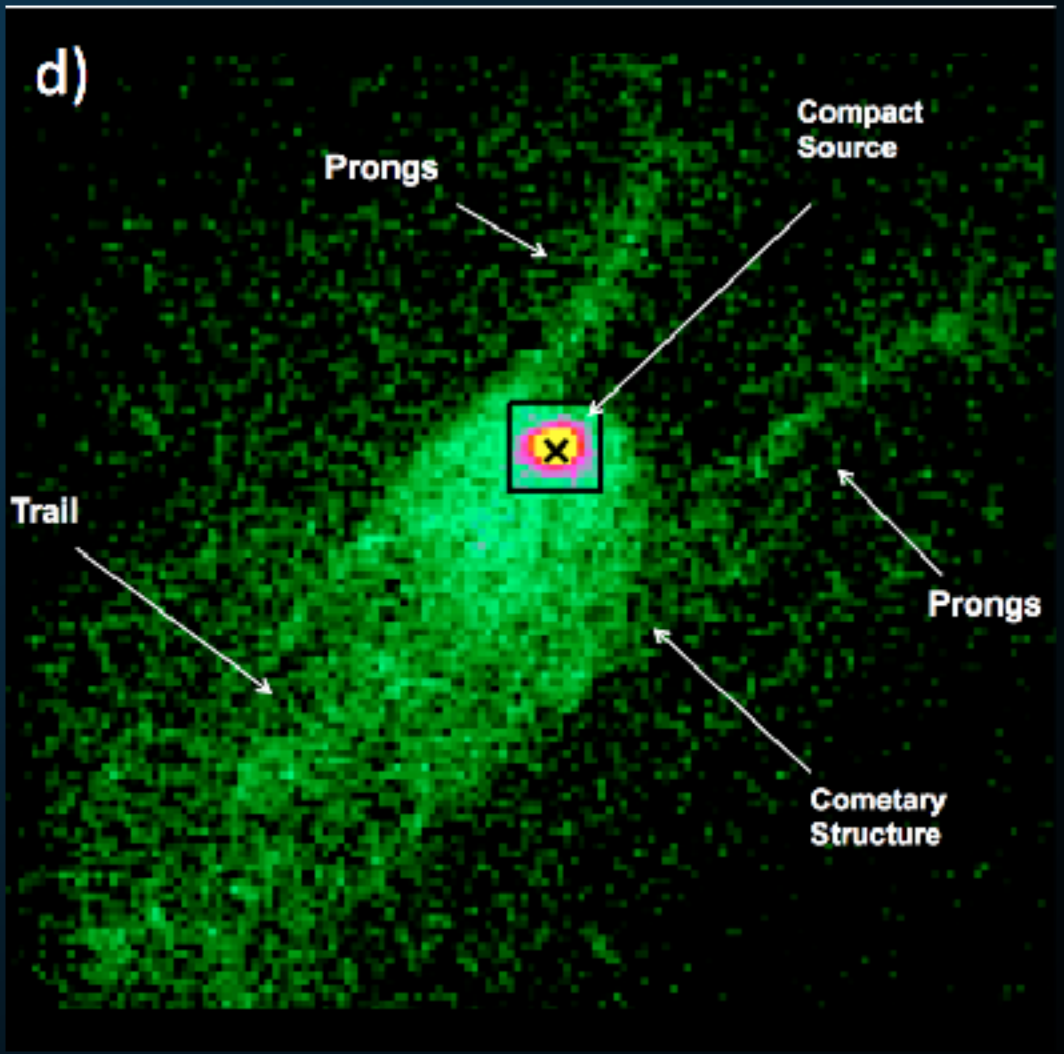

FERMI-LAT OBSERVATIONS OF PWN

1011.2076

- Gamma-Ray produced through ICS should accompany synchrotron emission.

- Synchrotron observations imply very hard GeV gamma-ray spectrum.

- Conclusively prove leptonic nature of emission.

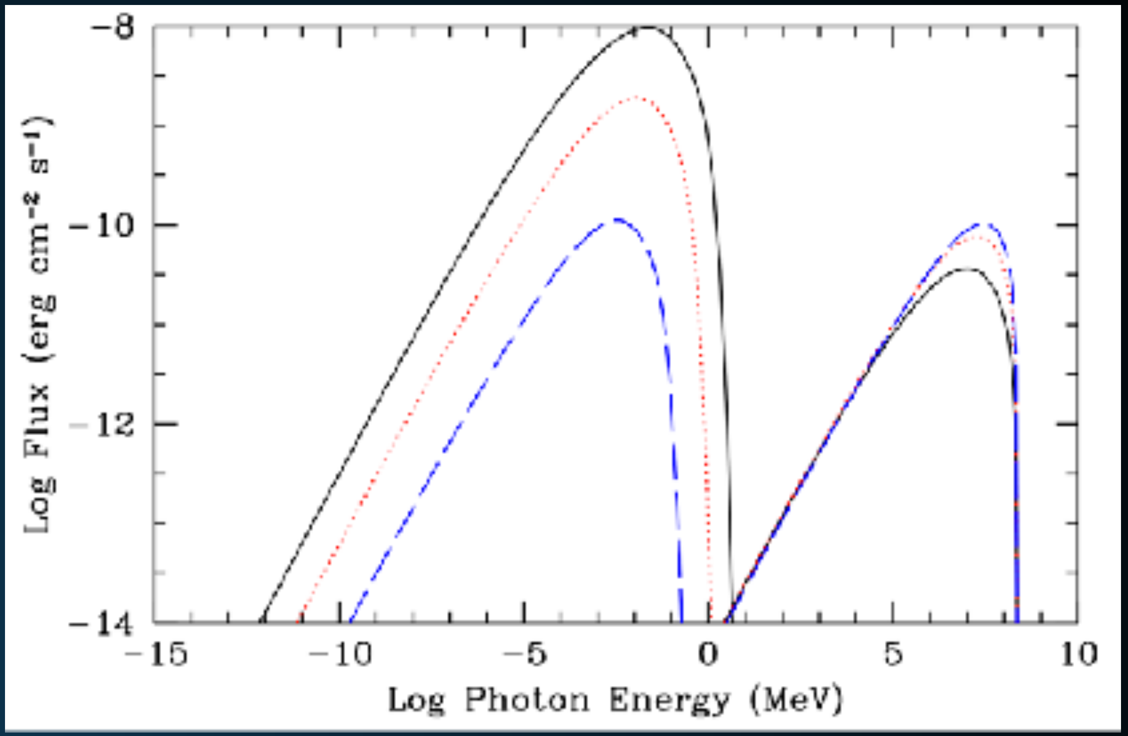

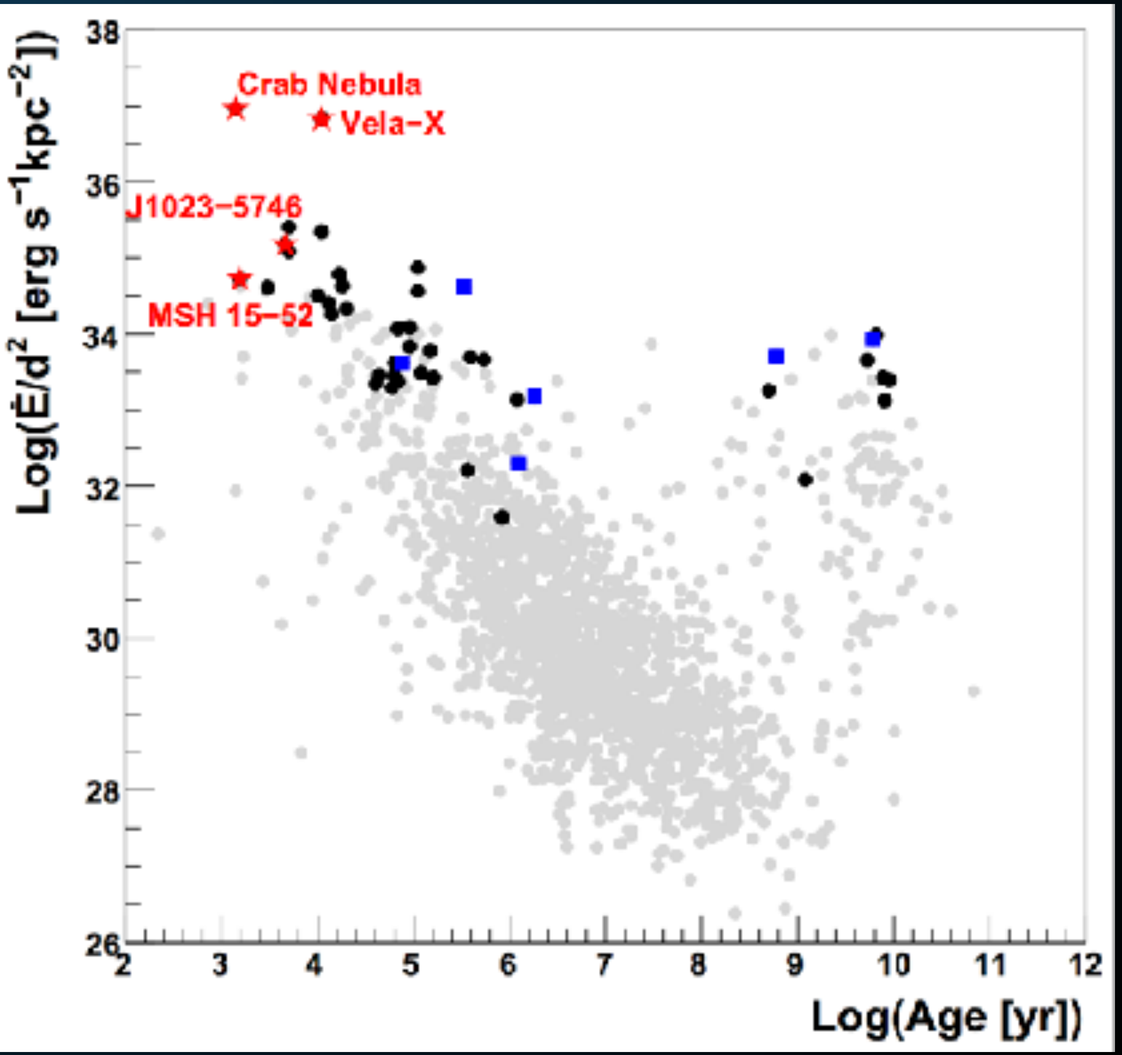

THERMAL PULSAR EMISSION

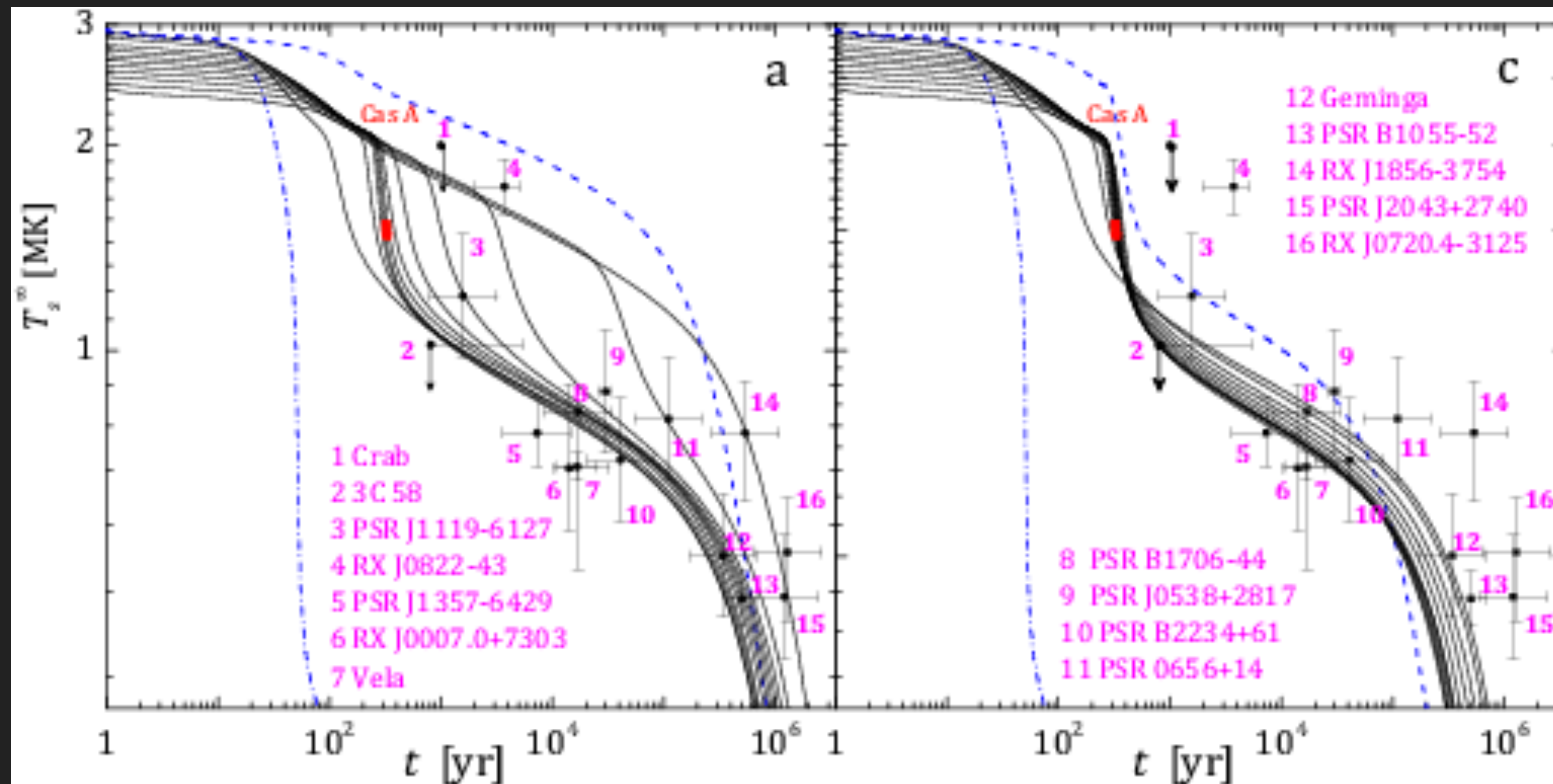

- Hot neutron stars can also be observed via their isotropic thermal emission.
- X-Ray observations can be sensitive to ~2 kpc for 10^6 K NS.
- Cooler NS extremely hard to see.
- Could potentially detect a system which has recently ceased producing TeV particles.

- HAWC sources are potential IceCube neutrino sources.
- Spectral measurements of HAWC sources are imperative to calculating the expected neutrino flux.

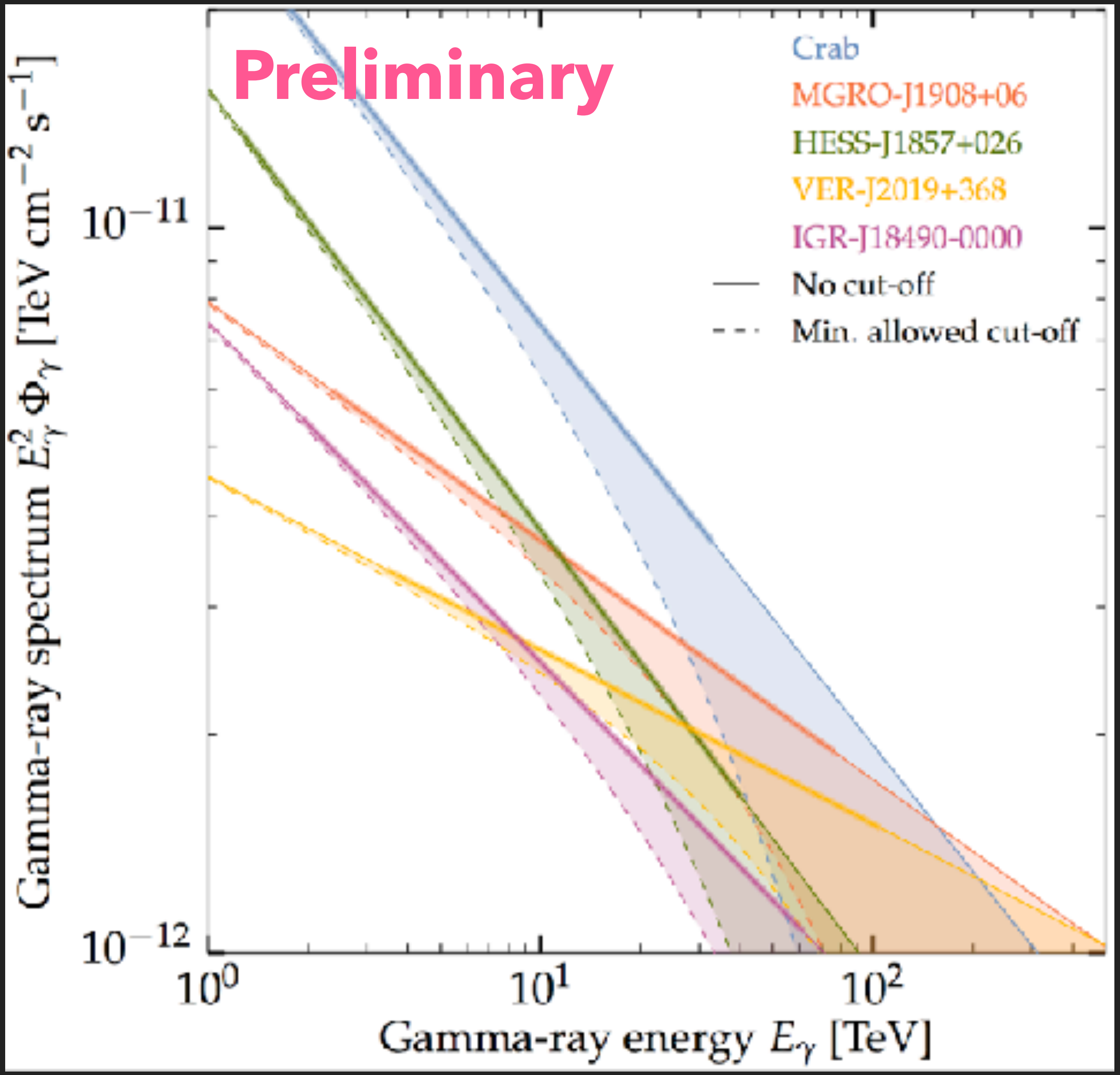

- Here we produce an analysis taking into account a 20% uncertainty in total flux, as well as spectral uncertainty due to an exponential cutoff.

Bustamante, Li, TL, Beacom (TBS)

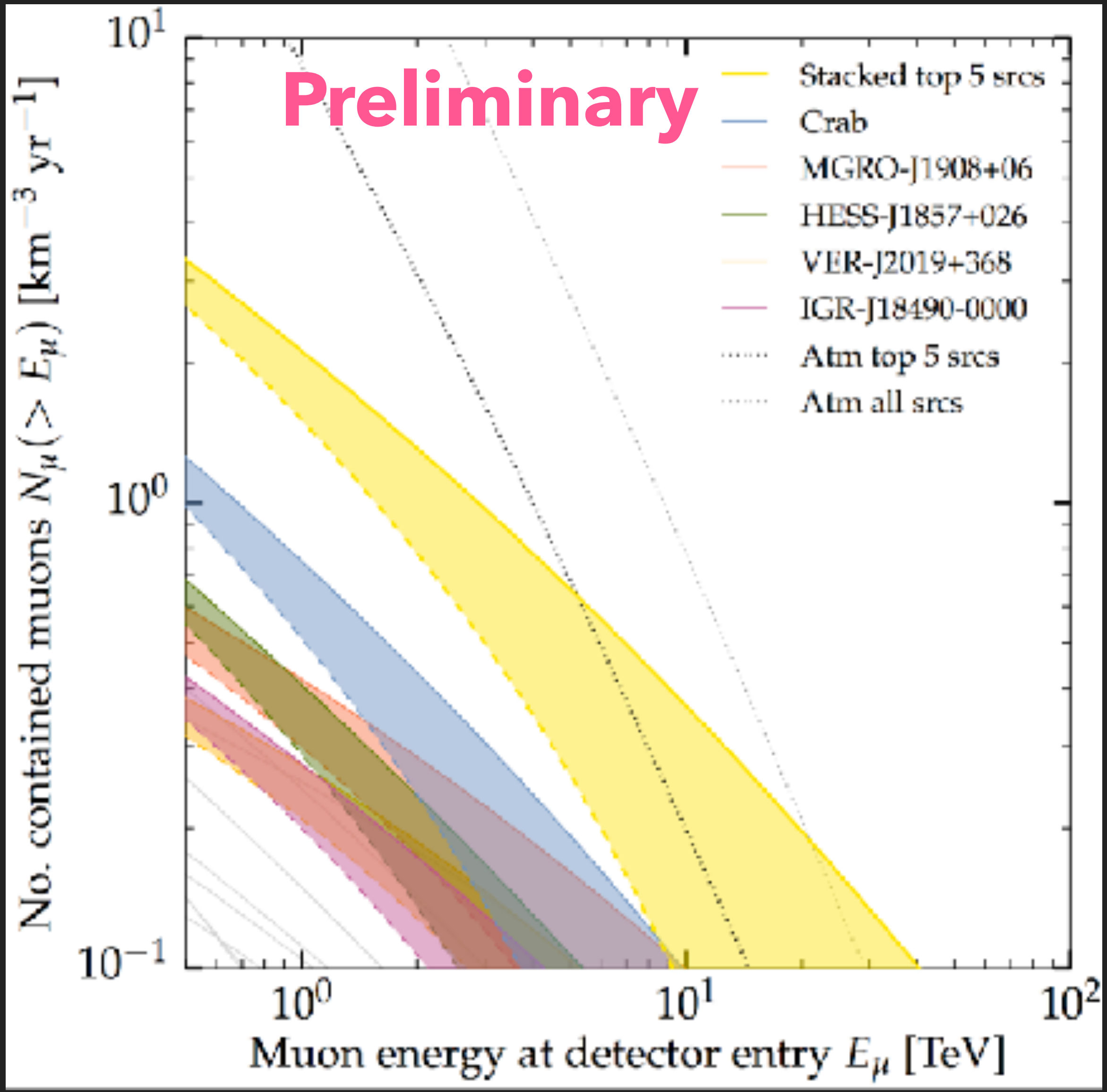

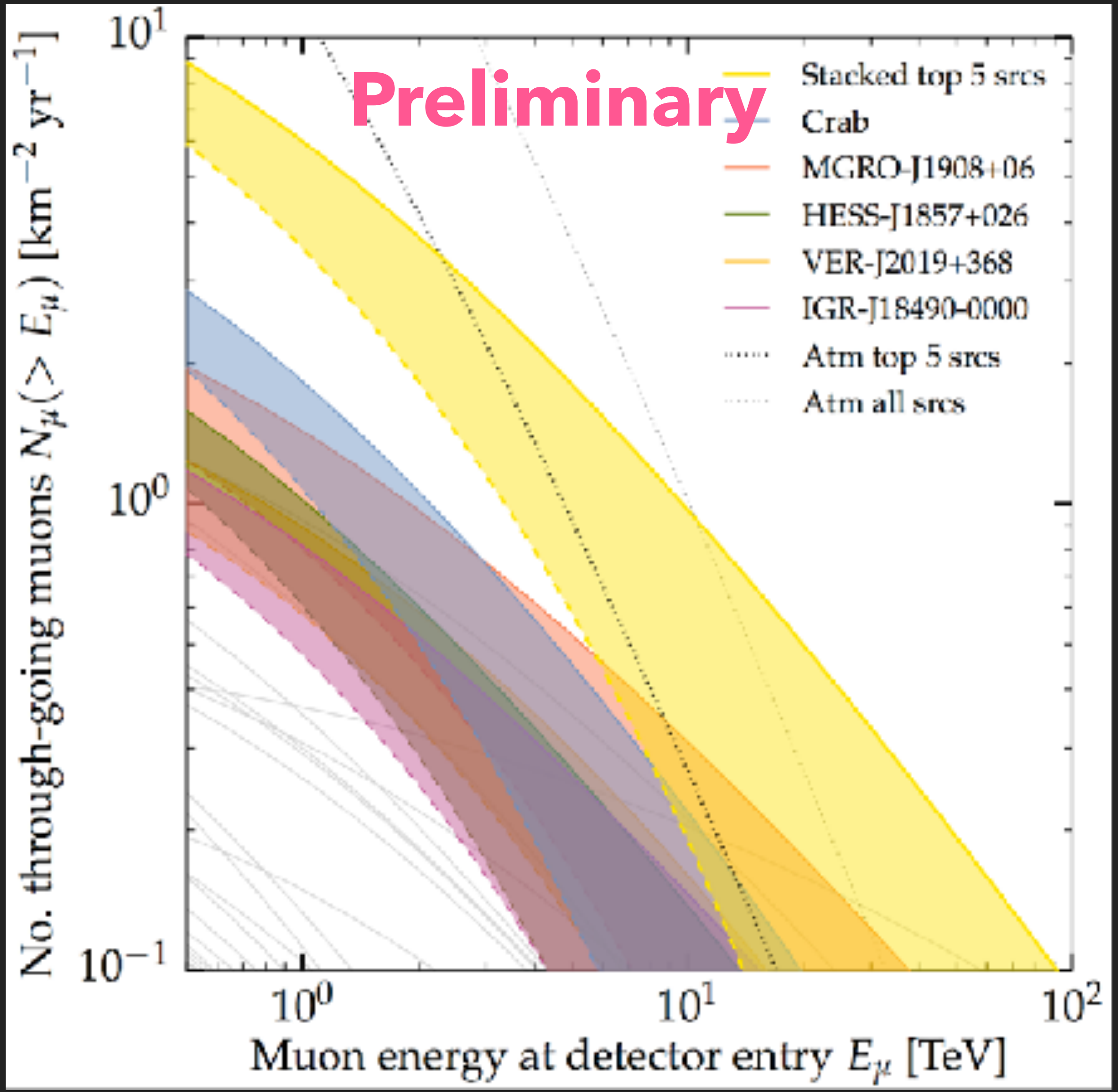

- If these sources are hadronic, their stacked neutrino flux is detectable in current IceCube data.
- Alternatively, can place a strong constraint on the hadronic fraction of the brightest HAWC sources.